UNIVERSITY *of the*
WESTERN CAPE

The identification of aptamers against serum biomarkers of human tuberculosis

Darius Riziki Martin

A thesis submitted in partial fulfilment of the requirements for the degree Magister Scientiae in the Department of Biotechnology, University of the Western Cape.

Supervisor: Prof. Mervin Meyer

Co-supervisor: Prof. Martin O. Onani

December, 2018

http://etd.uwc.ac.za/

Keywords

Aptamers

Binding constant

Diagnostics

Electrophoretic Mobility Shift Assay (EMSA)

Expression

In silico approach

Lateral flow devices

Magnetic bead-based SELEX

Recombinant DNA technology

Sequence analysis

Serum biomarkers

Surface Plasmon Resonance (SPR)

Systemic Evolution of Ligands by EXponential enrichment (SELEX)

Transformation

Transgelin-2 (TAGLN-2)

Tuberculosis

UNIVERSITY of the
WESTERN CAPE

http://etd.uwc.ac.za/

Abstract

The identification of aptamers against serum biomarkers of human tuberculosis

DRM, Martin

MSc. Thesis, Department of Biotechnology, University of the Western Cape

Tuberculosis (TB) is a global health problem and rated as the second leading cause of death after HIV/AIDS. Transmission of TB from one person to the next is very rapid in crowded communities. Therefore, it is crucial to identify people who are infected as quickly as possible not only to provide treatment but also to prevent the spread of the disease. Current TB diagnostic tests such as the culture and sputum smear tests are time-consuming, while rapid tests make use of antibodies that are costly and have low sensitivity and stability. Great improvement has been observed when aptamers are used in place of antibodies in rapid diagnostic tests such as lateral flow devices (LFDs). Therefore, the current study aims to synthesize and identify aptamers against serum biomarkers for development of rapid TB diagnostic tests such as a lateral flow assay. Several TB serum biomarkers have been identified and can be used for the diagnosis of TB.

TB biomarkers expressed in serum samples were identified through *in silico* approach. The biomarkers were expressed in bacterial systems using recombinant DNA technology. The recombinant proteins were purified by affinity chromatography and further used as targets for the selection of aptamers using Systemic Evolution of Ligands by EXponential enrichment (SELEX). Aptamers for the selected biomarkers were synthesized based on magnetic-bead based SELEX and characterized by electrophoretic mobility shift assay (EMSA), Surface Plasmon resonance (SPR) and MicroScale Thermophoresis (MST).

UNIVERSITY of the
WESTERN CAPE

http://etd.uwc.ac.za/

Six putative TB serum biomarker proteins were selected from literature, namely, Insulin-like Growth Factor Binding Protein 6 (IGFBP6), Interferon-stimulated Gene 15 (ISG15), Calcium Binding Protein (S100A9), Retinol Binding Protein 4 (RBP4), Granzyme A (GrA), and Transgelin-2 (TAGLN2).

The biomarkers were recombinantly expressed and purified after which they were used as targets in SELEX for aptamers synthesis. Aptamers were analysed by *in silico* method and the ones with highly conserved motifs were selected. The selected aptamers were synthesized and later characterized. The aptamers that show high affinity and specificity for the biomarkers will be used for the fabrication of a rapid lateral flow device for TB screening. Such a test would allow for a short diagnostic turnaround time, and hence expedite treatment.

UNIVERSITY of the
WESTERN CAPE

December, 2018

http://etd.uwc.ac.za/

Declaration

I declare that "*The identification of aptamers against serum biomarkers of human tuberculosis*" is my own work that has not been submitted for any degree or examination in any other university and that all the sources I have used or quoted have been indicated and acknowledged by complete references.

Signed: .....

Date: 20th of December, 2018

http://etd.uwc.ac.za/

Acknowledgements

First and foremost thank you Allah. For without your strength, guidance, love and grace upon my life none of my achievements would be possible. My sincere gratitude goes to my supervisors Professor Mervin Meyer and Professor Martin Onani for giving me the opportunity to work in such a competitive environment. Also, special thanks to the DST/Mintek Nanotechnology Innovation Centre (NIC) and the Ada and Bertie Levenstein Bursary for the financial support they gave me throughout the years. My special gratitude also to the NIC team including Professor Madiehe, Dr Nicole Sibuyi, Dr Mustafa Drah, Dr Kiplagat Ayabei, Dr Marius Tincho, Dr Dorcas Wusu, Mr Naser Eshibona, Mr Abdul Elbagory, Mr Mohammed Hassan, Ms Chipampe Lombe, Mr Olalekan Bakare, Mr Adewale Fadaka and Ms Phumuzile Dube. Thanks to Mr Phathutshedzo Mulisa Muthelo, Mr Atherton Mutombwera and Ms. Lauren Swartz for the training on synthesis and characterization of aptamers. Thanks to Ms Koena Moabelo, Litha Sisipho Gamnca, Philisiwe Molefe and Ms Shakeela Lucas for the good and bad times in the lab. My sincere gratitude also goes to the entire Biotechnology team.

To my supportive friends, including, Ida Okeyo, Shamsa Ali Hajj, Aden Mohamed, Wabomba Toili, Josphat Rotich, Fara Abdi, Adow, Harun and Daudi, thank you all for your precious times.

UNIVERSITY of the
WESTERN CAPE

http://etd.uwc.ac.za/

Table of content

UNIVERSITY of the
WESTERN CAPE

http://etd.uwc.ac.za/

UNIVERSITY of the
WESTERN CAPE

http://etd.uwc.ac.za/

UNIVERSITY of the
WESTERN CAPE

http://etd.uwc.ac.za/

UNIVERSITY of the
WESTERN CAPE

http://etd.uwc.ac.za/

UNIVERSITY of the
WESTERN CAPE

http://etd.uwc.ac.za/

UNIVERSITY of the
WESTERN CAPE

http://etd.uwc.ac.za/

UNIVERSITY of the
WESTERN CAPE

http://etd.uwc.ac.za/

UNIVERSITY of the
WESTERN CAPE

http://etd.uwc.ac.za/

List of figures

UNIVERSITY of the
WESTERN CAPE

http://etd.uwc.ac.za/

UNIVERSITY of the
WESTERN CAPE

http://etd.uwc.ac.za/

List of tables

UNIVERSITY of the
WESTERN CAPE

http://etd.uwc.ac.za/

Abbreviations

Abs – Antibodies

AFB - Acid-fast bacilli

AGE - Agarose gel electrophoresis

AIDS – Acquired Immunodeficiency syndrome

Amp - Ampicillin

A-PCR - Asymmetry PCR

ApoC - Apolipoprotein C

APS - Ammonium persulfate

Apt – Aptamer

ATP – Adenosine triphosphate

BLAST - Basic alignment tool

BLI - Biolayer interferometry

bp – Base pair

BSA - Bovine serum albumin

CD4 - Cluster of differentiation 4

cDNA – Complementary DNA

CFP-10 – Culture filtrate protein 10

CRP - C-reactive protein

CTLs - Cytotoxic granules of the T lymphocytes

DNA – Deoxynucleic acid

dNTPs - Deoxy ribonucleotide triphosphate

dsDNA – Double stranded DNA

E. coli – Escherichia coli

EDC - Ethyl-3-(3-dimethylaminopropyl)-carbodiimide

UNIVERSITY of the
WESTERN CAPE

http://etd.uwc.ac.za/

EDTA - Ethylene-diamine-tetra-acetic acid

EMSA - Electrophoretic Mobility Shift Assay

endA1 – Endonuclease 1 type A

EPTB - Extra pulmonary TB

ESAT – Early secretory antigenic target

F^+ - Forward primer

FDA - Food and Drug Administration

FL – Full length

Glu - Glutathione

GrA - Granzyme A

HEPES - 4-2- Hydroxyethyl-1-piperazineethanesulfonic acid

His – Histidine

HIV – Human Immunodeficiency virus

hMSCs - Human bone marrow-derived mesenchymal stem cells

UNIVERSITY of the
WESTERN CAPE

hrs - Hours

HSA – Human Serum Albumin

Hte – Human thioesterase

IDT - Integrated DNA Technologies

IFI15 – Interferon-induced protein ifi-15k

IFN γ – Interferon gamma

IGF-2 - Insulin growth factor-2

IGFBP6 - Insulin-like Growth Factor Binding Protein 6

IGFBP6 - Insulin-like growth factor binding protein 6

IGRAs - Interferon gamma release assays

http://etd.uwc.ac.za/

IL – Interleukin

IMD38 - Immunodeficiency 38

IPTG - Isopropyl β-D-1-thiogalactopyranoside

ISG15 - Interferon-stimulated Gene 15

ITC - Isothermal Titration Colorimetry

kb – Kilo bases

K_d - Dissociation constants

kDa – Kilo Daltons

LB - Lysogeny Broth

LFAs - Lateral flow assays

LFIs - Lateral flow immunoassays

Lib – Library

LJ - Löwenstein–Jensen

LTBI - Latent tuberculosis infection

UNIVERSITY of the
WESTERN CAPE

M. tb - Mycobacterium tuberculosis

MARAS - Magnetic-Assisted Rapid Aptamer Selection

MDR-TB - Multidrug-resistant TB

MEME – Multiple EM for motif elicitation

Met – Methionine

MGIT - Mycobacterial Growth Indicator Tube

min – Minute

MST – Microscale thermophoresis

MTBC - Mycobacterium TB complex

MUC – Mucin

http://etd.uwc.ac.za/

NALFA - Nucleic acid lateral flow assay

NC – Nitrocellulose

NCBI - National Center for Biotechnology Information

NGS - Next generation sequencing

NHS - N-hydroxysuccinimide

Ni-beads – Nickel

NIH – National Institute of Health

NK - Natural killer

NMR - Nuclear magnetic resonance

NMR - Nuclear magnetic resonance

nt – Nucleotide

OD – Optical density

OH – Hydroxide

OmpT – Outer membrane aspartyl protease

UNIVERSITY of the
WESTERN CAPE

PAGE – Polyacrylamide gel

PBMCs - Peripheral blood mononuclear cells

PBS - Phosphate buffered saline

PCR – Polymerase chain reaction

PDB - Protein data bank

POC - Point of care

PPD - Purified protein derivative

PPK2 - Polyphosphate kinase 2

PTB - Pulmonary tuberculosis

Pur – Purified

http://etd.uwc.ac.za/

QFT-GIT - QuantiFERON® TB Gold In-Tube

QMCB - Quarts micro crystal balance

R^- - Reverse primer

RBP4 - Retinol-binding factor protein 4

RefSeq - Reference Sequence

RIF – Rifampicin

RNA – Ribonucleic Acid

ROS - Reactive oxygen species

rRNA – ribosomal ribonucleic acid

RU – response unit

S100A9 - Calcium Binding Protein

SDS – Sodium Dodecyl Sulfate

SDS-PAGE - Sodium dodecyl sulphate polyacrylamide gel

SELEX - System Enrichment of Ligands by EXponential enrichment

UNIVERSITY of the
WESTERN CAPE

SiMAG – Superparamagnetic

SNP - single nucleotide polymorphism

SOC - Super optimal broth

SOD - Superoxide dismutase

SPR - Surface Plasmon Resonance

ssDNA – single stranded DNA

STRA6 – Stimulated by retinoic acid 6

TAGLN – Transgelin

TB – Tuberculosis

TEMED - N, N, N', N'- Tetramethylethane-1,2-diamine

http://etd.uwc.ac.za/

TH1 - T helper 1

TR – Truncated

Tris - Trisaminomethane

TST - Tuberculin skin test

USA – United States of America

VRs - Variable regions

WHO – World Health Organisation

XDR-TB - Extensively drug-resistant TB

µL – Microliter

µM – Micromolar

http://etd.uwc.ac.za/

Dedication

To my family, relatives and friends.

http://etd.uwc.ac.za/

CHAPTER 1
LITERATURE REVIEW

1.1 Introduction

TB is a worldwide health problem, and the 10th most common cause of death globally (WHOa, 2018). Tuberculosis (TB) is a disease which usually affects the lungs and is caused by the bacterium, *Mycobacterium tuberculosis.* TB can also affect other parts of the body, such as the brain, the kidneys, or the spine. TB is spread when droplets of nuclei containing *M. tuberculosis* are expelled into the air by infected individuals and inhaled by uninfected individuals (Warner, 2015). However, not everyone infected with *M. tuberculosis* becomes sick. As a result, two TB-related conditions exist; latent and active TB infection (Fogel, 2015). Individuals with active TB show symptoms such as chest pain, constant coughing for 3 weeks or longer, hemoptysis (i.e. coughing up blood), weight loss, loss of appetite, night sweats, fever and fatigue. These individuals are also infectious and can transfer the disease to other persons. Individuals who are latently infected with *M. tuberculosis* do not have the symptoms of the disease and are also not infectious (Fogel, 2015). It is estimated that one third of the world population is infected with *M. tuberculosis*, but only one tenth of these individuals will develop active TB in their lifetime (Falzon *et al.*, 2016; WHOa, 2018).

UNIVERSITY of the
WESTERN CAPE

The diagnosis of active TB can only be confirmed when there is definite evidence of *M. tuberculosis* presence in the patient's body. However, diagnosing TB promptly and accurately remains a significant medical challenge, particularly in poor resource settings (Huddart *et al.*, 2016).

http://etd.uwc.ac.za/

Commonly used TB diagnostic techniques include the sputum culture test, GeneXpert molecular test and the Line Probe Assay. The sputum culture test has been in practice for over a century and is still regarded as the mainstay technique for the diagnosis of TB (Zhou, 2015). However, this test has a number of limitations; it is widely used to detect acid-fast bacilli from the sputum (Davies and Pai, 2008), takes about 4 - 8 weeks and cannot be used for TB diagnosis in children under the age of 5 years (Boehme and Nabeta, 2010; Lange and Mori, 2010). Other molecular test TB tests such as the GeneXpert and the Line Probe Assay are quite expensive for use in low resource settings; it requires specialized equipment and highly trained personnel to perform the tests (Falzon *et al.*, 2016). Moreover, the antibodies used in these diagnostic tests for the detection of TB-specific antigens often have poor sensitivity and specificity (Steingart *et al.*, 2009). This poor sensitivity often stems from the low stability of antibodies in harsh environmental conditions. Thus, to overcome these challenges, effective diagnostic strategies that will be rapid, sensitive and cost-effective are urgently required. DNA aptamers are short oligonucleotides that can replace antibodies in diagnostic tests. These molecules can fold into specific 3D conformations, which is dependent on their nucleotide sequence. These 3D conformations can provide these molecules the structural specificity that is required for binding to biomarker proteins. DNA aptamers can be produced synthetically, which means their production costs are lower than that of antibodies (Shigdar *et al.*, 2013). They are also more stable than antibodies, which mean that they can be used to produce diagnostic tests that are more specific and more cost effective.

UNIVERSITY of the
WESTERN CAPE

http://etd.uwc.ac.za/

1.2 Tuberculosis

It is hyphothesized that the genus *Mycobacterium* originated more than 150 million years ago. Egyptian mummies, dating back to 2400 BC, showed skeletal deformities that are typical of tuberculosis. The French physician Theophile Laennac, was the first to identify signs of pulmonary and extrapulmonary TB in the 18th century. The organism causing TB was identified by Robert Koch in 1882 using the methylene blue staining developed by Paul Ehrlich. The term "tuberculosis" was first used by Johann Lukas Schönlein in the mid 19th century (Barberis, *et al*., 2017).

While *M. tuberculosis* causes TB in humans, other *Mycobacterium* species such as the *M. africanum, M. caprae, M. bovis, M. microti, M. mungi, M. pinnipedi* and *M. canetti* are known to cause TB in animals. There are over 190 species in the *Mycobacterium* genus. They share several common features; they are non-motile, aerobic, acid-fast bacteria, their cell wall is rich in mycolic acids, and as a result their cell wall is thicker than most bacteria (Blouin, 2015).

UNIVERSITY of the
WESTERN CAPE

Despite their several similarities, specific markers can be used to distinguish species in the *Mycobacterium* genus as shown in Table 1.1. Table 1.1 highlights some of the molecular markers used to differentiate the *Mycobacterium* strains, through single point mutations or combinations of polymorphisms found in *Mycobacterium* genes. For example, mutations in gene *OxyR* have been used to distinguish *M. caprae* and *M. bovis* from the other members of the *Mycobacterium* genus.

http://etd.uwc.ac.za/

Interestingly, *M. caprae* and *M. bovis* look similar but differ when a single nucleotide polymorphism (SNP) occurs in gene *gyrB* as shown in the Table 1.1.

Table 1. 1: An overview of the selected nucleotide markers present in the *Mycobacterium* strains (Rodriguez-Campos *et al*., 2014)

Mycobacterium strains	***M. tuberculosis***	***M. africanum***	***M. mungi***	***M. pinnipedii***	***M. microti***	***M. caprae***	***M. bovis*** ***M. bovis* BCG**
OxyR^{N285} mutation (G to A)[a]	G	G	ND	G	G	A	A
pncA^{C57} mutation (CAC to GAC)	CAC	CAC	ND	CAC	CAC	GAC	GAC
katG^{C203} (ACC to ACT) and ^{C463} (CTG to CGG)	ACC; V	ND; CTG	ND; ND	ACT; CTG	ACT; CTG	ACT; CTG	ACT; CTG
mmpL6^{n551} mutation (C to G)	C	C	ND	G	G	G	G
gyrA^{c95} mutation (AGC to ACC)	V	ACC	ND	ACC	ACC	ACC	ACC
gyrB mutation at n675 (C to T), 756 (G to A), 1311 (T to G), 1410 (C to T) and 1450 (G to T)	C,G,T,C, G	C,G,T,C,T	C,G,T,C, T	C,G,T,C,T	T,G,T, C,T	C,A,G,C, T	C,A,T,T,T
Rv2042c^{c38}	T	T	T	T	T	T	T

***Note**: The superscript denotes the mutation position at either the codon (c) or the nucleotide (n) of the gene while the V and ND represent variable and no data values respectively. OxyR, pncA, katG, mmpL, gyr and Rv2042 are the genes used in classical tests to determine the MTBC lineage and species based on SNPs.*

UNIVERSITY of the
WESTERN CAPE

1.3 Epidemiology of TB

Nearly 10 million TB infections were reported worldwide in 2017, and about 1.6 million people died due to this disease. About 95 % of these deaths occurred in low and middle-income countries (WHOa, 2018). While more men significantly contract and die from TB than women. However, women are severely affected during their productive years and during pregnancy. In 2017, an estimated 3.2 million women fell ill with TB where close to half a million of them died from it (WHOb, 2018). TB and HIV-AIDS are comorbidities.

http://etd.uwc.ac.za/

Patients with TB infection are often also infected with HIV, because HIV positive individuals have a compromised immune system that allows latent TB infection to become active (Bell and Noursadeghi, 2017).

South Africa is one of 6 countries accounting for 60% of the global TB burden (WHOa, 2018). Due to its rapid and ease of transmission, TB presents a threat to human health. Despite efforts to eradicate this disease, TB remains a threat. Socio-economic factors, inadequate therapeutics and failure to diagnose the disease at an early stage are among the reasons why this disease remains so prominent. The development of Multi-Drug Resistant TB (MDR-TB) is another major concern. Poor patient compliance with anti-TB treatment among TB patients and sporadic drug shortages are major contributing factors in the development of MDR-TB. An estimated of 480 000 global cases of MDR-TB have been reported in 2014 (Falzon *et al.*, 2016). Nearly 26 000 of these cases were South African patients. Approximately 6.7 % of these cases were patients who were previously on medication, while approximately 1.8 % were new MDR-TB cases (Budgell *et al*., 2016). Left untreated, patients with MDR-TB can develop Extensively Drug Resistant TB (XDR-TB). An estimated 10 % of MDR-TB patients develop XDR-TB within the same year of diagnosis (Falzon *et al.*, 2016). XDR-TB is considered untreatable and responds weakly to available TB medication, including the most effective second-line anti-TB drugs such as rifampicin, ethambutol, isoniazid and pyrazinamide.

UNIVERSITY of the
WESTERN CAPE

http://etd.uwc.ac.za/

1.4 Pathogenesis and the control of TB

It is quite challenging to fully understand the pathogenesis of TB and the protective role the immune system plays during TB infection because the bacteria interact with the host immunity in a sophisticated manner (Walzl *et al.*, 2011). In patients with active TB, *M. tuberculosis* triggers inflammation and induce an attack on the immune cells which is comparable to oxidative stress (Pieters, 2008). Upon TB infection, the *M. tuberculosis* induces the expression of superoxide dismutase (SOD) to prevent oxidative stress. This was confirmed in a study that observed high levels of expression of SOD in TB patients compared to the lung cancer patients (Wang *et al.*, 2013). SOD is a radical scavenging enzyme which inhibits inflammation in the extracellular spaces within the lungs (Nozik-Grayck *et al*., 2005; Gao *et al*., 2008). In the presence of SOD, lesions form within the affected regions, suggesting an active role for oxidative stress in the pathogenesis of the TB. The development of the lesions are caused by the difference in the homeostatic states between the enzyme and the reactive oxygen species (ROS) (Wang *et al.*, 2013). Nevertheless, in an uncompromised immune system, the *M. tuberculosis* infection can still be contained by the immune cells (Behar *et al*., 2010) as will be discussed in the mechanism of latent TB (Section 1.6).

UNIVERSITY of the
WESTERN CAPE

It is speculated that some individuals may combat *M. tuberculosis* by employing the effector mechanisms of neutrophils within the innate immune system (Warren *et al.*, 2017). Others clear the bacteria by adaptive immunity through the T cells (Jasenosky *et al*., 2015). The T cells are of two types, the short-time memory T cells and the central memory T cells.

http://etd.uwc.ac.za/

The short-time memory T cells remain for a short time when the bacteria are destroyed, while the central memory T cells are kept for life (Walzl *et al*., 2011).

When the host immunity fails to eradicate the *M. tuberculosis* during the latent state, the bacteria remains viable for an extended period, and only becomes active when the host defence weakens. This mechanism is, however, not fully understood (Walzl *et al*., 2011).

The host T cell-mediated immunity is crucial for the regulation of *M. tuberculosis* growth. The presence of the bacteria activates immune cells that express CD4 and interleukin (IL) 12 (e.g. macrophages, neutrophils and human B-lymphoblastoid). The CD4+ cells mature and promotes the activation of the interferon (IFN) –γ, while IL-12 cells activate T helper (TH1) cells to contain the bacteria (Lawn and Churchyard, 2009). However, when the immune system is weak, the risk of *M. tuberculosis* infection is elevated as evidenced in HIV^+ individuals. In fact, immune-compromised individuals are more susceptible to *M. tuberculosis* co-infection (Lawn and Churchyard, 2009).

UNIVERSITY of the
WESTERN CAPE

1.5 Animal-Borne TB transmission

As mentioned earlier, *M. tuberculosis* is also present in domestic animals such as the pets and the cattle (Angkawanish *et al.*, 2010; Parsons *et* a*l.*, 2008). *M. tuberculosis* infection in animals can also spread to humans especially when food products (e.g. raw cheese and unpasteurized milk) produced from *M. bovis* infected animals are consumed. Domestic cattle are more susceptible to bovine TB than other animals (Senthilingam, 2015).

http://etd.uwc.ac.za/

In fact, up to 2000 cases where TB was transferred from animals to humans was reported in the U.S./Mexico border, between 2006 and 2013.

1.6 Stages of TB infection

M. tuberculosis grows most successfully in tissues with high oxygen content, such as the lungs. There are two stages of TB infection, the latent and the active or virulent stages (Jeong *et al*., 2015). *M. tuberculosis* mostly enters the body through the inhalation of infected aerosols. The bacteria are then detected and engulfed by the macrophages. At this stage, the bacterial replication is stopped and if the infected person's immune systems functions optimally, they are eventually destroyed. If the bacteria are not destroyed, they remain functionless and are contained in the immune cells for some period and the infected individual is therefore latently infected. When the immune system weakens or the macrophages harbouring the bacterium die, they replicate abundantly spreading to the other parts of the body (Peruń *et al*., 2017). The infection spread through either lymphatic channels or the bloodstream to the distant tissues and organs such as regional lymph nodes, the apex of the lungs, kidneys, brain and the bones. At this stage, the latent bacteria become active and the person develops active or virulent TB as summarized in Figure 1.1 (Behar *et al*., 2010). Individuals with HIV co-infection have been reported to have an increased risk of latent TB reactivation (Montales *et al*., 2015).

UNIVERSITY of the
WESTERN CAPE

http://etd.uwc.ac.za/

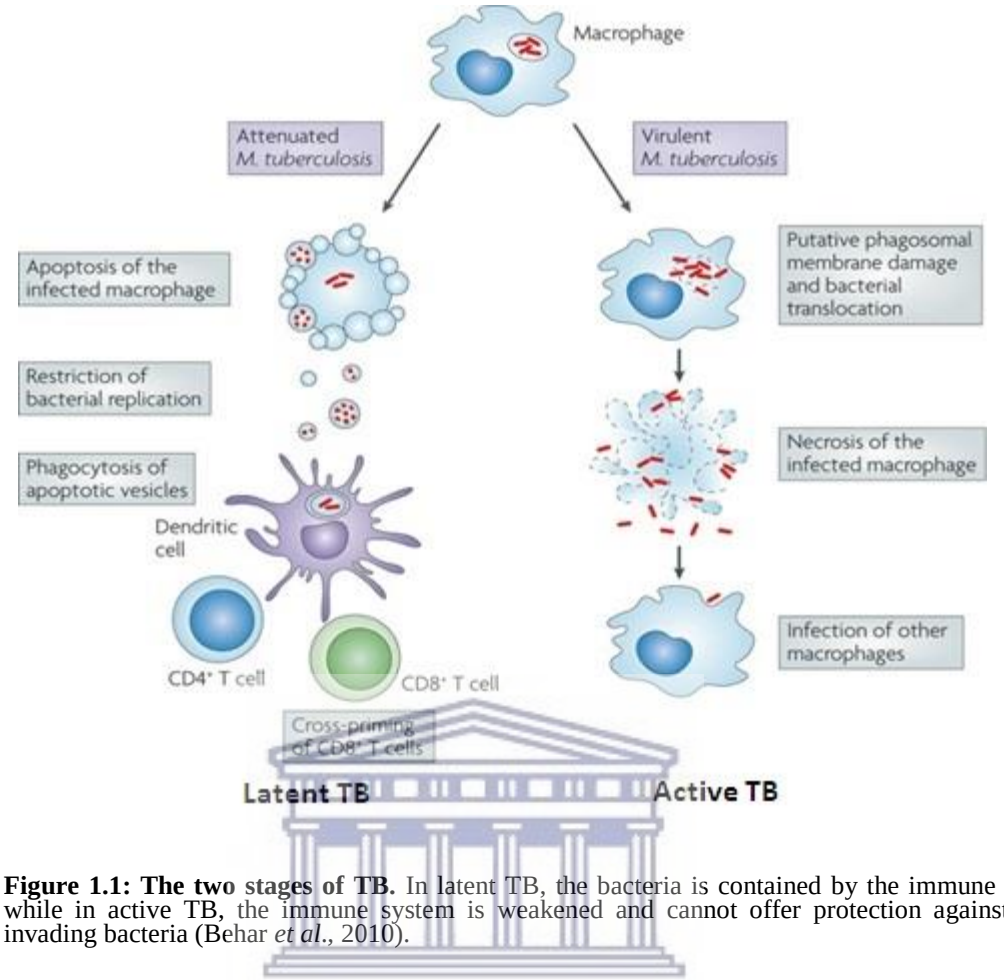

Figure 1.1: The two stages of TB. In latent TB, the bacteria is contained by the immune cells while in active TB, the immune system is weakened and cannot offer protection against the invading bacteria (Behar *et al*., 2010).

UNIVERSITY of the
WESTERN CAPE

Infection with *M. tuberculosis* either causes Pulmonary TB (PTB), Extra Pulmonary TB (EPTB) or lymph node infection. In PTB, the infection is initially localised at the upper area of the pulmonary lobe from where it spreads to other parts of the body if it escapes the immune defence system (Hunter, 2016). The infection might spread to the central nervous system, resulting in tubercular meningitis, which could be fatal if not treated (Michos *et al*., 2006). The infection might also spread to the extra-pulmonary sites resulting in the formation of EPTB diseases such as the cervical adenopathy and lymphatic TB (Lee, 2015). Lymph node infection begins from the neck region where the bacteria are mostly localised.

http://etd.uwc.ac.za/

This causes lymphadenitis or lymph node infection and is usually diagnosed in children below the age of 5 years. However, in countries that experience hot weather conditions, bacteria other than *M. tuberculosis* can also cause the symptoms. In adults, TB is manifested more in the lungs than in the lymph nodes. In fact, PTB occurs in 80 % of TB patients while the lymph node infection arises in only ±20 % of active TB patients, with the risk increasing in immune-compromised individuals such as those co-infected with HIV (Bell and Noursadeghi, 2017).

1.7 Current TB diagnostic techniques and their limitations

A number of clinical laboratory TB diagnostic tests are available. These tests are discussed below.

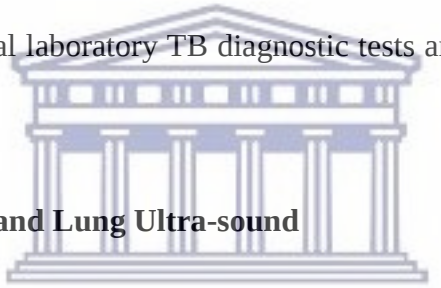

1.7.1 Chest X-ray and Lung Ultra-sound

M. tuberculosis infects primarily the lungs after which it then spreads to other parts of the body. When the lungs are infected, the immune cells trigger an inflammatory response that can damage the lungs and other organs. The lungs then gradually develop scar tissue which can be visualised by a chest X-ray or a lung Ultra-sound (Sperandeo *et al*., 2017; Ball *et al*., 2017). The chest X-ray Portable X-ray units capable of performing chest X-ray can approximately cost $600 to $800. If uninsured, patient cost of a chest X-ray in the US is $200 to $400 or, if insured, a co-payment of $10 to $50 is required (Wang *et al.*, 2018). On the other hand, the chest ultrasound is regarded cheaper than chest X-ray, costing on average one third to half as much as chest X-ray (Amatya, *et al.*, 2018).

http://etd.uwc.ac.za/

Despite extensive technological advancement, these techniques however cannot discriminate lesions caused by lung cancer from the ones arising from *M. tuberculosis* infection (Del Ciello *et al*., 2017). However, the presence of other lung diseases such as lung cancer and pneumonia can result in false positive TB result. Additionally, a negative diagnosis by chest X-ray does not mean the patient does not have EPTB.

Consequently, chest X-ray results should always be confirmed with other TB diagnostics tests. Although the turn-around time for the results of chest X-ray test is relatively quick when compared to some other TB tests, this test requires specialised equipment and trained personnel. In low resource settings such as South Africa this can be a major challenge.

1.7.2 Tuberculin skin test (TST)

The TST is used to test if a person has been exposed to *M. tuberculosis*, either from a previous tuberculosis vaccination, or from environmental exposure to the bacterium. TST involves the injection of a small amount of tuberculin fluid or TB protein (antigens) into the skin of the patient's forearm. The fluid contains Purified Protein Derivative (PPD), which is a protein extract of *M. tuberculosis.* When the body is exposed to *M. tuberculosis*, an active immunity develops and antibodies are produced that will remain in the body to provide protection against the organism in the future. When PPD is injected, it reacts with the antibodies and the inflammation causes swelling of the tissue at the site of injection within 48 – 72 hrs (Yang *et al*., 2012).

UNIVERSITY of the
WESTERN CAPE

http://etd.uwc.ac.za/

The larger the size of the swelling in the injected area, the higher the likelihood that the person is infected with *M. tuberculosis*. This test cannot discriminate between the latent and active TB (Yang *et al*., 2012). Individuals who have been vaccinated with the Bacillus Calmette–Guérin (BCG) vaccine against TB, will therefore also test positive for TB with the TST.

The TST is used in many developed and developing countries to diagnose TB. In countries with low rates of TB infection, it is regularly used to diagnose latent TB infection. However, this test is not very useful in countries with high rates of TB infection since the majority of people in these countries may have latent TB. Also, this test is still not affordable to developing countries. The annual cost of implementing and maintaining a TST program ranged from $66,564 to $332,728 for hospitals and $92,886 to $291,248 for health departments in the United States (Lambert, *et al.*, 2015). In addition, the cost per PPD Skin Test (including return visit for reading) was $49, and the 2-step PPD Skin Test for TB (including return visits for readings) was $98 (AITC, 2019).

UNIVERSITY of the
WESTERN CAPE

1.7.3 Interferon gamma release assays (IGRAs)

IGRAs measure a patient's immune response to the presence of TB-causing bacteria and are deemed to be more accurate than the TST (Caliskan *et al.*, 2014). The procedure involves drawing blood from a person suspected of having TB infection and exposing them to TB antigens (Lewinsohn *et al*., 2017). If the person is infected with *M. tuberculosis*, their peripheral blood lymphocytes will respond by producing IFN-γ. These assays are considered to be more sensitive and only require a single TB test.

http://etd.uwc.ac.za/

Recently, the U.S. Food and Drug Administration (FDA) approved two more IGRAs, the T-SPOT® TB test (T-SPOT) and the QuantiFERON® TB Gold In-Tube test (QFT-GIT) (Lewinsohn *et al*., 2017). The QFT-GIT assay measures the IFN-γ concentration, while T-SPOT determine the number of cells producing IFN-γ. The two assays are further compared in Table 1.2.

Table 1. 2: Comparison between the approved IGRAs (Lewinsohn *et al*., 2017).

Feature	**QFT-GIT**	**T-SPOT**
Test sample	Whole blood analysis	Process peripheral blood mononuclear cells (PBMCs) within 8 hours or if T-Cell Xtend® is used, within 30 hours.
***M.tuberculosis* antigens (for positive test results)**	Can detect the peptides singly such as the early secretory antigenic target 6 (ESAT-6) and the culture filtrate protein 10 (CFP-10).	Can detect both or separate a mixture of the peptides (ESAT-6 and CFP-10).
Measurement	IFN-γ concentration.	Number of IFN- γ producing cells (spots).
Possible Results	Positive, negative, indeterminate.	Positive, negative indeterminate, borderline.

UNIVERSITY of the
WESTERN CAPE

Despite the advantages highlighted above, these assays are also susceptible to errors introduced during sample collection, transportation, processing and interpretation of the assay. The tests must be processed within 8 - 30 hours of collection while the white blood cells are still viable. These tests are also costly which is again a challenge in low resource countries. T-SPOT is one of the options for screening for LTBI partly owing to the viewpoint of cost-effectiveness.

http://etd.uwc.ac.za/

The cost of one test was reported to be $46.61 for T-SPOT and $55.08 for QFT-GIT, while the total costs (including those incurred for retesting), were $6,525.42 and $7,711.86 for the T-SPOT and QFT-GIT tests, respectively (Mukai, *et al.*, 2017). Similarly, although the cost of diagnosis with IGRA and GeneXpert MTB/RIF was reported similar in a different study, however, the total healthcare cost of IGRA was nearly $15 million more than for the GeneXpert test. This was due to the large numbers of false-positive diagnoses triggering inappropriate treatment (Little, *et al.*, 2015). These assays may also have lower accuracy in HIV infected individuals, children younger than the age of 5, and in people who only recently got infected with *M. tuberculosis* (Falzon *et al.*, 2016). Furthermore, these tests cannot differentiate latent and active TB infection (Falzon *et al.*, 2016).

1.7.4 Microscopy tests

UNIVERSITY of the
WESTERN CAPE

This test involves the preparation of smear of the sputum sample of a patient, which is then viewed either using a light microscope or fluorescence microscope to detect the presence of *M. tuberculosis*.

This test is often used in countries with a high rate of TB infection and involves the examination of the sputum to detect a significant number of acid-fast bacteria by employing Ziehl-Neelsen (for light microscopy) or acridine-orange stain (for fluorescence microscopy) (Caulfield and Wengenack, 2016). A smear of sputum (a thin layer of the sample) is placed on a microscope slide, the morphology and the presence of the bacteria confirm TB infection (Caulfield and Wengenack, 2016). This test provides results within hours and is easy to perform.

http://etd.uwc.ac.za/

However, the sensitivity of the test is only about 50 – 60 % (Singhal and Myneedu, 2015; Caulfield and Wengenack, 2016), especially in countries with a high prevalence of HIV co-infection. The tests also have minimal detection rates due to the immuno-compromised nature of the sample, which can suppress the number of the viable *M. tuberculosis* (Siddiqi *et al*., 2003). Also, delays in sample collection and processing might render the test insensitive (Davis *et al*., 2013; Kirwan *et al*., 2016). While light microscopes are commonly available in diagnostic laboratories and relatively inexpensive, fluorescence microscopes are more expensive and requires specialized training. The costs of diagnosing tuberculosis using sputum smear microscopy were estimated to be lower than using rapid sputum-based test. The former ranged between $73 to $119 million per year, while the latter was $93 to $187 million per year (Pantoja, *et al.*, 2015).

1.7.5 Sputum culture test

UNIVERSITY of the
WESTERN CAPE

This test involves the sub-culture of bacteria that are present in the sputum of a patient on a suitable nutrient enriched medium. *M. tuberculosis* can be cultured in either the solid or the liquid media. The solid medium can be either egg or agar-based. The egg-based medium such as the Löwenstein–Jensen (LJ) is the most commonly used medium since it has a long shelf life and supports the growth of sevaral *Mycobacterium* species. However, it can be difficult to detect the presence of the *M. tuberculosis* in the early stages of infection (Boum *et al*., 2013; Palange *et al.*, 2016). Liquid media such as the Middlebrooks 7H9 and Dubos Tween albumin broths, or commercially available culture systems such as the Bactec 460TB system, the Bactec Mycobacterial Growth Indicator Tube (MGIT) 960 system, VersaTREK (ESP II) culture system and MB/BacT system

http://etd.uwc.ac.za/

can also be used to detect *M. tuberculosis* (Whitelaw and Sturm, 2009). Antimicrobial agents (such as penicillin, nalidixic acid, leucomycin and cycloheximide) can be added to both solid and the liquid media to prevent contamination with other micro-organisms (Whitelaw and Sturm, 2009).

Upon culturing the *M. tuberculosis*, a single bacterial colony is isolated from a culture with a mixture of different bacteria. An antibiotic resistant colony, which is usually composed of tens of millions cells derived from a single cell, is isolated after many sub-cultures (Pingle *et al*., 2014). However, the sputum culture test has some drawbacks. In a clinical setting, sub-culturing of the micro-organism is more complex, time consuming and expensive than microscopy. Also, with the novel diagnostic strategies, each patient requires only one test. In cases of human immunodeficiency virus (HIV)-positive people who are presumed to have tuberculosis but have a negative detection test result with any of the tests (such as rapid sputum or non-sputum biomarker-based test), the liquid culture is used as a confirmatory test despite the expenses involved (Pantoja, *et al.*, 2015). The estimated unit cost for culture test ranged from $1.63 to $62.01 (Lu, *et al.*, 2013). Unit costs for all the tests include only reagents, chemicals, and consumables but exclude costs for labor, overhead, space used, and transport. This figure amounted to $162 million in an estimated 1.5 million tuberculosis cases (Pantoja, *et al.*, 2015). Furthermore, the turn-around time for the results of the sputum culture test is 4 weeks due to the slow growth of *M. tuberculosis* on solid media (Palomino *et al*., 2007; Pingle *et al*., 2014).

Specialized equipment and a level 3 biosafety laboratory facilities are also required to perform these procedures.

http://etd.uwc.ac.za/

1.7.6 Molecular tests for TB Diagnosis

Molecular diagnostic techniques are based on the detection of genomic, proteomic or metabolomic markers that are associated with the disease and can be used in diagnostics to indicate the presence of the disease state. It can also be used in prognosis to predict the outcome of a treatment.

1.7.6.1 GeneXpert Test

This is a recently developed rapid TB test (~2 hours), which detects *M. tuberculosis* DNA from a sputum sample (Walzl *et al*., 2015). GeneXpert is a cartridge-based, automated and rapid molecular diagnostic technique that performs sample processing and hemi-nested real-time polymerase chain reaction (PCR) analysis in a single, hands-free step. It is also used to determine genetic mutations in patients that have developed resistance to the antibiotic, rifampicin (Tang *et al*., 2017). Owing to the fact that, it can detect the DNA mutations that confers the *M. tuberculosis* resistance to the antibiotics, it is ideal for the rapid diagnosis of MDR-TB with a high sensitivity and specificity. The overall sensitivity, specificity, positive predictive value (PPV) and negative predictive value (NPV) values reported by Pandey and colleagues were 98.6 %, 100 %, 100 % and 93.8 % (Pandey *et al*., 2017).

When this test was launched in 2008, South Africa and India were among the countries chosen to perform clinical validation (Boehme and Nabeta, 2010). Despite bringing new hope for countries with high risk of TB, this test is very costly.

http://etd.uwc.ac.za/

The unit cost of the test was estimated to be $9.98 (Pantoja, *et al.,* 2015). Also, the total capital cost (including instruments, additional space, security, and training) between 2011 to 2012 and 2016 to 2017, was estimated to be $20 million (149 million ZAR). These also require an additional annual budget of 53 to 57% or $48 to $70 million per year (Stevens, 2012). In addition, the GeneXpert test is also not reliable for individuals that are co-infected with HIV, and cannot differentiate between latent and active TB (Davis *et al*., 2013). They require highly trained personnel and a level 3 biosafety laboratory facilities (Pandey *et al*., 2017). Despite all these challenges, this test is currently the best performing TB diagnostic test and is used as the gold standard for the detection of antibiotic resistant TB. Compared to the conventional drug susceptibility tests, the GeneXpert test has a rapid turn-around time and is more accurate (Pandey *et al*., 2017).

UNIVERSITY of the
WESTERN CAPE

1.7.6.2 Line Probe Assays

This test incorporates both the PCR and reverse hybridisation techniques to rapidly detect *M. tuberculosis* and the genetic mutations associated with antibiotic resistance. Just like the GeneXpert test, these tests provide rapid results but require biosafety level 3 precautions, and highly trained personnel. In addition, chances of contamination are also high because they employ open-tube formats, which expose the samples to the external environment. Ninan and colleagues demonstrated this when they detected *M. tuberculosis* DNA from dead bacteria yielding false positive results (Ninan *et al*., 2016).

http://etd.uwc.ac.za/

These assays are also expensive to handle and to maintain. The assay costs $23.46 per sample. This is influenced by cost of consumables (60-80%), high labor costs ($3.46 per test) and overhead costs ($4.28 per test) due to the time involved and extensive laboratory facilities needed for test performance (Shah *et al.*, 2013).

1.7.7 Serological tests for TB

Serodiagnostic tests are used to diagnose TB by detecting host antibodies against *M. tuberculosis* in the blood samples of infected hosts. These tests make use of Lateral Flow Immune Assays (LFIAs) to diagnose the infectious disease (Broger *et al*., 2017). However, antibody-based tests have low sensitivity and specificity resulting in false negative and false positive results. Patients can test positive in response to other organisms not necessarily *M. tuberculosis.* Nevertheless, these tests are cost effective compared to the above mentioned tests such as GeneXpert and Line Probe Assays.

UNIVERSITY of the
WESTERN CAPE

More than a million commercial serological tests were carried out in India every year, where each test cost up to $30 per patient (WHO, 2011). The cost of serological tests in India is conservatively estimated at $15 million per year (Steingart, *et al.*, 2012). However, such countries have no published evidence to support their claims of accuracy and it was estimated that serological testing would result in 121,000 false-positive diagnoses, compared to the other TB tests endorsed by WHO. Research also suggested that for each additional smear-negative TB case found by serology, more than six additional false-positive cases would be inappropriately diagnosed (WHO, 2011).

http://etd.uwc.ac.za/

Therefore, despite the cost effectiveness of these tests, however, the WHO has cautioned against the use of them to diagnose active TB (Broger et al., 2017; WHO, 2011).

1.8 Putative TB serum biomarkers

Biomarkers are signature molecules or molecular indicators within body fluids and tissues that can be used to detect the presence of a particular biological condition or disease (Strimbu and Tavel, 2010). Biomarker discovery is the first step towards the development of rapid disease diagnostic systems.

Recent efforts in the field of TB diagnostics have revealed the urgent need for biomarker-based assays that will enable more efficient, affordable, and accessible diagnostic tools. Technologies such as DNA microarrays and proteomics have been used for biomarker discovery. However, despite the fact that huge volumes of data have been generated, less than 100 biomarkers have been validated for TB diagnosis by 2011 (Poste, 2011). Several biomarkers that were identified through proteomics have been validated clinically. Some of these biomarkers have already been used in the TST and IGRA tests.

UNIVERSITY of the
WESTERN CAPE

Proteomics technologies has demonstrated an improved efficiency for the identification of biomarkers that are present at very low concentrations in blood (Lee *et al.*, 2015). Blood has been used for decades as the preferred biological fluid for the detection of disease conditions. It is a rich source of biomarkers that can be used to provide insights into pathological and physiological processes that are linked to disease states (Marko-Varga *et al*., 2005).

http://etd.uwc.ac.za/

For this reason, the identification of biomarkers that can be used to detect TB at a very early stage (during latent infection) and during active TB will be of utmost importance, this would help prevent individuals from transmitting the deadly pathogen. This will in turn also hinder individuals from developing active TB and subsequently will foster the commencement of treatment programs, as recommended by WHO (Falzon *et al.,* 2016). Hence research into the serum proteome has a good prospect of providing biomarkers associated with the pathophysiology of TB (Cho *et* a*l*., 2006).

The ease of accessibility of serum samples from patients makes it attractive to identify potential biomarkers that appear in the blood circulation after *M. tuberculosis* infection. The ease of identification of the potential biomarkers will in turn allow the development of less invasive diagnostic tests (Phillips *et* a*l*., 2010; Ray *et* a*l*., 2011; Wallis *et al*., 2010). Several biomarkers for TB which includes Insulin-like growth factor binding protein 6 (IGFBP6), Apolipoprotein C (ApoC), C-reactive protein (CRP), Retinol-binding factor protein 4 (RBP4), Interferon-stimulated gene 15 (ISG15), Calcium-binding protein (S100A9), Rv1475c, Rv0578c PE-PGRS, Granzyme A (GrA) and Transgelin-2 (TAGLN2) have been discovered employing proteomics approaches (Mahmoudi *et al.,* 2016; Young *et al.,* 2014; Achkar *et al.,* 2015).

UNIVERSITY of the
WESTERN CAPE

1.8.1 Insulin-like growth factor binding protein 6 (IGFBP6)

IGFBP6 is an immune-stimulated protein released when the immune system detects the presence of bacterial infection (Achkar *et al*., 2015). IGFP6 is derived from the human bone marrow-derived mesenchymal stem cells (hMSCs).

http://etd.uwc.ac.za/

Little is known about its role during *M. tuberculosis* infection, but had been shown to be up-regulated on the serum of patients with active TB (Le Bouc *et al*., 1997).

Patients who have respiratory diseases other than TB do not overexpress this protein, making it specific for *M. tuberculosis* infection in patients with active TB (Le Bouc *et al*., 1997).

1.8.2 Interferon-stimulated gene 15 (ISG15)

ISG15, also known as interferon-induced protein ifi-15k (IFI15), Immunodeficiency 38 (IMD38) or human C reactive protein (CRP), is an interferon-induced protein that is released in a homeostatic body state to foster communication between cells (Gagoski *et al.*, 2016). When the host is invaded by *M. tuberculosis*, the infected macrophages induce an increase in the expression of the interferon-inducible proteins including ISG15 to enhance the release of the pro-inflammatory cytokines (Hare *et al*., 2015). This has been demonstrated using both *in vitro* and *in vivo* studies (Walters *et al*., 2013). Coincidentally, pro-inflammatory cytokines such as the IFN-γ have been used in IGRA tests (described in Section 1.7.3). This therefore suggests that ISG15 can be a potential biomarker for *M. tuberculosis* infection.

UNIVERSITY of the
WESTERN CAPE

ISG15 is induced when the immune system detects the presence of bacteria. ISG15 is released by extracellular vesicles that are shed into the extracellular matrix due to the presence of the bacteria (Al-Nedawi *et al*., 2008; Walters *et al*., 2013).

http://etd.uwc.ac.za/

It was also shown that ISG15 expression, through the type I IFN signalling pathway (innate immunity), increases abundantly in *M. tuberculosis*-infected macrophages (Hare *et al*., 2015; Walters *et al.*, 2013).

1.8.3 Calcium binding protein (S100A9)

S100A9 is a calcium-binding protein which play a role when the bacteria spread to the extra-pulmonary regions (Foell *et al.,* 2007). S100A9 induces the activation and aggregation of the neutrophils promoting accumulation of pro-inflammatory chemokines and cytokines in the affected area.

This was demonstrated in a mouse model of TB where the affected lung area was rich in leukocytes (Gopal *et al*., 2013). S100A9 is also a member of the SOD that plays a vital role in the protection against TB. It facilitates a balance between the ROS released in the presence of the pathogen and the antioxidants available within the affected region (Wang *et al*., 2013). In another study, S100A9 expression levels were compared amongst PTB patients, patients with other pulmonary-related diseases such as pneumonia and lung cancer, and healthy volunteers (Rodríguez-Piñeiro *et al*., 2010). The study found that S100A9 serum levels were significantly higher in the PTB group than the other two groups suggesting that this protein may be a good biomarker to distinguish patients with TB from those that have other respiratory diseases (Rodríguez-Piñeiro *et al.*, 2010).

UNIVERSITY of the
WESTERN CAPE

1.8.4 Retinol-binding protein 4 (RBP4)

RBP4 is an adipocyte secreted serum protein and a molecular marker for both diabetes and TB.

http://etd.uwc.ac.za/

In obese and insulin resistance patients, RBP4 levels are increased in the blood circulation when compared to control individuals (Comucci *et al*., 2014). Increased levels of RBP4 were also found in patients with active TB infection.

However, the expression level of the RBP4 reduces when active TB patients have chronic energy deficiency (Taslim *et al*., 2017). These findings contribute to the novelty of RBP4 as a prognostic biomarker for TB.

1.8.5 Granzyme A (GrA)

GrA is a tryptase (serine proteinase) that is up-regulated in patients with active TB infection (Lieberman, 2010). It is released by the natural killer (NK) cells and the cytotoxic granules of the T *lymphocytes* (CTLs) (Lieberman, 2003; Guggino *et al*., 2015). GrA induces death of the cells infected with *M. tuberculosis* bacteria by activating an apoptosis-like death (Guggino *et al*., 2015). GrA induce cell death in a caspase-independent programmed cell death and use unique substrates and mediators. The caspase-dependent death is characterized by loss of cell membrane integrity, single-stranded DNA damage and mitochondrial dysfunction (Zhu *et al*., 2009). GrA, *in vitro* cleave other proteins such as the nucleolin, IL 1β, fibronectin, type IV collagen, thrombin receptor, and pro-urokinase-type plasminogen activator. Recent research reported that GrA can be used to discriminate latent TB from the active TB (Guggino *et al*., 2015; Mahmoudi *et al*., 2016).

UNIVERSITY of the
WESTERN CAPE

1.8.6 Transgelin-2 (TAGLN2)

TAGLN2 was recently identified as a potential biomarker for both the latent and active TB infection.

http://etd.uwc.ac.za/

TAGLN2 belongs to the family Transgelin (TAGLN) proteins, which are actin-binding proteins of the calponin family, and are recognized for their rapid actin-gelling properties (Assinder *et al.*, 2009). The transgelin family is made up of three members named TAGLN1, 2 and 3. TAGLN1 is localized at the site of its expression in the smooth muscle cells, while TAGLN2 is highly expressed in TB-infected and individuals co-infected with HIV (Stanier *et al*., 1998; Achkar *et al*., 2015).

It is also expressed in several cancer cells such as prostate, breast, colon and lung cancers (Stanier *et al.,* 1998). TAGLN3 on the other hand, is highly expressed in the brain cells. TAGLN2 is highly expressed in TB-infected cells. It has five splice variants, with the fifth variant unable to translate to any protein. The rest of the variants are translated into proteins is not yet fully understood (Stanier *et al.,* 1998). The role of TAGLN2 in several infectious diseases is still unknown (Achkar *et al.,* 2015).

UNIVERSITY of the
WESTERN CAPE

TAGLN2 was also reported to interact with the immunological synapse of the host in the presence of an attack either by a bacteria or any pathogen, and enhances T cell response by controlling actin stability at the immunological synapse (Na *et al*., 2016). This suggests its critical role and involvement in the immune response.

In fact, in patients with active TB, TAGLN2 has been shown to be over-expressed and can thus be used to accurately distinguish between active TB, latent TB and other respiratory diseases in both HIV^+ and HIV^- individuals (Achkar *et al*., 2015).

http://etd.uwc.ac.za/

TAGLN2 was also detected in almost all the TB patients across the globe including Asia, Africa, North and South America (Achkar *et al*., 2015). Therefore, TAGLN2 can potentially be used to detect TB not only at the early stages, but also TB individuals co-infected with HIV (Achkar *et al*., 2015).

Most of the selected potential TB biomarkers listed above have roles that are relevant to the host's response to TB, and can be considered for development of a rapid TB-diagnostic test.

Thus detection of such serum biomarkers can be recognised as a practical approach not only for diagnosis, but for monitoring treatment efficacy and prognostic evaluation of patients with TB (Heo *et al*., 2009). These kinds of diagnostic tools would be a huge boost for developing countries that cannot afford expensive diagnostic laboratories.

UNIVERSITY of the
WESTERN CAPE

1.9 Aptamers

Once suitable biomarker proteins have been identified, the next step in the development of rapid disease diagnostic systems is the identification of molecules that can bind to these proteins with high specificity and be used in the detection of these biomarker proteins. Antibodies have traditionally been used for this purpose, but aptamers are emerging as alternative and more superior molecules for this application.

The term aptamer comes from two words, "*aptus*" which is Latin for "to fit", and "*meros*" which is Greek for "part" or "region" (Ellington and Szostak, 1990; Robertson and Joyce, 1990; Tuerk and Gold, 1990).

http://etd.uwc.ac.za/

Aptamers are synthetic single-stranded oligonucleotides (DNA, RNA) or peptide molecules that bind to a specific target (Darmostuk *et al*., 2014). They are shorter than 100 nucleotides (nt) in length and have an increased binding affinity and selectivity for specific targets, ranging from proteins to small molecules (Song *et al.*, 2008). Their typical structural motifs include stems, internal loops, purine-rich bulges, hairpin structures, pseudo-knots, kissing complexes, and G-quadruplet structures (Chen and Yang, 2015).

1.9.1 Comparison between aptamers and antibodies

It was demonstrated that aptamers have an increased selectivity, specificity and affinity towards a variety of targets (from small drugs to whole cells) (Ozer *et al.*, 2014). In some cases aptamers have been able to discriminate between targets with only subtle structural differences (Wilson *et al.*, 2001).

Some of the features that make aptamers more appealing than antibodies for application in diagnostics are summarized in Table 1.3. They are considered to be superior to most targeting molecules, which include antibodies and targeting peptides. Aptamers can fold into three-dimensional structures that have a much higher affinity for binding its target compared to antibodies and other targeting ligands. The large-scale production of aptamers is more cost effective when compared to antibodies. Aptamers are tolerant to high temperatures, which imply that diagnostic devices using aptamers will have a longer shelf life.

Most importantly, they can be easily modified for conjugation and biomedical application.

UNIVERSITY of the
WESTERN CAPE

http://etd.uwc.ac.za/

Table 1. 3: Comparison of aptamers with antibodies (adapted from Chen and Yang, 2015).

Feature	Antibody	Aptamer
Oriented immobilization	Difficult through protein A/G	Easy through various modifications
Selection	Limited to animal immunisation	*In vitro* and *in vitro* selection under a variety of conditions
Application target	Proteins or haptens. Difficult for non-immunogenic or toxic targets	Any targets from ions to whole cells, including non-immunogenic or toxic target
Production	Time-consuming and costly	Efficient with chemical synthesis at low costs
Detection range	Good	Better
Modification	Difficult and expensive to modify	Cheap and easy to modified with other active groups in a large scale.
Reusability	Poor reusability due to irreversible conformational changes	Good reusability through a reversible conformational switch
Shelf life	Short shelf life and require a continuous cold storage	Long shelf life and does not require special storage conditions.
Stability	Sensitive to pH and temperature	Tolerant of pH and temperature

1.10 Selection of aptamers using SELEX technology

Unlike antibodies, aptamers can be synthesized *in vitro* by System Enrichment of Ligands by EXponential enrichment (SELEX). SELEX is one of the techniques used for synthesis and selection of aptamers used in diagnostics and therapeutics (Sun *et al.,* 2014). SELEX is used for isolation and production of single stranded oligonucleotides (aptamers) that binds to specific targets with high affinity. SELEX have significantly improved over the years, with this technique producing aptamers with high specificity and selectivity. The aptamer structures can be modified pre- or post-SELEX process to prevent degradation by nucleases and to increase binding efficiency (Shigdar *et* a*l*., 2013).

The SELEX process is a series of steps that are repeated several times (8-25 rounds) until the aptamers are highly enriched for the target molecule.

http://etd.uwc.ac.za/

These steps include incubation of the random DNA library with the target (such as a biomarker protein), separation, amplification, single-strand generation, elution and purification as shown in Figure 1.2 (Chen *et al.*, 2016; Tsao *et al.*, 2017).

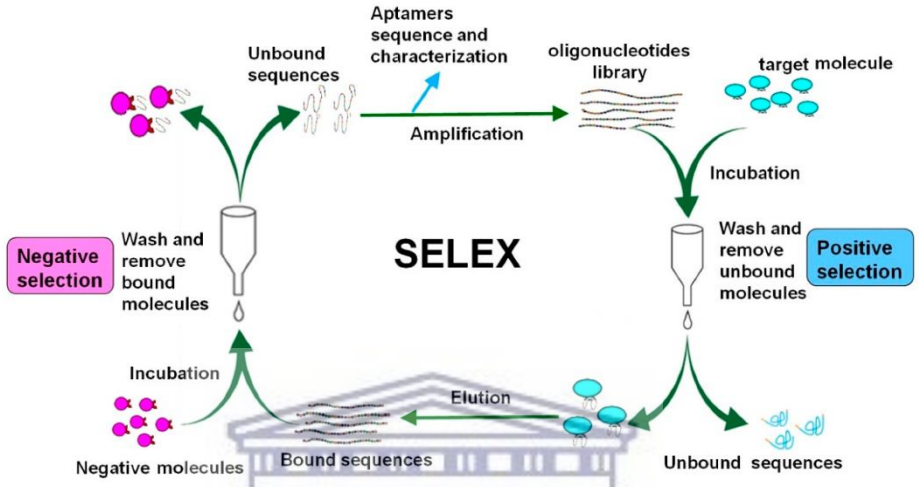

Figure 1. 2: SELEX overview. Summary of the major steps involved in aptamer selection through SELEX, these include incubation of the target molecule with the random DNA library and isolation of target specific aptamers. Positive and negative selection steps are included to increase aptamers specificity (Chen *et al.*, 2016).

The selection of aptamers requires a serial incubation of the DNA libraries with its target to allow binding between the two molecules. The desired DNA sequences are obtained during SELEX by partitioning and amplification. PCR amplification of the template is a critical tool to generate efficient dsDNA (Grote *et al.*, 2002).

Since the introduction of SELEX for aptamer selection in the 1990's, (Ellington and Szostak, 1990; Robertson and Joyce, 1990; Tuerk and Gold, 1990), improvements have been made to either modify the existing method or to develop other strategies in-line with SELEX to rapidly and efficiently produce aptamers (Darmostuk *et al.*, 2014; Lin *et al.*, 2014; Yüce *et al.*, 2015).

UNIVERSITY of the WESTERN CAPE

http://etd.uwc.ac.za/

Several strategies are available that can efficiently isolate aptamers, these methods include cell-based SELEX, nitrocellulose (NC) membrane filtration-based SELEX, affinity-based chromatography, capillary electrophoresis-based SELEX, microfluidic-based SELEX, magnetic bead-based SELEX and tailored-SELEX (Lin *et al*., 2014; Vater *et al*., 2003).

1.10.1 Nitrocellulose (NC) membrane filtration-based SELEX

This strategy is based on the use of NC membrane for aptamer immobilisation. The target molecules are then incubated with the immobilized aptamers for a certain period of time before being eluted. The aptamers can be selected easily using this strategy due to their smaller sizes (Song *et al*., 2012). This strategy however generates false positive aptamers and with low sensitivity and specificity for the target molecule.

This is because the generated aptamers could bind to the membrane with higher affinity than the proteins, resulting into a low sensitivity (Ozer *et al*., 2014).

UNIVERSITY of the
WESTERN CAPE

1.10.2 Affinity-based chromatography SELEX

Aptamers against smaller molecules as well as proteins can be selected using this method. This method employs an affinity column, which has the target molecule immobilised on beads. The random nucleic acid library is incubated with the target molecules after which they are selected randomly by PCR.

However, a significant drawback of this method is that it only targets molecules modified with affinity tags or functional groups (Wang *et al*., 2011; Song *et al.*, 2012).

http://etd.uwc.ac.za/

This method is also less sensitive if the target lacks an affinity tag or a functional group is needed for capturing the beads. Also, enrichment of the aptamers towards the target is not guaranteed (Song *et al*., 2012).

1.10.3 Tailored SELEX

The tailored SELEX involves incubation of a randomised library (that lacks primer-binding regions) with the target molecule. Special adaptors are used to replace the primer binding regions in each SELEX round (Vater *et al*., 2003). This process produces aptamers that lack the primer regions that might have enhanced the binding to the target molecule. The method is time-consuming as it requires cloning of the pool (selected oligonucleotide) to the primer binding sequences after each selection step before the final round (Amano *et al.*, 2017; Jarosch *et al.*, 2006).

1.10.4 Microfluidic-based SELEX

UNIVERSITY of the
WESTERN CAPE

The use of microfluidics in SELEX has reduced the time it takes to generate aptamers because SELEX is done and processed on a chip, and it can enhance selection efficiency on a small scale (Song *et al*., 2012). For example, the DNA aptamer specific for Neurotoxin type B was obtained after a single round of selection using the continuous flow magnetic activated chip based separation device (Song *et al*., 2012). However, the use of microfluidics is very costly, requires specialized instruments, and not readily available.

http://etd.uwc.ac.za/

1.10.5 Neutral SELEX

This method differs from the classical SELEX due to the exclusion of the selection step. The DNA/target complexes are PCR amplified at each and every step, and the sequences are selected afterwards (Amano *et al*., 2017). In this method, no sequences will be enriched for, as no target will be used during the selection process. Also, the sequences produced are less stable and have a high rate of mutation because the amplified products are used as the template for the next round (Chen and Yang, 2015).

1.10.6 Capillary electrophoresis-based SELEX

A mobility shift can be used to select aptamers from the mixture containing a target molecule and the random DNA library. This method uses a capillary electrophoresis system, allowing the aptamers to interact with targets without steric hindrance. Selection of aptamers can be achieved within a very few rounds (2-4 rounds) compared to other methods (Song *et al*., 2012).

UNIVERSITY of the
WESTERN CAPE

Unfortunately, enrichment of the aptamers towards the target is not guaranteed when using the capillary electrophoresis strategy (Song *et al*., 2012).

1.10.7 Cell SELEX

This process aims at searching for aptamers against a whole cell compared to the other SELEX methods whose primary target is a single small molecule. In this strategy, the targets can be combination of extracellular or transmembrane proteins or unique structures of the cell (Reinemann and Strehlitz, 2014).

http://etd.uwc.ac.za/

This method however can result in false positivity due to the target location, and the specificity of the aptamers can be affected by the binding pockets of the target (Meyer *et al*., 2013).

1.10.8 Magnetic bead-based SELEX

This method starts with the incubation of a randomised DNA library with the target molecule. The target molecule has a tag on one of its end for binding to the tagged beads. An external magnet will then be used to attract the protein/DNA complexes captured on the beads to separate the bound from the unbound nucleic acids. This method can be employed to partition aptamers that have high affinity and selectivity towards target proteins (Chen *et al*., 2015; Gong *et al*., 2013; Lai and Hong, 2014; Stoltenburg *et al*., 2015; Xi *et al.*, 2015). This strategy was selected for this study and it is described in detail in Section 2.2.16.1.

1.11 Applications of Aptamers in the diagnosis of TB and other infectious organisms

UNIVERSITY of the
WESTERN CAPE

Aptamer-based LFIAs have been developed the past years to target various agents such as thrombin, cocaine, adenosine (Liu and Lu, 2006a, 2006b; Niu *et al*., 2014; Wang *et al.*, 2007; Wei *et al*., 2007) and (1→3)-β-d-glucans (Low *et al*., 2009). Attempts were made to select aptamers against the whole *M. tuberculosis* bacterium (Chen *et al*., 2007) and proteins related to TB infections such as the MPT64 (Qin *et al*., 2009) and polyphosphate kinase 2 (PPK2) (Shum *et al*., 2011). However, these strategies were not effective as the aptamers lacked sensitivity against these proteins.

http://etd.uwc.ac.za/

Other studies have also selected aptamers that can detect active TB from the sputum, aptamers were synthesized against the immuno-dominant antigens like the CFP-10, ESAT-6 and CFP-10-ESAT-6 heterodimer (Rotherham *et al.*, 2012). Nevertheless, these aptamers have not been applied in any practical diagnostic tool due to lack of specificity and sensitivity. These proteins (CFP-10 and ESAT-6) were used as targets by Mozioglu and colleagues (2016), the H37Ra (a *M. tuberculosis* protein) were used as targets in two different SELEX selection protocols (Mozioglu *et al*., 2016). However, the dissociation constants (K_d) for the aptamers identified in that study was less than the one obtained by Chen and co-workers when the team studied aptamers that recognize whole *M. tuberculosis* bacterium. The H37Rv aptamers were shown inhibit bacterial invasion of macrophages and decrease bacterial growth in the lungs. This study also demonstrated that aptamers can be used for diagnosis of TB and in development of anti-TB agents (Chen *et al*., 2012).

UNIVERSITY of the
WESTERN CAPE

1.12 Lateral flow assays for point of care rapid diagnosis

Point of care (POC) diagnostics is defined as medical diagnostic testing at or near the time and place of patient care. POCs are mostly used as a screening rather than a diagnostic tool. These tests are cost effective and do not require expensive laboratory equipment or highly trained personnel to perform the test. The test can be carried out at a primary healthcare facility and the test results are available immediately. This means that when a patient visit a primary healthcare facility, they can be tested and the results are available immediately. The patient can then be referred for additional testing or treatment immediately.

http://etd.uwc.ac.za/

The results of these tests can normally be interpreted very easily, which means that POCs can even be used for self-testing. For these reasons POCs are ideal for low resource settings. Lateral Flow Assays (LFAs) are good examples of POCs.

LFAs can be categorized into either lateral flow immunoassays (LFIAs) or nucleic acid lateral flow assay (NALFA) depending on their recognition elements used in the assay as indicated in Figure 1.3. The LFIAs make use of antibodies (such as the IgG) as recognition elements while the NALFAs use probes for the detection of amplicons, which are formed during PCR (Haridas and Thiruvengadam, 2014). The LFAs make use of membranes assembled in strips with antibodies mounted on them for the detection of antigens. The test results are obtained within few minutes, generally 5-30 min (Koczula and Gallotta, 2016). These tests are gaining interest as more companies are inspired to develop lateral flow devices that will provide rapid diagnosis for infectious diseases such TB (Koczula and Gallotta, 2016).

UNIVERSITY of the
WESTERN CAPE

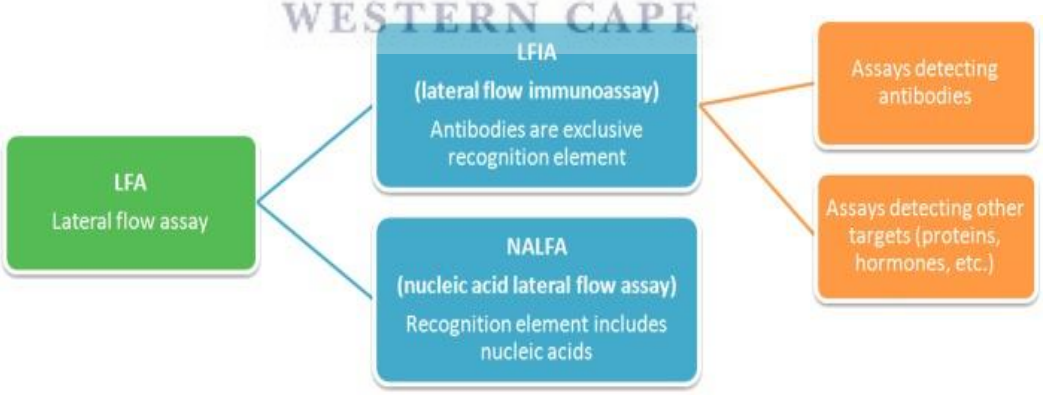

Figure 1. 3: Different types of LFAs employed in the diagnosis of molecules in complex biological samples (Koczula and Gallotta, 2016).

More than 100 companies worldwide have developed screening assays over the past thirty years.

http://etd.uwc.ac.za/

Their annual growth rate was compounded at 7 %, with the global market of this technology estimated to reach $4675 million by 2020 (Koczula and Gallotta, 2016).

The antibody-based platform has been widely used for the direct detection of antigens present in patients' samples. The stability of antibodies is a major challenge in the development of LFAs (Chen and Yang, 2015). The current TB diagnostic assays have limited sensitivity (43 – 71 %) and show inconsistency (84 – 100 %) (Fu and Xie, 2011; Steingart *et al*., 2011). The introduction of a rapid, cost-effective, and sensitive POC diagnostic device that can detect the TB at an early stage of infection, can differentiate between latent and active TB, and can differentiate between TB and other pulmonary diseases will significantly improve treatment outcomes for many TB patients. The application of aptamers that can recognize serum biomarkers can lead to the development of such POC diagnostic devices.

UNIVERSITY of the
WESTERN CAPE

1.13 Aims and objectives of the study

1.13.1 Aims of the study:

1. To identify and select potential serum TB biomarkers from published studies (proteomics studies).

2. To generate aptamers against the selected biomarkers using magnetic-bead based SELEX.

http://etd.uwc.ac.za/

1.13.2 Objectives of the study:

1. Identify potential serum biomarkers for TB.

2. Clone, express and purify TB biomarker protein through recombinant DNA technology.

3. Use magnetic-bead based SELEX for selection of aptamers against the biomarker proteins.

4. Study binding efficiency of aptamers to the target proteins.

http://etd.uwc.ac.za/

CHAPTER 2
MATERIALS AND METHODS

2.1 Materials and buffers

Table 2. 1: Reagents and their suppliers

Reagent	Supplier
Absolute Ethanol	Kimix Chemicals (South Africa, SA)
40 % Acrylamide Bis Solution (37:5:1)	Bio–Rad (United States of America, USA)
Certified low range ultra-agarose Bovine serum albumin (BSA) Bromophenol blue Glycine Phosphate buffered saline (PBS) pH 7.4 ready mix Sodium Acetate Sodium Azide N,N,N',N'-tetramethylethane-1,2-diamine (TEMED)	Sigma Aldrich Co. (USA)
Ammonium persulfate Boric acid Ethylene-diamine-tetra-acetic acid (EDTA) Glycerol Magnesium Chloride Potassium Chloride Sodium Hydroxide Tris(hydroxymethyl)aminomethane	Merck (Pty) Ltd (SA)
Deoxynucleotide mix Ethidium bromide	Promega (USA)
DNA loading dye	Inqaba Biotechnical industries (Pty) Ltd (Inqaba® biotech, SA)
DNA oligonucleotides Ethanolamine-HCL	Integrated DNA Technologies (IDT, USA)
1-Ethyl-3-(3-dimethylaminopropyl)-carbodiimide (EDC) N-hydroxysuccinimide (NHS)	GE Healthcare (Pty) Ltd (SA)
Gel Red Stain HC 1000M SPR chips	Biotium Inc (SA)
4-2-hydroxyethyl)-1-piperazineethanesulfonic acid (HEPES) buffered solution with sodium chloride	Xantech bioanalytics (Germany)
Human Serum Albumin (HSA) Transcriptor First Strand cDNA Synthesis Kit	Roche Diagnostics (SA)
Kapa Taq ready mix	Kapabiosystems (Pty) Ltd (SA)
Magnesium Acetate Potassium Acetate T7 gene 6 Exonuclease with Lambda Exonuclease	New England Biolabs (United Kingdom, UK)
Nickel-NTA coated magnetic beads SiMAG-IDA/Nickel beads	Chemicell GmbH (Germany)
O'GeneRuler® 100bp Plus DNA ladder	Life Technologies (Pty) Ltd (SA)
O'GeneRuler® 1kbp Plus DNA ladder	Fermentas Life Sciences (Canada)
Velocity taq polymerase kit	Bioline (UK)

UNIVERSITY of the
WESTERN CAPE

http://etd.uwc.ac.za/

Table 2. 2: Equipment and their suppliers

Equipment	Supplier
PowerPac™ Basic Power Supply	Bio–Rad (USA)
Eppendorf Thermomixer comfort	Merck (Pty) Ltd (SA)
Dynamag®-2 Magnetic Particle concentrator Shaker Eppendorf 5414 Water-Jacketed CO_2 Incubators	Thermo Scientific (SA)
Eppendorf® Microcentrifuge 5415	DJB Labcare (UK)
GeneAmp® PCR System 2700	Applied Biosciences (SA)
ProteOn XPR36	Rhodes University (SA)
Qubit® 2.0 Fluorometer	Invitrogen by Life technologies (USA)
Stuart Block Heater	Stuart Scientific (UK)
UVP BioSpectrum® Imaging System	The Scientific group (Pty) Ltd (SA)

Table 2. 3: Composition of buffers used in the study

Buffers	Composition
SELEX buffer	PBS with 1.5 mM Mg^{2+} pH 7.4.
EMSA loading buffer	60 mM Pottasium chloride, 10mM Tris (pH 7.6), 5 % Glycerol, 0.01 % Xylene cyanol, 0.01 % Bromophenol blue.
TBE buffer	0.089 M Tris, 0.089 M Boric acid, 0.002 M EDTA
TE buffer	10 mM Tris (pH 8.0), 1 mM EDTA.
Sample buffer	0.5 M Tris-HCl pH 6.8, glycerol (100 %), 0.2 mL of β mercaptoethanol, 0.01 g of bromophenol Blue and 0.2 g of SDS.
1 X SDS Running buffer	3.03g Tris (250 mM), 14.4g Glycine (1.92M) and 10g SDS (1 %).
Coomasie stain solution	50 % ethanol, 10 % acetic acid and 0.25 % brilliant blue R-250
De-stain solution	16.5 % ethanol and 5 % acetic acid
Lysis buffer	50 mM potassium phosphate, pH 7.8, 400 mM NaCl, 100 mM KCl, 10 % glycerol, 0.5 % Triton X-100 and 10mM imidazole.

UNIVERSITY of the
WESTERN CAPE

http://etd.uwc.ac.za/

2.2 Methodology

2.2.1 *In silico* identification and selection of serum TB biomarkers

Intensive literature mining using various search engines (such as Google scholar, PubMed, UniProtKB, SciFinder, NCBI gene bank, RefSeq, protein data bank, PDB) was performed to identify TB serum biomarkers. The potential biomarkers were selected from recent TB proteomics case studies, published between 2014 and 2017. The biomarkers were selected based on the following criteria:

i. The biomarkers must be expressed or shed in the serum samples of TB-infected patients.

ii. The biomarkers must have been identified by more than one independent study.

iii. They must be able to discriminate between the active TB and the latently infected patients.

UNIVERSITY of the
WESTERN CAPE

iv. Interest is on the proteins that have not been previously used for development of aptamer-based TB diagnostics.

v. Biomarkers must be expressed through recombinant DNA technology with ease.

vi. Biomarkers must be specific to *M. tb* strain, and be able to discriminate individuals infected with the other MTBC strains.

http://etd.uwc.ac.za/

2.2.2 RNA extraction

Total RNA was extracted from several human cancer (SKOV-3, CaOV-3, LNCaP, MCF-7) and normal (KMST-6 and MCF-12A) cell lines, the cells were shown to encode the genes of selected TB biomarkers. The cells were cultured in T-25 (25 cm^2) flasks until ≃70 % confluent. The cells were obtained from DST/Mintek NIC laboratory (Biotechnology Department, UWC).

Total RNA was extracted from the cells using the High Pure RNA Isolation Kit (Roche Diagnostics) according to manufacturer's instructions. Briefly, the cells were lysed by adding 400 µL Lysis buffer and vortexed for 15 seconds. The lysate was transferred to High Pure Filter tube, followed by addition of 90 µL DNase incubation buffer and 10 µL DNase enzyme. The tubes were centrifuged for 45 seconds. The pellets were washed first with 500 µL wash buffer I then 500 µL wash buffer II. RNA was eluted with 50 µL elution buffer. The RNA was quantified using the Qubit® 2.0 Fluorometer (Invitrogen) following the manufacturer's instructions. The RNA integrity was evaluated by electrophoresis on a 1 % agarose gel. The gel was visualised and the images were captured using the UVP BioSpectrum® Imaging System (The Scientific group (Pty) Ltd).

UNIVERSITY of the
WESTERN CAPE

2.2.3 cDNA synthesis

The cDNA was synthesised using the Transcriptor First Strand cDNA Synthesis Kit (Roche Diagnostics) in accordance with the instructions set by the manufacturer. One µg of the total RNA was added to the solution containing the Random Hexamer Primer and the volume was adjusted to 13 µL using nuclease-free water.

http://etd.uwc.ac.za/

The RNA secondary structures were denatured by heating the sample for 10 min at 65 ^{0}C. The tube containing the template-primer mix was cooled immediately on ice, followed by addition of 4 µL Transcriptor Reverse Transcriptase Reaction buffer, 0.5 µL Protector RNase Inhibitor, 2 µL Deoxynucleotide Mix and 0.5 µL Transcriptor Reverse Transcriptase. The reaction mixture was mixed gently and incubated at 50 ^{0}C for 1 hour. The enzyme was deactivated at 85 ^{0}C for 5 min. The synthesised cDNA was quantified by the Qubit® 2.0 Fluorometer and stored at -20 ^{0}C until required for downstream applications.

2.2.4 Primer design

The DNA sequences for the genes encoding the selected biomarkers were obtained from NCBI gene bank. The sequences were used to design PCR primers for the genes. The primers were designed manually and confirmed using Primer3Plus software

UNIVERSITY of the
WESTERN CAPE

(http://www.bioinformatics.nl/cgi-bin/primer3plus/primer3plus.cgi).

The primer sequences are shown in Table 2.4. The CACC sequence was incorporated into the forward primers for cloning in the Champion™ pET100 Directional TOPO® vector (TOPO^R vector).

http://etd.uwc.ac.za/

Table 2. 4: Primers designed for the TB genes

Gene Name	Primer Sequence
ISG15	F^+ 5'**CACC**ATGGGCTGGGACCTGACGGTGAAGATG'3
	R^- 5'GCTCCGCCCGCCAGGCTC'3
IGFBP6	F^+ 5'**CACC**ATGACCCCCCACAGGCTGC'3
	R^- 5'GCCGCTACTCCCAGTGGGGC
S100A9	F^+ 5'**CACC**ATGACTTGCAAAATGTCGCAGCTGGAAC'3
	R^- 5'GGGGGTGCCCTCCCCGAG'3
GrA	F+ 5'**CACC**ATGGCCAACTGTGAGCGTACCTTCATTG'3
	R^- 5'TTCATAGATCCAGTTCTGAGCACAGCTC'3
RBP4	F^+ 5'**CACC**ATGAAGTGGGTGTGGGCGCTCTTG'3
	R^- 5'CAAAAGGTTTCTTTCTGATCTGCCATCG'3
TAGLN2	F^+ 5'**CACC**ATGGCCAACAGGGGACCTGCATATG'
	R^- 5'TTAACCATTCGTGGGAGGGCAGGG'3

***Notes**: F^+- Forward primer,R^- - Reverse primer, ISG15 – Interferon-stimulated gene 15, IGFBP6 – Insulin-like growth factor binding protein 6, S100A9 – Calcium binding protein, GrA – Granzyme A, RBP4 – Retinol binding protein 4, TAGLN2 – Transgelin-2.*

UNIVERSITY of the
WESTERN CAPE

2.2.5 PCR amplification of genes encoding TB biomarkers

The genes of interest were amplified from the cDNA synthesized in Section 2.2.3 as the template. A thermostable, proofreading DNA polymerase (velocity DNA polymerase) was used to produce blunt-end PCR products compatible for cloning in the Champion™ pET100 Directional TOPO® vector. The PCR conditions were as follows:

Step 1: initial activation of the Taq polymerase at 95 ^{0}C for 3 min

Step 2: denaturation of the template at 95 ^{0}C for 30 seconds

Step 3: annealing of the dNTPs to the template at 66.9 ^{0}C

Step 4: an extension of the template at 72 ^{0}C for 30 seconds

Step 5: final elongation at 72 ^{0}C for 5 min

http://etd.uwc.ac.za/

Steps 2-4 cycles were repeated 30 times. Gradient PCR was performed for all the genes (*IGFBP6, ISG15, S100A9, GrA, RBP4* and *TAGLN2*) to determine the optimum PCR conditions.

The genes were all observed to anneal at different temperatures ranging from 55 ^{0}C to 72 ^{0}C, however 66.9 ^{0}C was chosen for all the genes.

2.2.6 Purification of PCR-products

The PCR products were cleaned and purified using the GeneJet™ Gel Extraction Kit (Fermentas) following manufacturer's instructions. All the purification steps were carried out at room temperature (25 ^{0}C), and all the centrifugations were carried out in a table-top microcentrifuge at 16 000 rpm. For every 100 µL of the PCR reaction mixture, 100 µL of binding buffer was added. The solution was thoroughly mixed and the colour of the solution was checked. A yellow colour indicated an optimal pH for DNA binding, an orange or violet colour required addition of 10 µL 3M sodium acetate solution (pH 5.2). For genes <500 bp such as ISG15, S100A9 and GrA, 100 % isopropanol was also added at a ratio of 1:2 (i.e, 100 µL of isopropanol, 100 µL of PCR mixture, and 100 µL of binding buffer) and the solution was mixed thoroughly. The solution was then transferred to the GeneJET purification column and centrifuged for 45 seconds. The flow-through was discarded; the column was washed with 700 µL wash buffer and centrifuged for 45 seconds. The flow-through was discarded, the purification column was centrifuged for an additional 1 min to remove residual wash buffer. The column was transferred into a clean 1.5 mL microcentrifuge tube, 500 µL of elution buffer was added to the column and the tube was centrifuged for 1 min.

UNIVERSITY of the
WESTERN CAPE

http://etd.uwc.ac.za/

The purified PCR products were quantified using the Qubit™ fluorometer and stored at -20 ^{0}C until further analysis.

2.2.7 Quantification of the DNA samples using the Qubit™ fluorometer

DNA was quantified using the Qubit® 2.0 Fluorometer following manufacturer's instructions. A working solution was prepared as follows; (1 µL x n) of Quanti-iT Reagent was combined with (199 µL x n) Quant-iT buffer; where n is the number of samples to be quantified. 198 µL of the working solution was aliquoted into 0.5 mL tubes and 2 µL of the sample of interest (PCR products) was added. The mixture was vortexed carefully and incubated for 2 min at 25 ^{0}C. The concentration of the samples was read using Qubit™ fluorometer.

2.2.8 Cloning of genes into TOPO vector

The TOPO^R Cloning Reaction was performed as described by the manufacturer, the reaction was prepared as summarised in Table 2.5. For optimal results 0.5:1 to 2:1 molar ratio of PCR product to TOPO^R vector was used, the concentration of the insert was calculated using the formula below:

$$\frac{\text{ng of vector x kb size of insert}}{\text{kb size of vector}} \text{x molar ratio of } \frac{\text{insert}}{\text{vector}} = \text{ng of insert}$$

UNIVERSITY of the
WESTERN CAPE

http://etd.uwc.ac.za/

Table 2. 5: Reaction mixture for cloning of selected genes in the TOPO^R vector

Reagent	Volume (µL)	Concentration (M)
PCR product	1	1
NaCl and $MgCl_2$	1	1.2 and 0.06
Sterile water	3	-
TOPO^R vector (20 ng)	1	1
Total volume	6	

The reagents were mixed gently and incubated at 25 ^{0}C for 5 min and then placed on ice. The ligation mixture was used to transform One Shot^R TOP10 chemically competent *Escherichia (E.) coli* cells. Briefly, 3 µL of the TOPO Cloning reaction was added into a vial of One Shot^R TOP10 *E. coli* cells and mixed gently. The mixture was incubated on ice for 30 min. The cells were then heat-shocked in a 42 °C water bath for 30 seconds and the tube was immediately transferred to ice. Super optimal broth (SOC) medium (250 µL) was added to the tube and incubated at 37 °C for 3 hours with shaking (300 rpm). The bacterial culture was spread on a pre-warmed selective agar plate (containing 100 µg/mL ampicillin) and incubated overnight at 37 °C.

UNIVERSITY of the
WESTERN CAPE

2.2.9 Colony PCR screening

Following transformations, the positive clones were screened for the presence of inserts using the gene-specific primers and vector specific primers. The reaction mixture was prepared as summarised in the Table 2.6.

http://etd.uwc.ac.za/

Table 2. 6: Reaction mixture for colony PCR screening

Reagents	Volume (µL)	Final Concentration
Template DNA	Scratch of colonies	-
10 µM Gene specific primers	-	0.1 µM
2x Kapa Taq Extra HotStart Ready MasterMix	-	1 X
50 mM $MgCl_2$	-	3 mM
25 mg/mL BSA	-	0.5 mg/mL
Final volume adjusted with nuclease-free water	10 µL	

The inserts were amplified using the conditions described in Section 2.2.5. The colony PCR products were electrophoresed on a 1.2 % ultra-low agarose gel. The gel was viewed and imaged on a UVP BioSpectrum® Imaging System.

2.2.10 DNA plasmid extraction

UNIVERSITY of the
WESTERN CAPE

Positive colonies were inoculated in 10 mL ampicillin positive (Amp^+) Lysogeny Broth (LB) and grown overnight at 37 ^{0}C while shaking. Glycerol stocks of the bacterial cultures were prepared and stored at -80 ^{0}C. The rest of the bacterial cultures were used to isolate plasmid DNA using the Wizard Plus SV minipreps DNA Purification Systems (Promega) following manufacturer's instructions. The cultures were centrifuged at a maximum speed in a microcentrifuge for 5 min.

The pellets were thoroughly resuspended with 250 µL of Cell Resuspension Solution, followed by addition of same amount of Cell Lysis Solution. The solutions were mixed by inversion of the tubes.

http://etd.uwc.ac.za/

Then 10 µL of Alkaline Protease Solution was added and mixed by inversion. The samples were incubated for 10 min at 25 ^{0}C, followed by the addition of 350 µL of Neutralization Solution and mixed by inversion. The samples were centrifuged at top speed for 15 min, the cleared lysate was decanted into the spin column and the samples were centrifuged at top speed for 3 min. About 750 µL of Wash Solution was added and this was followed by centrifugation at top speed for 3 min, this step was repeated using 250 µL of the Wash Solution. The plasmid DNA samples were electrophoresed on a 1.2 % ultra-low agarose gel and the gel was analyzed on a UVP BioSpectrum® Imaging System. The DNA was stored -20 ^{0}C.

2.2.11 DNA sequence analysis

The respective glycerol stocks were streaked on amplicillin containing agar plates. The plates were subsequently incubated at 37 ^{0}C for 16 hours and sent to Inqaba® biotech for sequence analysis. The analysis was done using the universal T7 primers (sequences: Forward primer 5'-TAA TAC GAC TCA CTA TAG GG-3'; Reverse primer 5´-TAG TTA TTG CTC AGC GGT GG-3´). The resultant raw DNA sequence data was uploaded and analysed in Basic alignment tool (BLAST)

(http://www.mbio.ncsu.edu/BioEdit/bioedit.html).

2.2.12 Transformation of the BL21 Star™ (DE3) One Shot® Cells

Upon confirmation of successful cloning, the BL21 Star™ (DE3) *E. coli* strain was used to express the TB-biomarkers.

UNIVERSITY of the WESTERN CAPE
http://etd.uwc.ac.za/

Transformation of the BL21 Star™ (DE3) One Shot® Cells followed a similar protocol described in Section 2.2.8. The entire transformation reaction was streaked in a LB agar plates containing 100 μg/ mL ampicillin and 1 % glucose and grown overnight at 25 °C.

2.2.13 Pilot protein expression of the TB biomarker

Several positive colonies were cultured in 10 mL LB containing 100 μg/ mL ampicillin and 1 % glucose overnight. The cultures were diluted 1: 10 with fresh LB and grown for three hours at 25 °C with shaking at 300 rpm until the sample reached OD_{600nm} of 0.5 - 0.8. The cultures were then split into two 5 mL cultures, 1 mM IPTG was added to one of the cultures and the other sample was uninduced. The cultures were further cultured under the same conditions for ~16 hours. The following day, the culture was centrifuged at maximum speed for 5 min, the cell pellets were analysed for the expression of the proteins by sodium dodecyl sulphate polyacrylamide gel (SDS-PAGE).

UNIVERSITY of the
WESTERN CAPE

2.2.13.1 Screening of protein expression by SDS-PAGE

The samples obtained from the pilot expression (2.2.13) were resuspended in 10 mL PBS, then 80 μL of the samples were mixed in a 1:1 ratio with 2X laemmli sample buffer.

The samples were boiled for 5 min at 95^0C and pulse spun, both the pellet and the supernatant (10 μL) were resolved by 15 % SDS-PAGE. The components for making the stacking and the separating gels are shown in the Table 2.7.

http://etd.uwc.ac.za/

Table 2. 7: Reaction mixture for SDS-PAGE screening of the proteins

Reagents	12 % Separating Gel	5 % Stacking gel
0.5M Tris-Cl pH 6.8	-	750 µL
1.5M Tris-Cl, pH 8.8	2.5 mL	-
10 % SDS	0.2 mL	60 µL
Acrylamide/Bis (40 %)	3.76 mL	372 µL
10 % Ammonium persulfate (APS)	0.1 mL	30 µL
TEMED	10 µL	10 µL
Water	3.76 mL	3 mL

The gel was electrophoresed in 1 X SDS Running buffer at 90 V for 30 min then the voltage was adjusted to 150 V and continued to run for 60 – 90 min. The gel was stained with coomassie stain for 30 min and de-stained overnight. The gel was visualised and the images were captured using the UVP BioSpectrum® Imaging System and Canon CanoScan LiDE 120 electronic scanner. The remaining samples were stored at -20 °C.

2.2.13.2 Analysis of recombinant protein solubility

The pellet samples were resuspended in 500 µL Lysis buffer. The cells were subjected to freezing and thawing cycles in dry ice and at 42 °C, three times. The cells were then sonicated briefly in a three cycles at 10 second interval. The samples were centrifuged at 16 000 rpm for 5 min. The supernatant was transferred to a fresh microcentrifuge tube. An equivalent amount of both supernatant and the pellet was mixed with 2X SDS-sample buffer, the mixture was boiled for 5 min at 95 °C. The samples (10 µL supernatant and 5 µL pellet) were loaded onto a 15 % SDS-PAGE and electrophoresed. The gel was stained and destained as above and imaged with a UVP BioSpectrum® Imaging System.

UNIVERSITY of the
WESTERN CAPE

http://etd.uwc.ac.za/

2.2.14 Large-scale expression of the TB biomarkers

The protein was expressed as described in Section 2.2.13, with few adjustments. The inoculation culture and the temperature were increased to 2 L and 37 ^{0}C, respectively.

2.2.15 Protein purification

The His-tagged samples were purified in a column by nickel-bead affinity chromatography and analysed by SDS-PAGE. They were used to screen for protein expression as well as protein solubility. The purified proteins were quantified by the Qubit™.

The purified samples were concentrated in a small-sized concentrator before dialysis in PBS. The dialysed samples were lyophilized and stored at 4 ^{0}C until further downstream applications.

UNIVERSITY of the
WESTERN CAPE

2.2.16 Selection of Aptamers for TB biomarkers

2.2.16.1 Magnetic-bead based SELEX

TAGLN2 was used for aptamer selection by Magnetic-bead based SELEX following the protocol described in the Figure 2.1.

http://etd.uwc.ac.za/

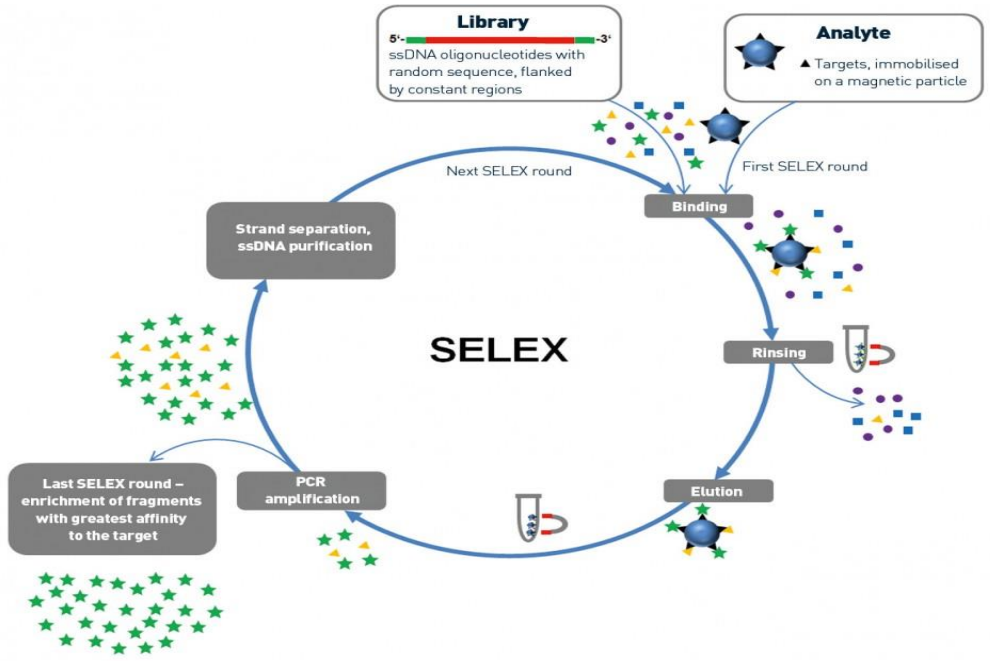

Figure 2. 1: An overview of the magnetic bead-based SELEX. A random library was incubated with the target recombinant protein for 30min. The bound and unbound pools were separated using magnetic beads, and then amplified by PCR. The process was repeated 8 - 15 times. The final pool was characterized and sent for sequence analysis (Kurt, 2013).

2.2.16.2 Preparation of DNA library for SELEX

The DNA aptamer library was a gift from Prof C.K O'Sullivan (Universitat Rovira I Virgili, Spain). The library was initially purchased from IDT Technologies. The library was made up of random 10^{13} to 10^{15} oligonucleotide sequences. Each aptamer in the library contained a 53 bp variable/random region (to which a target sequence can bind) that was flanked by 21 and 23 bp conserved/fixed primer sequence as shown in Figure 2.2.

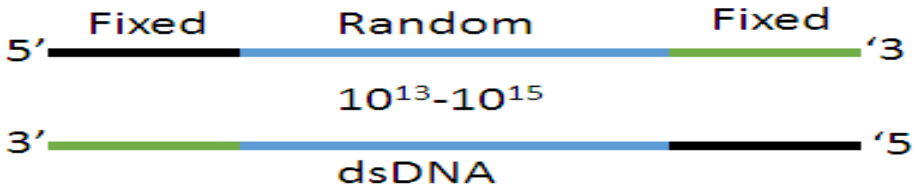

Figure 2. 2: The oligonucleotide aptamer library was made up of the random DNA region flanked by target primer sequences.

http://etd.uwc.ac.za/

The library was prepared by diluting 300 pmoL of DNA library in 100 µL of 1X SELEX buffer (PBS, pH 7.4; 1.5 mM $MgCl_2$). The DNA library was denatured at 95 °C for 5 min, followed by gradual cooling of 10 °C every 1 min, until it reached 25 °C. The denatured DNA library was kept at 25 °C prior to incubation with the purified recombinant protein. The DNA library and aptamer sequences used for SELEX are summarized in the Table 2.8.

Table 2. 8: SELEX DNA library and aptamer sequences and their suppliers

Name	Sequence	Supplier
SELEX library	5'-AGC TCC AGA AGA TAA ATT ACA GG-(53N)- CAA CTA GGA TAC TAT GAC CCC-3'	IDT Technologies
5'phosphorothioate modified aptamer	F^+ 5'-A*GCTCCAGAAGATAAATTACAGG-3' R^- 5'-GGGGTCATAGTATCCTAGTTG-3'	Whitehead Scientific (Pty) Ltd (South Africa)
Apt_1 (Full length region, FL)	5'AGCTCCAGAAGATAAATTACAGG**TTGAATGGTCAGAGGATTGCATGGACTGCCGGTGGGTGGGTGGGGGGTGGCAT**CAACTAGGATACTATGA**CCCC**3'	Inqaba Biotechnical industries (Pty) Ltd (South Africa)
Apt_1 (Truncated Region, TR)	5'**TTGAATGGTCAGAGGATTGCATGGACTGCCGGTGGGTGGGTGGGGGGTGGCAT**3'	
Apt_2 (FL)	5'AGCTCCAGAAGATAAATTACAGG**ATTTATAAGGGTGGCTAGTTAATAGGGGATGGGGTGGGTGGTTGTGGGTTCGT**CAACTAGGATACTATGA**CCCC**3'	
Apt_2 (TR)	5'**ATTTATAAGGGTGGCTAGTTAATAGGGGATGGGGTGGGTGGTTGTGGGTTCGT**'3	
Apt_7 (FL)	5'AGCTCCAGAAGATAAATTACAGG**GGTGGGTGGGAGGGTTTTTGTAGTTAGAGGAAGGGGAGCTGTGGTCTTAACAC**CAACTAGGATACTATGA**CCCC**'3	
Apt_7 (TR)	5'**GGTGGGTGGGAGGGTTTTTGTAGTTAGAGGAAGGGGAGCTGTGGTCTTAACAC**3'	
Apt_9 (FL)	5'AGCTCCAGAAGATAAATTACAGG**CAGTAATAGAGGGGAGGTATGTGTGTTGCTTAATTGTGGGTGGGCGGGTGGAA**CAACTAGGATACTATGA**CCCC**3'	
Apt_9 (TR)	5'**CAGTAATAGAGGGGAGGTATGTGTGTTGCTTAATTGTGGGTGGGCGGGTGGAA**3'	
T7 Primers	F^+ 5´TAATACGACTCACTATAGGG3´ (327pMol) R^- 5'TAGTTATTGCTCAGCGGTGG3' (325pMol)	Invitrogen

**Indicates the phosphorothioate modification; F^+ = forward primer; R^- = reverse primer*

http://etd.uwc.ac.za/

2.2.16.3 Selection of TAGLN2 aptamers by magnetic bead-based SELEX

The recombinant histidine-tagged TAGLN2 protein was diluted in deionized water to a concentration of 30 pmoL. The first round of SELEX involved incubation of the prepared DNA library with the 30 pmoL protein target (at a ratio of 10:1 library DNA to target) for 30 min 25 °C with shaking at 500 rpm. SiMAG/Nickel beads (Chemicell GmbH, Germany) were added to the DNA library-protein mixture. About 0.15 mg of the SiMAG-IDA-Nickel beads was incubated for 30 min at 25 °C with the DNA library-protein mixture. To remove unbound DNA, the immobilised DNA library-protein mixture was placed on a magnet for 2 min. The bead complex containing the bound DNA library-protein was then washed by re-suspending the bead pellet in 100 µL 1X SELEX buffer, after which the beads were again captured using the magnet. This was repeated three times. After the 3rd wash the bead mixture was re-suspended in 25 µL nuclease-free water. The re-suspended DNA (in a complex mixture with beads and protein) was used as template in a Pilot PCR. This constituted the positive SELEX. The steps employed for all the rounds are summarized in the Table 2.9.

UNIVERSITY of the
WESTERN CAPE

http://etd.uwc.ac.za/

Table 2. 9: Steps for isolation of aptamers using *in vitro* SELEX

SELEX round	Negative SELEX	Counter SELEX	Positive SELEX
Round 1	-	-	300 pmol DNA library + 30 pmol TAGLN2 protein (30 min)
Round 2 – 4	Purified ssDNA + SiMAG-IDA-Ni beads (30 min; 500 rpm)	-	Unbound ssDNA + 30 pmol TAGLN2 protein (30 min; 500 rpm)
Round 5 - 7	Purified ssDNA + SiMAG-IDA-Ni beads (20 min; 500 rpm)	-	Unbound ssDNA + 15 pmol TAGLN2 protein (20 min; 500 rpm)
Round 8 - 14	Purified ssDNA + SiMAG-IDA-Ni beads (20 min; 500 rpm)	Unbound ssDNA + 15 pmol HSA 10 min; 15 pmol TAGLN2 protein (10 min)	Counter SELEX; (20 min; 500 rpm)

2.2.16.4 Negative SELEX to increase aptamers specificity

To ensure specificity of the aptamers selected against the target protein, SELEX was repeated 14 times. The resultant PCR products were analysed on a 3 % agarose gel and then used for the next round of SELEX and the ssDNA was stored at -20 ^{0}C until further analysis. After the first round, a negative selection step was introduced to remove DNA that was bound non-specifically. This was done by incubating the eluted DNA with SiMAG/ Glu beads in binding buffer for 30 min at 25 °C under the conditions mentioned earlier (Section 2.2.16.3). The unbound DNA was used as a template for the next cycle of SELEX. The bound sample was then used as the template for the pilot PCR.

The pilot PCR was used to determine the optimal number of cycles for PCR scale-up. The lib-protein-bead complex was added to the master mix and subjected to PCR conditions as described in Section 2.2.5.

UNIVERSITY of the
WESTERN CAPE

http://etd.uwc.ac.za/

The samples were removed manually from the PCR at cycle numbers 5, 10, 15, 20 and 25 to obtain the optimal number of cycles that produces the best products. The samples (10 µL) were analyzed on a 3 % agarose gel and viewed on a UVP BioSpectrum® Imaging System.

2.2.16.5 Scaled-up PCR

The optimum number of cycle that produced the distinct band without any non-specificity (determined in Section 2.2.16.4) was used to scale up the PCR reaction volume to 100 µL prior to enzyme digestion for ssDNA production. The amplified products were subjected to agarose gel electrophoresis on a 3 % agarose gel and then analysed by UVP BioSpectrum® Imaging System.

2.2.16.6 Counter SELEX

Counter SELEX was introduced after the seventh rounds of selection to increase the specificity of the sequences that bind to the target (protein of interest). The supernatant containing the unbound DNA was incubated with the protein of interest (15 pmoL) for 10 min, at 25 ^{0}C, while shaking at 500 rpm. Human serum albumin (HSA) was selected as the counter protein. HSA was added at a final concentration of 15 pmoL and incubated for a further 10 min, at 25 ^{0}C, while shaking at 500 rpm. About 0.15 mg of the SiMAG-IDA-Nickel beads was added to HSA/lib complex, the bound bead complex was isolated and resuspended in 20 µL of PCR grade water. The samples (10 µL) were analyze on a 3 % agarose gel and viewed on UVP BioSpectrum® Imaging System.

UNIVERSITY of the
WESTERN CAPE

http://etd.uwc.ac.za/

2.2.16.7 T7 enzymatic digestion

Degradation of the unmodified dsDNA strands was done using a strand-specific enzyme, the T7 Gene 6 Exonuclease. The PCR amplicons were incubated with 1 X NEBuffer 4 and 40 units of the enzyme for 6 hours at 25 °C. This was followed by enzyme inactivation at 65 °C for 5 min. The samples were loaded onto the agarose gel for electrophoresis and viewed by UVP BioSpectrum® Imaging System.

2.2.16.8 ssDNA Concentration and purification

The generated ssDNA was purified using the Oligo Clean and Concentrator™ kit (Zymo Research, USA), according to the manufacturer's instruction. The digested products were transferred into a clean 2 mL Eppendorf tube; to which twice the volume of the Oligo binding buffer was added. Absolute ethanol (400 µL) was then added and the mixture was pipetted a few times then transferred into a Zymo-Spin™ Column that was suspended in a collection tube. The DNA solution was centrifuged at 10 000 rpm; (30 sec) and the flow-through was discarded. The DNA Wash Buffer (750 µL) was added to the column, followed by centrifugation as above. The flow-through was discarded and the column was transferred into a clean 1.5 mL Eppendorf tube. Nuclease-free water (35 µL) was added into the column and centrifuged to elute the DNA. The purified DNA was quantified using the DNA Qubit Assay and analysed by agarose gel electrophoresis.

UNIVERSITY of the
WESTERN CAPE

http://etd.uwc.ac.za/

2.2.16.9 Monitoring the evolution of the aptamers

The SELEX process was repeated 14 times until the aptamers were highly enriched for their target. Before monitoring evolution, SELEX rounds were selected based on the stringencies introduced in different rounds (Table 2.10). The samples were PCR amplified using the optimum number of cycles (25 cycles), the PCR products were analysed on a 3 % agarose gel and then viewed on UVP BioSpectrum® Imaging System.

Table 2. 10: The criteria used for monitoring the evolution

Recommended no. of SELEX rounds	SELEX category	Description of activities	Selected rounds for monitoring the evolution
1 – 4	Normal selection of aptamers	30 min incubation of beads and target protein (30 pMol) for both negative and positive SELEX	Round 3
5 – 7	Introduction of the selection stringency on aptamers (exclude counter SELEX)	20 min of incubation of beads and target protein (15 pMol) for both negative and positive SELEX	Round 7
8 - 14	Stringency and counter SELEX introduction	20 min of incubation of beads (negative SELEX) and 10 min incubation of counter and target proteins (15 pMol) for both counter and positive SELEX	Round 11 and 14

UNIVERSITY of the WESTERN CAPE

http://etd.uwc.ac.za/

2.2.16.10 Characterization of the selected aptamers

2.2.16.10.1 Electrophoretic Mobility Shift Assay (EMSA)

Binding of the aptamers to TAGLN2 was analyzed through a native gel electrophoresis mobility shift assay (EMSA). The aptamers were conditioned for binding by heating at 95 °C followed by 60 min incubation at 25 °C. The full length and variable aptamers (5 µM) were incubated in the presence of an increasing amount of protein target (ranging from 5 to 500 nM) for 30 min at 25 °C (30 µL final volume). Control proteins and aptamers were introduced to increase aptamer selectivity to the target protein (TAGLN2). The proteins used as controls included HSA and 6X His peptide, while MUC1-aptamers were used as the control aptamers (Muthelo and Meyer, 2015). After incubation, 10 µL of the samples were loaded onto a 8 % non-denaturing polyacrylamide gel. The gel was run in TBE buffer (1 X) at 105 V for 1 hour. The gel was stained with 2.5 µg/mL Ethidium Bromide for 20 min. The gel was visualised in the UVP BioSpectrum® Imaging System and analysed with Vision Works™ LS Image Acquisition and Analysis Software.

UNIVERSITY of the
WESTERN CAPE

2.2.16.10.2 Surface Plasmon Resonance (SPR)

SPR studies were conducted using the SPR ProteOn XPR36. The HTE chip was activated by nickel sulphate (10 mM) at a flow rate of 30 µL/min. The His-tagged TAGLN2 ligand was injected immediately to avoid nickel (II) ion leakage. The ligand was immobilized on the chip at a concentration range of 5 to 10 µg/mL, 30 µL/min flow rate and association/dissociation time of 300 seconds in a final volume of 150 µL.

http://etd.uwc.ac.za/

The ligands were stabilized with 1M NaCl. The analytes (FL and TR aptamers) were then injected into the chip at a flow rate of 25 uL/min flow rate at 300 seconds association/dissociation constants. The analytes were injected at different concentrations ranging from 0.1 to 20 µM. Imidazole was introduced in one of the channels as a control. The experiment was repeated thrice. The results were analysed by the Bioevaluation software to assess binding between the TAGLN2 and the aptamers.

2.2.16.11 DNA Sequence analysis and *in silico* analysis of the generated aptamers

2.2.16.11.1 Quantification of the evolving aptamers using Image J

The intensity of the bands on the agarose gel was quantified by the ImageJ software (NIH, USA). The relative band intensity was plotted against the selected aptamer rounds during enrichment. The program was employed as described by the manufacturer's manual (https://imagej.nih.gov/ij/download.html). A bar graph was constructed to distinguish the negative SELEX from the positive SELEX.

UNIVERSITY of the
WESTERN CAPE

2.2.16.11.2 Aptamers preparation and DNA sequence analysis

The dsDNA samples generated from PCR scale-up were analyzed on agarose gel and then purified using the Oligo Clean and Concentrator™ kit (Zymo Research, USA), according to the manufacturer's instruction. The DNA sample (10 ng/µL) was sent for sequence analysis by next generation sequencing (NGS) at Inqaba® biotech.

http://etd.uwc.ac.za/

A basic service of sequencing reactions without repeat, and analysis of the DNA sequences (Bioanalyzer) upto 11 samples per DNA chip (IB MiSeqBioAna) was requested. The Miseq Library Prep was prepared according to Inqaba® biotech's standard operating protocols using IB MiSeq Lib_DNA and MiSeq run. The resulting sequences were merged with Galaxy version 16.07 open web server (https://usegalaxy.org; Afgan *et al*., 2016) by Pair-End read merger. The data was analysed using Geneious 10.0.5 software (http://www.geneious.com; Kearse *et al.*, 2012).

2.2.16.11.3 Analysis of the aptamers by Geneious Software

The DNA sequence analysis results obtained from Section 2.2.16.11.2 were sent as raw data, and they were imported into the Geneious software for analysis. The software was used to pair and merge the sequences amplified by the forward and reverse primers to form dsDNA. The sequences were used as the starting material for analysis. The sequences that showed non-complementary forward and reverse sequences were discarded and considered to be the background noise. The complementary DNA strands (paired reads) were extracted based on the length of the library pool used during SELEX. The forward primer sequence was used as a reference when the merged sequences were blasted to identify aptamers with similar sequences. The sequences with the correct nucleotide sequences at the 5' end were isolated from the sequences that lacked the correct nucleotide sequence at the 3' end. Sequences that appeared as duplicates were selected for further analyses as they were enriched to the target during SELEX.

UNIVERSITY of the
WESTERN CAPE

http://etd.uwc.ac.za/

Top ten duplicates were aligned using the ClastalW Alignment, the sequences obtained from the TR and the FL aptamers were aligned to determine enriched aptamers. A phylogenetic tree was constructed for both the TR and the FL aptamers. The aptamer DNA sequences were then divided into clades based on their conserved sequences. The selected aptamers were subjected to MEME Suite to confirm the conserved motifs.

2.2.16.11.4 Analysis of the motifs in the aptamers by MEME Suite Software

The MEME Suite software was used to confirm the conserved motifs identified from Section 2.2.16.11.3. The selected aptamer sequences were imported into the MEME Suite software. Sequences that showed conserved motifs within the aptamer pool were compared to each other; their secondary structures were predicted by Mfold web server.

2.2.16.11.5 Aptamers secondary structure prediction using the Mfold web server

UNIVERSITY of the
WESTERN CAPE

Secondary structure predictions of the candidate aptamer sequences were constructed using an online software tool, Mfold (http://unafold.rna.albany.edu/?q=mfold; Zuker, 2003). The parameters set for *in silico* analysis were as follows: temperature (25°C), Mg ions (1.5mM) and Na ions (0.138M).

http://etd.uwc.ac.za/

CHAPTER 3

RECOMBINANT EXPRESSION AND PURIFICATION OF POTENTIAL TB BIOMARKER PROTEINS IN *E. COLI*

3.1 Introduction

In silico approaches were used to identify potential TB biomarkers, the proteins were selected by profiling serum proteins that were shown through proteomics studies to be differentially expressed in TB patients. Human serum has proved to be a reliable source of biomarkers that are related to pathological and physiological processes of diseases (Marko-Varga *et al*., 2005) and the blood samples of TB patients are also used in several TB diagnostic tests.

Proteins that are upregulated in the sera of TB patients can potentially be used as TB biomarkers (Achkar *et al*., 2015). Six serum proteins (IGFBP6, ISG15, S100A9, RBP4, GrA and TAGLN2) were shown to be upregulated in the sera of TB patients (Achkar *et al*., 2015; Guggino *et al*., 2015; Hare *et al*., 2015; Xu, *et al*., 2015). The first step towards using these potential biomarker proteins in diagnostics is the identification of molecules that can detect these proteins. Although antibodies can be used, these molecules have several limitations as discussed in Section 1.9.1. DNA aptamers are more suitable for applications in the recognition of proteins. The identification of DNA aptamers using the SELEX procedure requires large amounts of the purified biomarker protein. In this study recombinant DNA technology was used to clone genes encoding the potential biomarker proteins into protein expression vector (pET100/D-TOPO®). Large scale expression of the protein was then performed in *E. coli.*

UNIVERSITY of the WESTERN CAPE
http://etd.uwc.ac.za/

3.2 Results and discussions

3.2.1. Identification of TB biomarker proteins

Six TB biomarker proteins were identified as potential TB biomarkers from literature using methods described in Section 2.2.1. These proteins are Insulin-like Growth Factor Binding Protein 6 (IGFBP6), Interferon-stimulated Gene 15 (ISG15), Calcium Binding Protein (S100A9), Retinol Binding Protein 4 (RBP4), Granzyme A (GrA) and Transgelin-2 (TAGLN2) (Table 3.1).

Table 3. 1: Potential biomarker proteins identified from literature

TB Biomarkers	Acronym	Source
Insulin-like growth factor binding protein 6	IGFBP6	Achkar *et al*., 2015
Interferon- stimulated gene 15	ISG15	Hare *et al*., 2015
Protein S 100A9	S100A9	Xu *et al*., 2015
Retinol binding protein 4	RBP4	Xu *et al*., 2014
Granzyme A	GrA	Guggino *et al*., 2015
Transgelin 2	TAGLN2	Achkar *et al*., 2015

UNIVERSITY of the
WESTERN CAPE

3.2.1.1. *IGFBP6* gene

IGFBP6 gene is preferentially expressed in the soft tissues in the presence of *M. tb* (Fagerberg *et al.,* 2014; Kiso *et al.,* 2017). It is also expressed in human cancerous cells such as the prostate cancer cell line (LNCaP). The gene encodes the serum potential TB biomarker IGFBP6 protein.

http://etd.uwc.ac.za/

3.2.1.2. *ISG15* gene

The *ISG15* gene is secreted by the interferon (IFN) due to presence of *M. tb.*

The gene is preferentially expressed in the blood (Li *et al.,* 2009) and can also be expressed in human cancerous cells including the human lung carcinoma (A549), cervical cancer (HeLa cells) and the human liver cancer *(*HepG2 cell line). The *ISG15* gene encodes the potential TB biomarker ISG15 protein.

3.2.1.3. *S100A9* gene

The *S100A9* gene is preferentially expressed in the bone marrow (Li *et al.,* 2009) and encodes the secretory potential TB biomarker S100A9 protein. The gene can also be expressed from human cancerous cervical lesions such as HeLa, CasKi and CaVO-3 cell lines.

3.2.1.4. *RBP4* gene

UNIVERSITY of the
WESTERN CAPE

The *RBP4* gene is differentially expressed in the blood due to immunity. The immune system is stimulated in response to diabetes and cancer such as the one affecting the ovaries (ovarian cancer, SKOV-3 and SW626 cell lines) (Cheng *et al.,* 2014).

3.2.1.5. *GrA* gene

GrA gene is preferentially expressed in the larynx (Guggino *et al.,* 2015) where it encodes the cytosolic potential TB biomarker GrA protein.

http://etd.uwc.ac.za/

3.2.1.6. *TAGLN2* gene

The *TAGLN2* gene is expressed in several cancer cells such as prostate, breast, colon and lung cancers (Stanier *et al.,* 1998).

It encodes the serum TAGLN2 protein, recently identified as a potential biomarker to detect the presence of *M. tb* in both the latent and active TB infection (Achkar *et al.,* 2015). The TAGLN2 protein can potentially also be used to detect TB not only at the early stages, but also progressive TB since it is also expressed in the TB individuals co-infected with HIV (Achkar *et al*., 2015).

3.2.2 PCR amplification of genes encoding TB biomarker proteins

Genes encoding these biomarker proteins were amplified from cDNA prepared from several human cell lines. This include skin fibroblast cell line (KMST-6) and cancer cell lines (CaoV-3, MCF-7and SKOV-3). RNA was isolated from these cells and the cDNA was synthesized as described in Sections 2.2.2 and 2.2.3, respectively. Gene specific PCR primers were designed as described in Section 2.2.4. These primers were used to amplify the 6 genes. Table 3.2 shows the 6 genes (and their expected sizes) identified from literature.

UNIVERSITY of the
WESTERN CAPE

Table 3. 2: Potential biomarker proteins identified from literature and their sizes

TB Biomarkers	Acronym	Gene Size (bp)
Insulin-like growth factor binding protein 6	IGFBP6	616
Interferon- stimulated gene 15	ISG15	465
Protein S 100A9	S100A9	360
Retinol binding protein 4	RBP4	628
Granzyme A	GrA	456
Transgelin 2	TAGLN2	600

http://etd.uwc.ac.za/

The integrity of RNA extracted from the cells (SKOV-3, KMST-6 and MCF-7) was evaluated by agarose gel electrophoresis (AGE) (Figure 3.1).

The presence of both 28SrRNA and 18SrRNA subunits provides insights into the success of RNA extraction and its integrity before downstream applications (Jakovljevic *et al.,* 2004; Tabb-Massey *et al.,* 2003). As shown in Figure 3.1, the presence of 28S rRNA at ≃ twice the amount of 18S rRNA (as shown by the intensity of the bands) confirmed the quality and concentration of the extracted RNA. The rRNA is highly abundant, making up ≃ 95 % of the total RNA in all the mammalian cells (Fu and Gong, 2017). Majority of this is made up of the 28S and the 18S rRNA. Thus detection of these rRNA subunits can been used to confirm the presence of the intact RNA in a given sample (Fleige and Pfaffl, 2006; Strand *et al.*, 2007). From the Figure 3.1, the absence of smearing also indicated good quality RNA.

UNIVERSITY of the
WESTERN CAPE

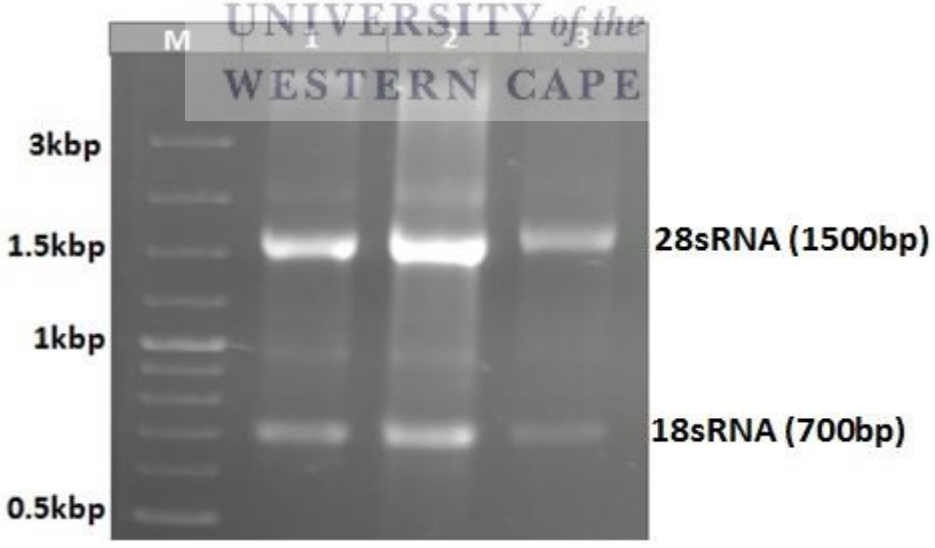

Figure 3. 1: Agarose gel electrophoresis (AGE) analysis of the RNA integrity extracted from human cell cultures.. The samples were extracted from human cancer (SKOV-3 and MCF-7 cells) and non-cancer cells (KMST-6 cells). M: O'GeneRuler™ 100bp Plus DNA Ladder, 1: SKOV-3, 2: KMST-6 and 3: MCF-7 cells extracted RNAs. The presence of the two rRNA subunits (18sRNA and 28sRNA) is indicated on the gel image.

http://etd.uwc.ac.za/

SKOV-3 and KMST-6 cells yielded a better quality and quantity of RNA (seen as intense bands in Figure 3.1) compared to MCF-7 cells (less bright bands).

It was expected that the different cell lines might vary in their expression profile for these genes. It is for this reason that more than one cell line was used. The extracted RNA was used to synthesise complementary DNA (cDNA) (as described in Section 2.2.3).

3.2.3 cDNA Synthesis

cDNA was synthesized using the Transcriptor First Strand cDNA Synthesis Kit (Roche Diagnostics) as described in Section 2.2.3. The protector RNase inhibitor supplied in the kit protected the degradation of the RNA by RNases while the reverse transcriptase (RT) was used to translate the RNA to cDNA. Like polymerase, reverse transcriptase needs a primer (Random Hexamer Primer) to start the DNA synthesis and this created one DNA (cDNA) strand complementary to the RNA strand in a DNA-RNA hybrid. The Reverse Transcriptase has RNase H activity that degrades the RNA strand in RNA: DNA hybrids, leaving single stranded cDNA ready for PCR. In this case, total RNA of which mRNA makes up 1-5% was used as a template for cDNA synthesis.

UNIVERSITY of the
WESTERN CAPE

Genes encoding the selected TB biomarker proteins were amplified from the cDNA obtained from various mammalian cells as shown in Table 3.3, using conventional PCR. The amplicons were analysed by AGE. As shown in Table 3.2, the genes vary in size. The expected size of each gene was correlated with their sizes on the gel (Figure 3.2 A-D). Figures 3.2 A and B showed amplification of the 4 genes (*ISG15*, *IGFBP6*, *S100A9* and *GrA*) from cDNA generated from

http://etd.uwc.ac.za/

MCF-7 and SKOV-3, while the other two genes (*RBP4* and *TAGLN2*) were amplified from KMST-6 and CaOV-3 derived cDNA (Figures 3.2 C and D).

Table 3. 3: Potential TB biomarkers and their source cell lines for PCR

Gene	Cell line
IGFBP6	Prostate cancer (LNCaP) cell line
ISG15	Cervical cancer (HeLa cells) Human liver cancer *(*HepG2 cell line)
S100A9	Cervical lesions (CaVO-3 cell lines)
RBP4	Ovarian cells (SKOV-3)
GrA	Cervical lesions (CaVO-3 cell lines)
TAGLN2	Cervical lesions (CaVO-3 cell lines)

UNIVERSITY of the
WESTERN CAPE

http://etd.uwc.ac.za/

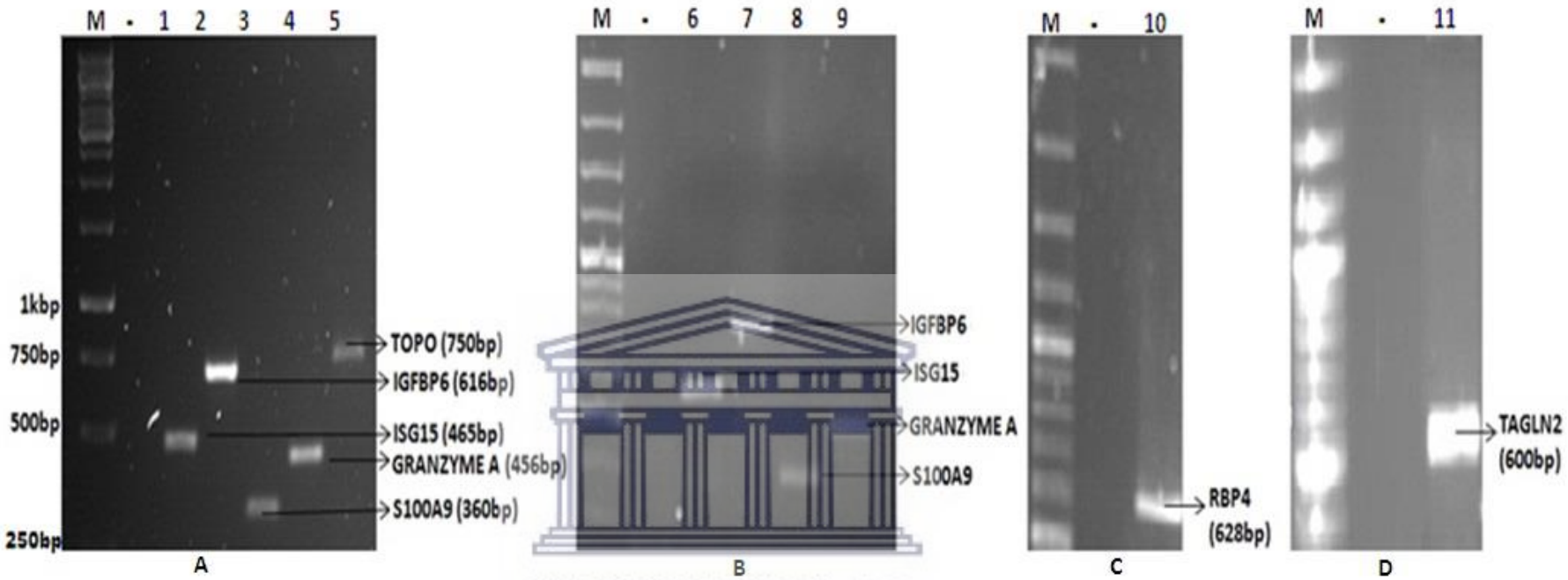

UNIVERSITY of the
WESTERN CAPE

Figure 3. 2: PCR amplification of the genes encoding the selected TB biomarker proteins from cDNA derived from human cell lines. Gel images A, B, C and D represents genes amplified from MCF 7, SKOV-3, KMST-6 and CaOV-3 cells, respectively. M: 1kbO'gene ruler, -: negative control, Lanes 1-11 where, PCR results for 1: *ISG15* (465bps); 2: *IGFBP6* (616bps); 3: *S100A9* (360bps), 4: *GrA* (456bps); 5: *TOPO* positive control (750bps); 6: *ISG15* (465 bps); 7: *IGFBP6* (616bps); 8: *S100A9* (360bps); 9: *GrA* (456bps); 10: *RBP4* (628bps) and 11: *TAGLN*2 (600bps).

http://etd.uwc.ac.za/

The amplified gene products (PCR amplicons) were purified using a commercial kit (Section 2.2.6) and quantified using the Qubit (Section 2.2.7). The samples were then stored at -20^{0}C until further analysis.

3.2.4 Cloning of the genes encoding the TB biomarker proteins

The six genes were cloned into the pET vector using the Champion™ pET 100 Directional TOPO® Expression Kit. The kit uses a five minute cloning strategy to directionally clone blunt-ended PCR products into the vector as shown in Figure 3.3 (Cheng and Shuman, 2000). The vector contains topoisomerase I (of the *Vaccinia* virus origin) which is responsible for the insertion of the blunt-ended PCR product (Figure 3.3). During cloning, the enzyme cleaves the phosphate group connecting two nucleotide bases in the opposite strands at the 3′ and the 5′ carboxyl groups. The cleavage occurs in the 5′-strand after the CCCTT sequence (Shuman, 1994), the GTGG overhang sequence in the vector initiates cloning by displacing the GTGG sequence in the 5' strand of the blunt-ended PCR products. The CACC sequence in the 3′ strand then anneal to the complementary GTGG overhang sequences in the vector (Figure 3.3) (Cheng and Shuman, 2000).

UNIVERSITY of the
WESTERN CAPE

http://etd.uwc.ac.za/

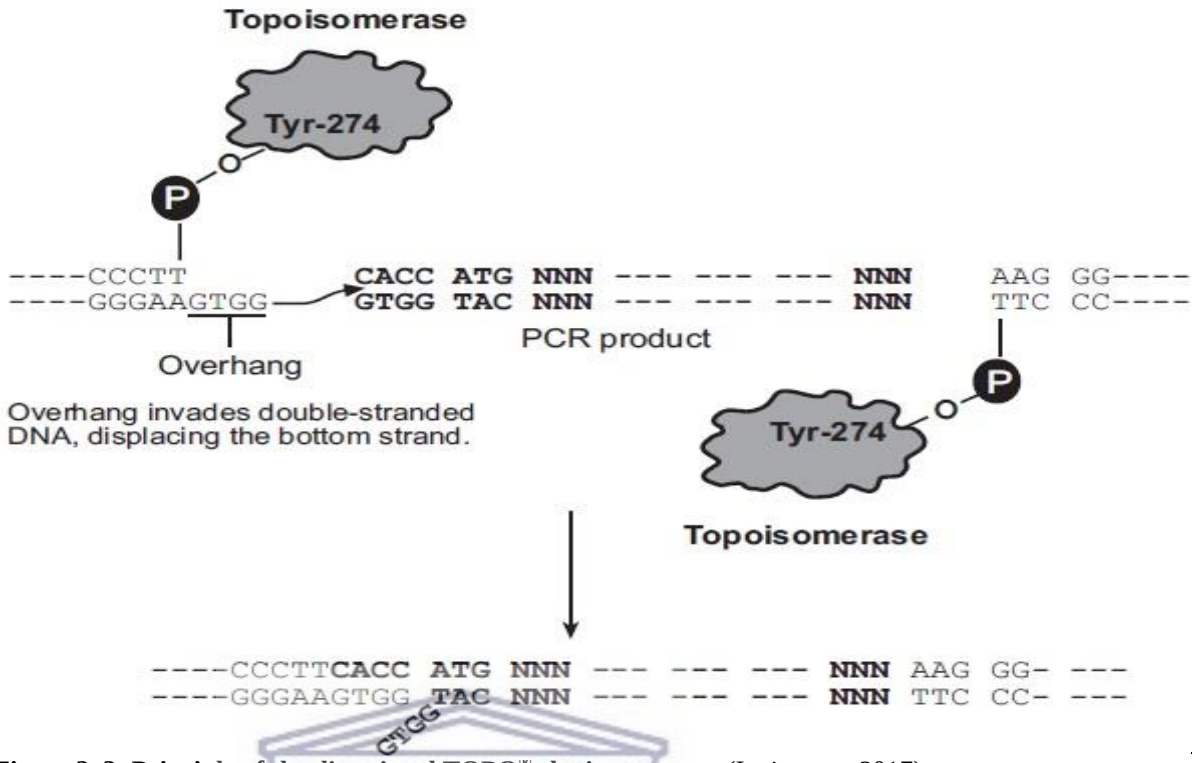

Figure 3. 3: Principle of the directional TOPO® cloning strategy (Invitrogen, 2017).

The amplified genes encoding the selected TB biomarker proteins were cloned into the pET vector in a 2:1 molar ratio of the PCR product: pET® vector (section 2.2.8). Randomly selected colonies were screened for the presence of the genes of interest. Colony PCR screening was performed using the gene-specific primers. Ten colonies per plate were selected for screening. The colonies were diluted 1:10 in distilled water and used as templates in the colony PCR (as described in Section 2.2.9). Figure 3.4 shows one of these ten colony PCRs for each of the 6 of the TB biomarker genes. The PCR amplicons for 3 of the genes (S100A9, GrA and TAGLN2) were the expected size (360bps, 456bps and 600bps, respectively). The clones were therefore considered positive for successful cloning.

UNIVERSITY of the WESTERN CAPE

http://etd.uwc.ac.za/

ISG15 (465 bps) showed non-specific PCR amplification as evidenced by the presence of multiple bands, while the *IGFBP6* (616 bp) PCR amplified a product that was less than the expected size, the amplicon was at ±100 bp. The positive control was provided in the kit to determine the PCR efficiency. Glycerol stocks were prepared for the positive colonies, *TAGLN2*, *GrA* and *S100A9*, (as described in Section 2.2.10) and stored at -80 ^{0}C until ready for downstream applications.

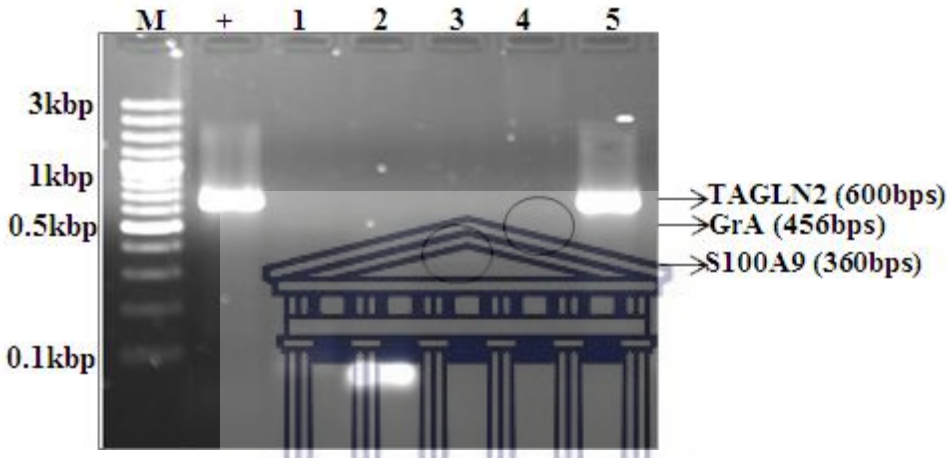

Figure 3. 4: Colony PCR screening for the genes encoding the potential TB biomarker proteins using gene-specific primers. M: 1kb O'gene ruler, +: positive control (TOPO DNA, 750 bps), 1: *ISG15* (465bps), 2: *IGFBP6* (616bps), 3: *S100A9* (360bps), 4: *GrA* (456bps) and 5: *TAGLN2* (600bps) genes. The circles represent genes S100A9 and GrA respectively.

UNIVERSITY of the
WESTERN CAPE

Based on Figure 3.4, only 3 of the 6 genes were successfully cloned. Because of this low success rate, it was decided to also confirm the presence or absence of genes by performing a PCR on the plasmid DNA that was produced from the clones. DNA minipreps were prepared for all the clones that were screened by colony PCR. The plasmid DNA samples were quantified using the Qubit. Using T7 primers, conventional PCR was used to amplify inserts present in the plasmid DNA (Figure 3.5).

http://etd.uwc.ac.za/

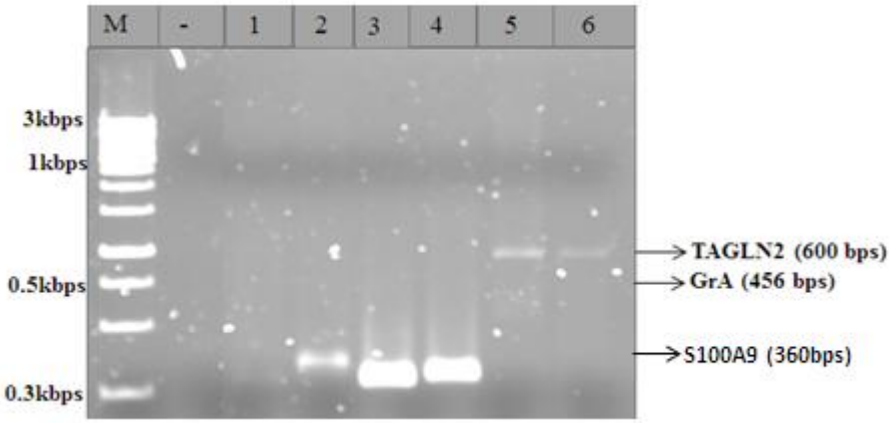

Figure 3. 5: PCR screening for the genes encoding the potential TB biomarker proteins from plasmid DNA using T7 primers. M: 1kb O'gene ruler, -: negative control, 1: *ISG15* (465bps), 2: *IGFBP6* (616bps), 3: *S100A9* (360bps), 4: *RBP4* (628bps), 5: *GrA* (456bps) and 6: *TAGLN2* (600bps). The arrows are pointing to the expected sizes of *S100A9*, *GrA* and *TAGLN2*.

From Figure 3.5, the clones for only two of the genes (*S100A9* and *TAGLN2*) were positive and produced amplicons at the expected sizes. There was no amplification for the *ISG15* gene. The sizes of the amplicon obtained from *IGFBP6, RBP4* and *GrA* were not corresponding to the expected sizes and were therefore considered as negative. The PCR for *GrA* produced an amplicon that was similar in size to *TAGLN*. It is possible that the *GrA* PCR reaction was contaminated with *TAGLN*. These results suggest that colonies for only TAGLN2 and possibly also *S100A9* were successfully cloned into the pET TOPO vector. The other genes produced false positive colonies during antibiotic selection this might be attributed to the recircularization of the vector during cloning. The vector can close up due to the possibility of a reverse reaction between the hydroxyl group in the 5′ end of the cleaved strand and phosphate group in the 3′ end of the complementary strand (Shuman, 1994). This consequently resulted in closing up of the vector by itself and producing false positive colonies without the inserts.

UNIVERSITY of the
WESTERN CAPE

http://etd.uwc.ac.za/

To validate the successful cloning and the orientation of the *TAGLN2* gene in the vector system, this clone was sent to Inqaba Biotech™ for DNA sequence analysis.

3.2.5 DNA Sequence analysis of TAGLN2 and S100A9 clones

Agar plates containing ampicillin resistant colonies of *TAGLN* and S100A9 were sent to Inqaba Biotech™ for DNA sequence analysis using the universal T7 primers, to confirm the presence of the *TAGLN* gene and to determine the orientation of the gene insert. The DNA sequence of the vector (including the cloning site and the sites where the T7 primer anneals) is shown in Figure 3.6. Using T7 primers will result in amplification of some part of the vector sequences from position 208 to 455.

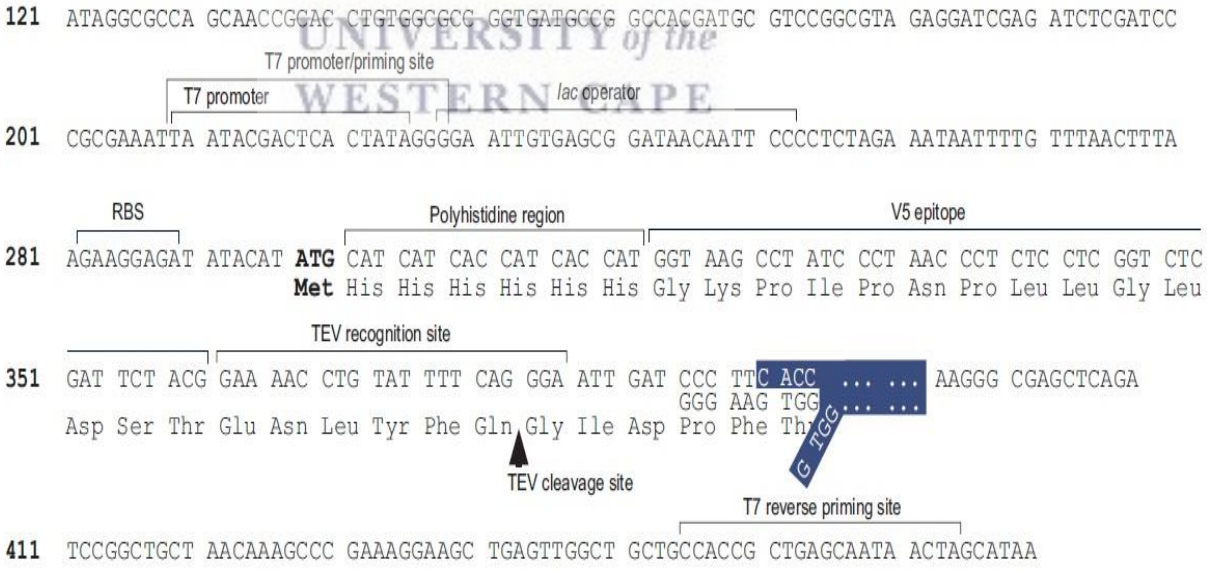

Figure 3. 6: TOPO 10 vector DNA sequences for the multiple cloning site from positions 121-480 (Invitrogen, 2017). Cloning of genes start from CACC sequence (shown in blue) at position ≃390 bp.

http://etd.uwc.ac.za/

After DNA sequence analysis, the sequence data was blasted in Addgene (https://www.addgene.org/analyze-sequence/), to confirm the presence of the inserts (gene of interests) within the plasmid DNA. Only *TAGLN2* gene sequence was correct and is shown in Figure 3.7. The *TAGLN2* gene sequence was in the correct orientation, as confirmed by the presence of the CACC sequence added at the 5′ end of the forward primer, to allow complementary base pairing with the GTGG overhang at the 3' end of the vector. There were no mutations observed in the *TAGLN2* DNA sequence.

http://etd.uwc.ac.za/

TAGLN2 sequences

1: TTCCCGTCTAGAATAATTTTGTTTAACTTTAAGAAGGAGATATACATATGCGGGGTTCTCATCA
64: TCATCATCATCATGGTATGGCTAGCATGACTGGTGGACAGCAAATGGGTCGGGATCTGTAC
126: GACGATGACGATAAGGATCATCCCTT**CACC**ATGGCCAACAGGGGACCTGCATATGGCCTG
186: AGCCGGGAGGTGCAGCAGAAGATTGAGAAACAATATGATGCAGATCTGGAGCAGATCC
244: TGATCCAGTGGATCACCACCCAGTGCCGAAAGGATGTGGGCCGGCCCCAGCCTGGACGC
303: GAGAACTTCCAGAACTGGCTCAAGGATGGCACGGTGCTATGTGAGCTCATTAATGCACTG
363: TACCCCGAGGGGCAGGCCCCAGTAAAGAAGATCCAGGCCTCCACCATGGCCTTCAAGCA
422: GATGGAGCAGATCTCTCAGTTCCTGCAAGCAGCTGAGCGCTATGGCATTAACACCACTGA
482: CATCTTCCAAACTGTGGACCTCTGGGAAGGAAAGAACATGGCCTGTGTGCAGCGGACGC
541: TGATGAATCTGGGTGGGCTGGCAGTAGCCCGAGATGATGGGCTCTTCTCTGGGGATCCCA
601: ACTGGTTCCCTAAGAAATCCAAGGAGAATCCTCGGAACTTCTCGGATAACCAGCTGCAAG
661: AGGGCAAGAACGTGATCGGGTTACAGATGGGCACCAACCGCGGGGCGTCTCAGGCAGGC
720: ATGACTGGCTACGGGATGCCACGCCAGATCCTCTGATCCCACCCCAGGCCTTGCCCCTGC
780: CCTCCCACGAATGG**TTA**AAGGGGCGAGCTCAACGATCCGGCTGCTAACAAAGCCCGAAAG
839: GAAGCTGAGTTGGCTGCTGCCACCGCTGAA (868)

UNIVERSITY of the
WESTERN CAPE

Figure 3. 7: DNA sequence generated for the TAGLN2 clone using the universal T7 primers. The DNA sequence in black shows the insert, starting with the CACC sequence (in bold and underlined) which is part of the forward PCR primer and the stop codon TTA (in bold and underlined). The DNA sequence in orange shows the ends of the pET vector.

http://etd.uwc.ac.za/

The *TAGLN2* gene sequences were further validated by BLAST analysis using the NCBI online tools. A translated BLAST against the Homo sapiens gene database produced *Homo sapiens TAGLN2* gene (Accession number: NM_001277224.1) as the gene inserted into the pET vector (Figure 3.8). The insert in the pET clone matched the TAGLN2 protein sequence with a 100% identity. This confirmed that the *TAGLN2* gene was successfully cloned into the pET vector into the correct orientation.

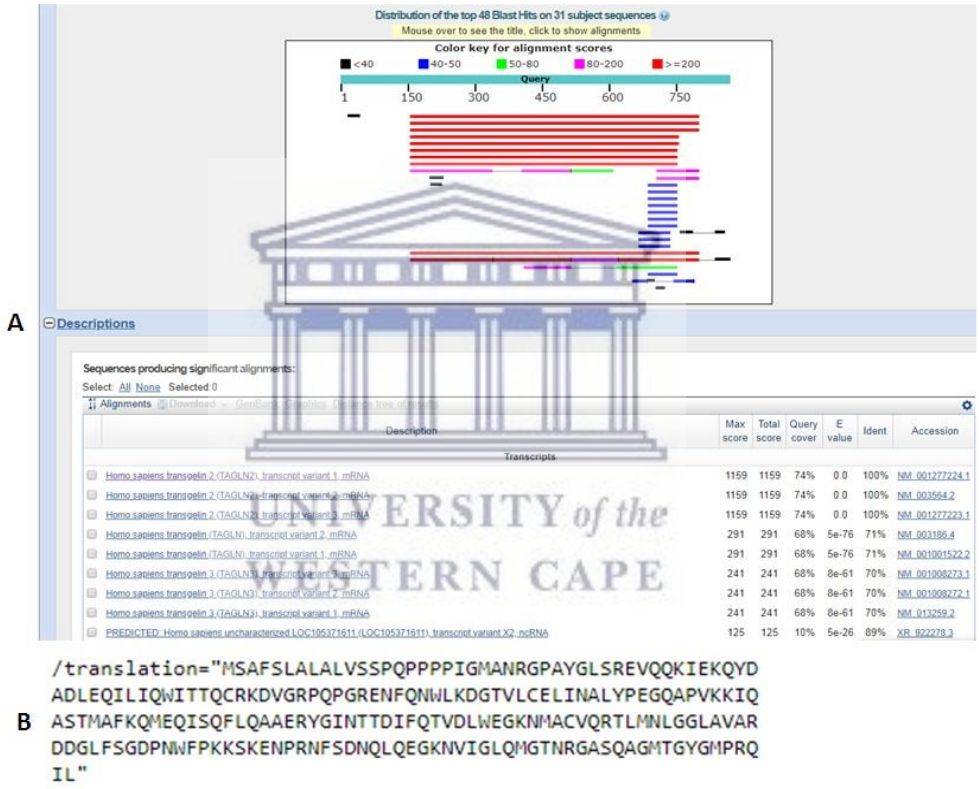

Figure 3. 8: BLAST analysis of the DNA sequence generated for the TAGLN2 clone. A shows a map of the alignments and their identities of the top 25 sequences in the database that is similar to the DNA sequence of the TAGLN2 clone. B shows the translated amino acid sequence for the sequence with the best match to the TAGLN2 clone.

Cloning of *S100A9* was not successful since the DNA sequence generated for this clone did not match the protein sequence of S100A9. It is possible that this clone too was generated as a false positive colony during antibiotic selection, which may be attributed to the recircularization of the vector during cloning.

http://etd.uwc.ac.za/

3.2.6 Expression and purification of TAGLN2 recombinant protein

3.2.6.1 Screening of TAGLN2 expression in *E. coli* cells

Expression of TAGLN2 protein was screened in two bacterial strains, the BL21 CodonPlus™ and the BL21 Star™ (DE3) *E. coli* cells. The *TAGLN2*-TOPO construct was transformed into the BL21 cells as described in Section 2.2.12 where 5 colonies were picked from each strain for expression screening.

Pilot protein expression was induced by addition of 1mM IPTG in 5 mL bacterial cultures, and then allowed to grow for ~16 hrs. Bacterial systems provide the merits of simplicity, speed, low costs and recombinant protein expressions in large biomass (Carstens *et al*., 2001). Protein expression in the two bacterial strains, the BL21 CodonPlus™ and BL21Star™ was analysed by SDS-PAGE, not much differences between the uninduced and induced samples was observed in the gels (data not shown). To further investigate protein expression, the samples were purified using nickel-bead affinity chromatography. The purified proteins were used to screen for protein expression as well as protein solubility. Figure 3.9 represent the expression and affinity purification profile of TAGLN2 protein from the two different bacterial strains, the BL21 CodonPlus™ (Figure 3.9 A) and the BL21Star™ (Figure 3.9 B). The HIS–tagged TAGLN2 protein was successful expressed and purified in the two bacterial strains as indicated by a single protein band (E1-2, Figure 3.9 A and B); the purified protein had a size equivalent to TAGLN2 molecular weight of ≃24 kDa in both strains.

UNIVERSITY of the
WESTERN CAPE

http://etd.uwc.ac.za/

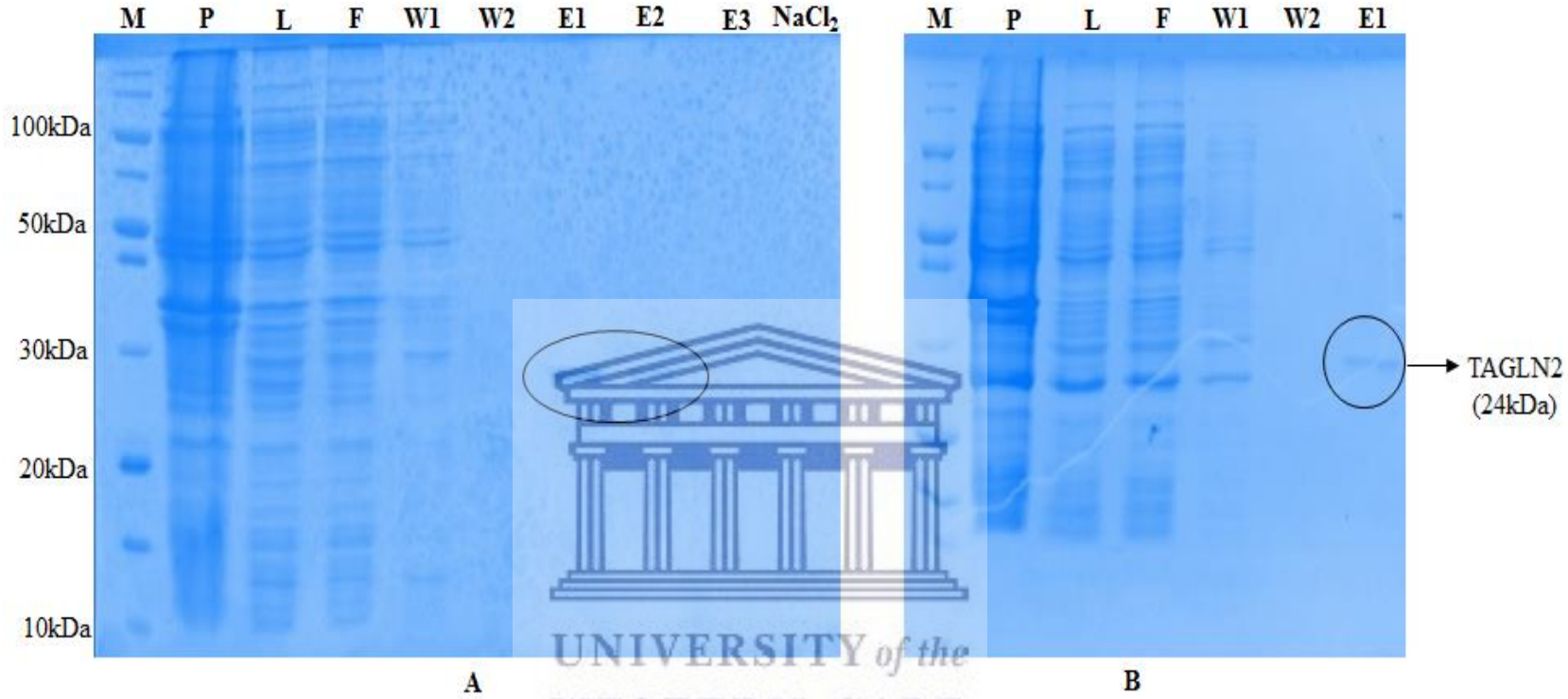

UNIVERSITY of the
WESTERN CAPE

Figure 3. 9: Large scale expression of the HIS-tagged TAGLN2 protein and purification by affinity chromatography. The protein was expressed in BL21 CodonPlus™ (A) and BL21 Star™ (DE3) (B) *E. coli* cells. M: 250 kDa Unstained Broad Range Protein Ladder; P: pellet; L: lysate or supernatant fraction; F: flow through; W1: first wash with 5mM imidazole; W2: second wash with 20mM imidazole; E1-3: elution fraction with 400 mM imidazole; and $NaCl_2$: elution of protein with 400 mM imidazole and 1M $NaCl_2$.

http://etd.uwc.ac.za/

The BL21 Star™ *E. coli* strain was recommended by the TOPO cloning kit supplier, and expected to have higher activity than the BL21CodonPlus™ strain. However, the opposite was true as the latter showed higher protein quantities than the BL21 Star™. The BL21 Star™ was recommended because it contains both the lacUV5 promoter and the λ DE3 lysogen which is capable of enhancing the expression of the desired proteins through T7 RNA polymerase. The polymerase is coded by genes in the λ DE3 lysogen and also lacks two of the key protease activities including the Lon protease and a mutation in the outer membrane OmpT protease. The lack of these two key proteases reduces degradation of heterologous proteins expressed in the strain. In addition, these strains also had mutated rne 131 gene that is encoded by RNase E which in turn improves the yield of the desired protein (Invitrogen, 2006).

The solubility of the protein was also assessed; there was no indication of overexpression in the pellet fraction (Figure 3.9, P). The recombinant protein was present in the supernatant, and proves to be soluble. If the protein was present in the pellet fraction, then the protein would have been considered insoluble and a membranous protein and not a cytosolic protein (Thoring *et al.*, 2016). The recombinant protein (HIS-TAGLN2) seemed to be stable as there was no degradation (multiple bands) from both gels. The protein was then dialysed for 16 hours and then quantified by the Qubit™. The concentration from small scale sample was 550 ng/μL. The sample was then stored at -20 ^{0}C until ready for downstream applications. Due to the increase in the yield of TAGLN2 protein from Figure 3.9A compared to Figure 3.9B, the CodonPlus™ strain was selected for the scale-up protein expression.

http://etd.uwc.ac.za/

3.2.6.2 Large-scale expression of TAGLN2 protein

TAGLN2 recombinant protein expression was up-scaled to 2L using the BL21 CodonPlus™ strain. The enhanced protein expression in CodonPlus *E. coli* cells have been associated with the presence of extra copies of *tRNA* genes that are rare in other *E. coli* strains (Carstens *et al.*, 2001), the *tRNA* genes promote protein expression that would otherwise be prevented. The CodonPlus™ strains also have protease deficiency as they lack both the Lon and OmpT (as mentioned in Section 3.2.6.1). The deficiencies in these proteases help to preserve the integrity of the recombinant proteins. Advantages the CodonPlus™ strain has over Star™ are Hte modifications that are responsible for elevating the transformation efficiency. In addition, they also lack *endA*1, which prevent degradation of the plasmid DNA during transformation. These factors may help to maintain the integrity of the mRNA, stabilizing it and improve the yield of the translated protein (Carstens *et al.*, 2001).

UNIVERSITY of the
WESTERN CAPE

The soluble protein fraction (supernatant) was purified as before and analysed by SDS-PAGE. As shown in Figure 3.10, the recombinant protein (HIS-tagged TAGLN2) from large-scale expression was eluted with 400 mM imidazole buffer. Two protein bands were observed (Figure 3.10, E1) at 24 kDa. This probably might have been due to protein degradation attributed to poor storage conditions of the samples. The samples were stored at 4 ^{o}C after purification. Thus, it is important to store the samples at -80 ^{0}C prior to their downstream applications.

http://etd.uwc.ac.za/

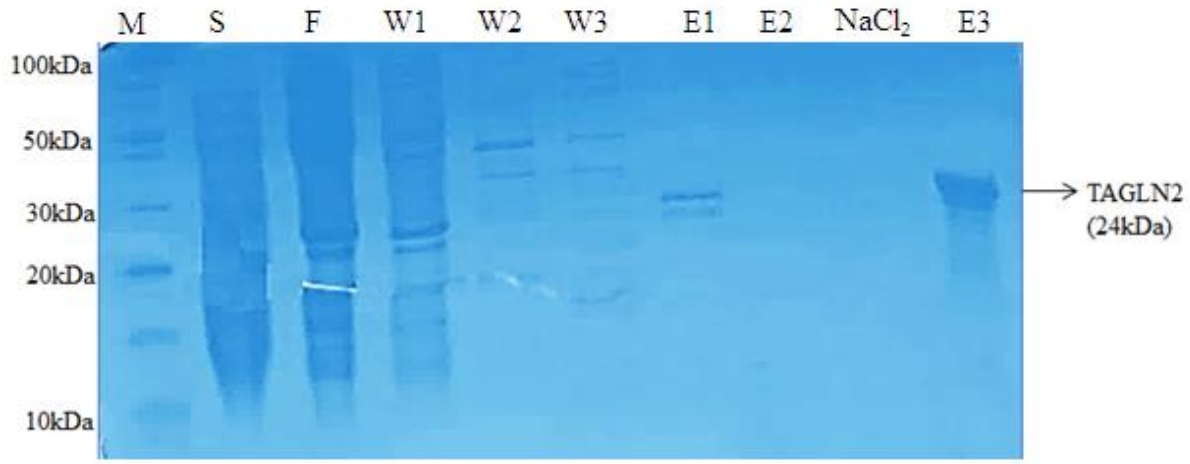

Figure 3. 10: Affinity purification of HIS-tagged TAGLN2 recombinant protein expressed in BL21 CodonPlus™. M: 250 kDa Unstained Broad Range Protein Ladder; S: supernatant fraction; F: flow through; W1-2: first wash with 5mM imidazole; W3: washed with 20mM imidazole; E1-2: fraction of the eluted protein with 400 mM imidazole; E3: small-scale purified protein (control).

The purified protein sample was quantified by the Qubit™, the concentration was 360 ng/µL. Surprisingly, this concentration was lower than the concentration obtained during pilot expression (550 ng/µL, Section 3.2.6.1). Most of the protein washed off as the flow through (F) and wash 1 (W1) samples, an indication that the concentration of Ni-beads was not enough to bind all the protein (i.e. the beads were over-loaded). The purified sample was concentrated in a 10 kDa concentrator, since the protein of interest (HIS-tagged TAGLN2) has a higher molecular weight (24 kDa) and would not pass through the pores of the membrane, resulting in the concentration of the protein. The protein was dialysed in PBS overnight at 4 °C and subsequently freeze-dried. The dry weight of the lyophilized protein was 69 mg. The lyophilized HIS-TAGLN2 protein was then stored at 4^{0}C for future use.

UNIVERSITY of the
WESTERN CAPE

http://etd.uwc.ac.za/

3.3 Conclusion

Computational tools were used to identify 6 potential serum biomarker proteins for TB diagnosis. The identification of DNA aptamers against these proteins required large quantities of these proteins. This required the cloning of the genes encoding these proteins and their recombinant expression in *E. coli*. Although all 6 genes were successfully amplified by PCR from human cell cultures, only one of these genes, *TAGLN2* was successfully cloned into the protein expression vector, pET100/D-TOPO®. This was confirmed by DNA sequence analysis. Through large expression of TAGLN2, a significant amount of this protein was purified from *E. coli* that was transformed with the pET100/D-TOPO® vector.

UNIVERSITY of the
WESTERN CAPE

http://etd.uwc.ac.za/

CHAPTER 4

THE SELECTION OF APTAMERS AGAINST TAGLN2 AND SEQUENCE ANALYSIS BY BIOINFORMATICS

4.1 Introduction

Systematic Evolution of Ligands by EXponential enrichment (SELEX) is an *in vitro* process that is used to produce DNA aptamers that are highly enriched for a specific target molecule (e.g. small molecules, proteins, nucleic acids, viruses, bacteria, whole cells and tissues). These aptamers bind to these target molecules with high affinity and specificity. These features of aptamers can be exploited in the development of diagnostic systems, which require molecules that can recognize protein biomarker targets with high specificity. The SELEX process is divided into several steps that are repeated several times (8 - 25 rounds). The affinity and specificity of the aptamers for the target generally increases with increasing rounds of selection. Dissociation constants (K_d) in the nanomolar ranges can be attained. The steps are as follows: incubation of the random DNA aptamer library with the target molecule which is immobilized in a matrix, separation of the pools of bound and unbound aptamers, amplification of bound aptamers through PCR, the generation of single-strand DNA nucleotides that will serve as a template for the next round of selection, elution of bound aptamers from their matrix, followed by aptamer purification and lastly the determination of the aptamer sequence (Tsao *et al*., 2017).

In this study nickel - nitrilotriacetic acid (Ni-NTA) magnetic beads were used as the matrix to immobilize a potential TB biomarker protein, TAGLN2. The NTA-moiety is covalently attached to the particle surface and facilitates the binding of a polyhistidine-tag.

http://etd.uwc.ac.za/

This method separates bound and unbound aptamers by using a magnet to capture aptamer/protein-complexes on magnetic beads. Binding of the aptamer/protein-complex to the magnetic bead is facilitated by a fusion tag on the protein of interest. In this study a commercial TAGLN2 protein (Abcam Biotech^{TM}) with a polyhistidine-tag was used as the target for SELEX since the recombinant TAGLN2 protein produced and discussed in Chapter 3 was not available at the time SELEX was performed.

http://etd.uwc.ac.za/

4.2 Results and Discussion

As indicated above SELEX is a repetitive selection process, which involves incubation, separation and PCR amplification. Section 4.2.1 will describe and discuss the results obtained for one SELEX round in detail, while the full data set for the selection of aptamers against TAGLN2 will be discussed in Section 4.2.2.

4.2.1 Processes involved in the selection of aptamers

A DNA aptamer library with short fragments (97 bp) and short random regions (≃53 nucleotides) were used in this study as such libraries were demonstrated to be sufficient for selection of aptamers against several target molecules (Svobodova *et al*., 2013). Bock and colleagues (1992) showed that a 96 bp DNA aptamer library was able to target a human thrombin protein (Bock *et al*., 1992). Also, Legiewicz and co-workers (2005) demonstrated that interference in the aptamer selection process could occur when longer (90 nucleotides) and shorter (16 nucleotides) randomized regions are employed to recognize the same target (Legiewicz *et al*., 2005). Randomized regions of ≃30-60 nucleotides are considered the ideal length. DNA aptamers were preferred for this study since DNA is more stable than RNA molecules. Due to the presence of a 2'OH group, RNA molecules are more unstable and prone to hydrolysis when exposed to a higher temperatures and an environment with a basic pH (James, 2000; Kusser, 2000).

UNIVERSITY of the
WESTERN CAPE

http://etd.uwc.ac.za/

4.2.1.1. Determining the optimal number of PCR cycles by pilot PCR

A random single stranded DNA library was incubated with the target protein (histidine-tagged TAGLN2) at a fixed concentration (300 pM ssDNA and 30 pM TAGLN2 protein) for 30 min as described in Section 2.2.16.3.

The DNA aptamer library comprised of millions of random oligonucleotide sequences each with a length of ≃97 bp. Each oligonucleotide (full length/ FL) sequences consisted of a random (variable) region of ~53 bp flanked by a ~21 to 23 bp primer sequences at the 5′ and 3′ ends of the aptamer. Following the separation of the bound and the unbound aptamers, the next step of SELEX requires the PCR amplification of the bound aptamer sequences. Mutations are often introduced during PCR amplification and can result in non-specific PCR products, which can reduce the success of the downstream applications of the aptamer (Lorenz, 2012). Several methods have been used to step-wise monitor the evolution of the DNA pools after each round of SELEX (Qu *et al.,* 2016; Takahashi *et al.,* 2016). These include the use of the nuclear magnetic resonance (NMR) which is efficient in the analysis of the structures of RNA molecules (Amano *et al*., 2017). The use of Surface Plasmon Resonance (SPR) and Electrophoretic Mobility Shift Assays (EMSA) have also been employed to assess the affinity of the DNA pools to the target molecule (Qu *et al.*, 2016). However, SPR requires sensor chips onto which the target molecules or aptamers are immobilized. EMSA experiment requires that the aptamer pools or target molecules must be labelled with tags such as radioisotopes or fluorophores. Immobilization of

http://etd.uwc.ac.za/

the reagents to the sensor chips and the use of fluorophores are time-consuming and expensive. Aside from being expensive, all these methods might alter the structure and the binding properties of the target molecule to the aptamer library. Pilot PCR, which involves monitoring of the PCR amplicons by simply subjecting the PCR product to AGE and visualising the quality of the PCR product, is more cost effective. Pilot PCR was used in this study to determine the optimal number of PCR cycles that does not result in non-specific amplification or PCR artefacts. Pilot PCR was used to follow the progression of the PCR by analysing the PCR products periodically over the 25 cycles. Following the separation of the bound and the unbound aptamers, the aptamer-TAGLN2 conjugate was used a template in a pilot PCR.

Figure 4.1 shows that using more than 15 PCR cycles results in non-specific amplifications as indicated by multiple bands present in lanes C20 and C25, representing 20 and 25 PCR cycles, respectively. Figure 4.1 shows that a single PCR product is produced at 10 PCR cycles, but that the yield is low. As the number of PCR cycles are increased from 10 the amount of non-specific products are also increased.

UNIVERSITY of the
WESTERN CAPE

http://etd.uwc.ac.za/

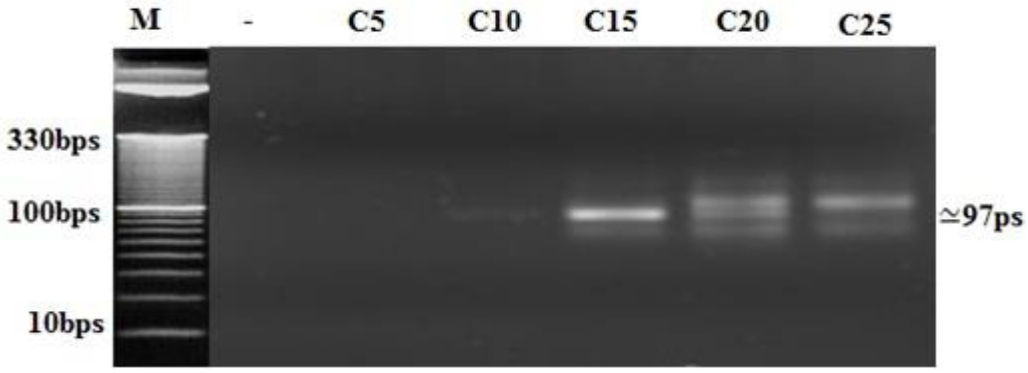

Figure 4. 1: Pilot PCR to determine the optimum number of cycles that can generate more specific PCR products in SELEX. M: 10 bp marker, - : negative control while C5 to C25 are the number of PCR cycles.

4.2.1.2. Large-scale PCR amplification of aptamers using the optimized PCR conditions

Twelve cycles were chosen as the optimal number of PCR cycles based on the pilot PCR in Figure 4.1. Twelve cycles were used to PCR amplify the aptamers using the aptamer/TAGLN2 complex as template. These products were analysed by AGE. Figure 4.2 shows single amplicons at the expected size, ≃100 bp (97 bps). Replicates of this reaction were performed to increase the amount of PCR product for the next step of SELEX.

UNIVERSITY of the
WESTERN CAPE

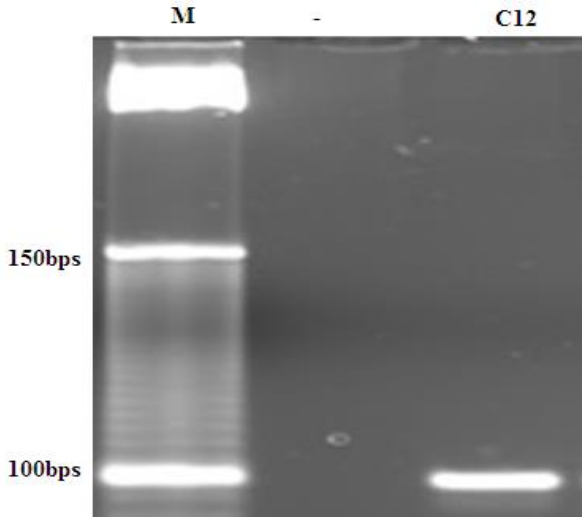

Figure 4. 2: Large scale amplification of aptamers using the optimum PCR cycles.. M: 10bp O'gene ruler, –: negative control, C12: PCR cycles.

http://etd.uwc.ac.za/

4.2.1.3. Generation of ssDNA by asymmetry PCR

PCR amplification during SELEX produces dsDNA, however ssDNA are required for binding to the target protein. Several methods have been employed to produce ssDNA from the PCR amplified dsDNA. The use of phosphorothioate modified forward or reverse primer in the PCR allows for the degradation of the unmodified strand in the dsDNA using an exonuclease enzyme.

This can also be achieved by using a biotinylated strand that will bind to the streptavidin-activated membrane, separating the two strands of dsDNA. The use of a radioactive labelling of the sense strand works on the same principle as biotin-streptavidin separation. Asymmetry PCR (A-PCR) can also be used to generate ssDNA aptamers. In A-PCR unequimolar ratios between the forward and the reverse primers is used to produce both ssDNA and dsDNA (He *et al.*, 2013). These methods however have some limitations, for instance, A-PCR requires thorough optimization of factors such as primer ratios, annealing temperatures and number of PCR cycles for each individual library (He *et al.*, 2013). Changing parameters used in normal (symmetric or pilot PCR) PCR will also reduce PCR reaction efficiency (Pierce *et al.*, 2005).

UNIVERSITY of the
WESTERN CAPE

Asymmetry PCR (A-PCR) was used to generate ssDNA aptamers. This was achieved by using unequimolar ratios between the forward and the reverse primers. To protect the sense strand from nuclease degradation the forward primer was also modified by adding phosphorothioate to the 5' end. During A-PCR, both ssDNA and dsDNA are produced and since the interest is in ssDNA, nucleases are used to digest DNA strands that are not protected by

http://etd.uwc.ac.za/

phosphorothioate. A-PCR result in low PCR reaction efficiency (60 - 70 %) as a consequence of unequal primer concentrations, (Sanchez *et al.*, 2004). A-PCR will promote amplification of the 5' strand and generate mainly the ssDNA (Sanchez *et al.*, 2004).

PCR products from symmetry pilot PCR were used as template for A-PCR, a 5:1 ratio of forward to reverse primer was used to generate ssDNA. The PCR products were analysed by AGE.

Figure 4.3 shows dsDNA and the ssDNA products generated by A-PCR, the majority of the products were ssDNA based on the band intensities on the gel image. The dsDNA had a higher molecular weight than the ssDNA, as such ssDNA migrates faster than the dsDNA on the gel. The dsDNA products are likely to interfere with the binding affinity of the aptamers to their target during the selection process and they were removed by nuclease digestion.

UNIVERSITY of the
WESTERN CAPE

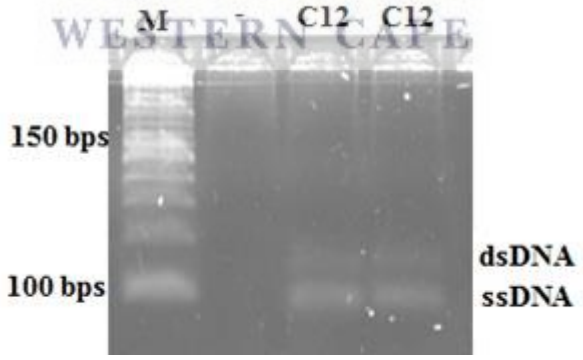

Figure 4. 3: Generation of ssDNA aptamers by assymetry PCR. M: 10bp O'gene ruler, –: negative control, C12: PCR cycles.

The fact that the random DNA library used was 97 bp long, chances of aptamer diversity for the target pool was reduced and the efficiency of the selection

http://etd.uwc.ac.za/

process was thus improved. A-PCR was used in the first two rounds of selection. This is expected to increase the yield of the ssDNA and to decrease chances of forming non-specific products (He *et al.,* 2013). The scale-up PCR was followed by a nuclease digestion step to remove the dsDNA.

In this study, the A-PCR product was subjected to the T7 gene 6 exonuclease digestion to remove dsDNA. The exonuclease digested samples was analysed by AGE, as shown in Figure 4.4A. The dsDNA observed in the A-PCR samples disappeared from the digested samples (T7). The resulting ssDNA was then purified (Figure 4.4 B) and resuspended in SELEX buffer in preparation for the next round of SELEX.

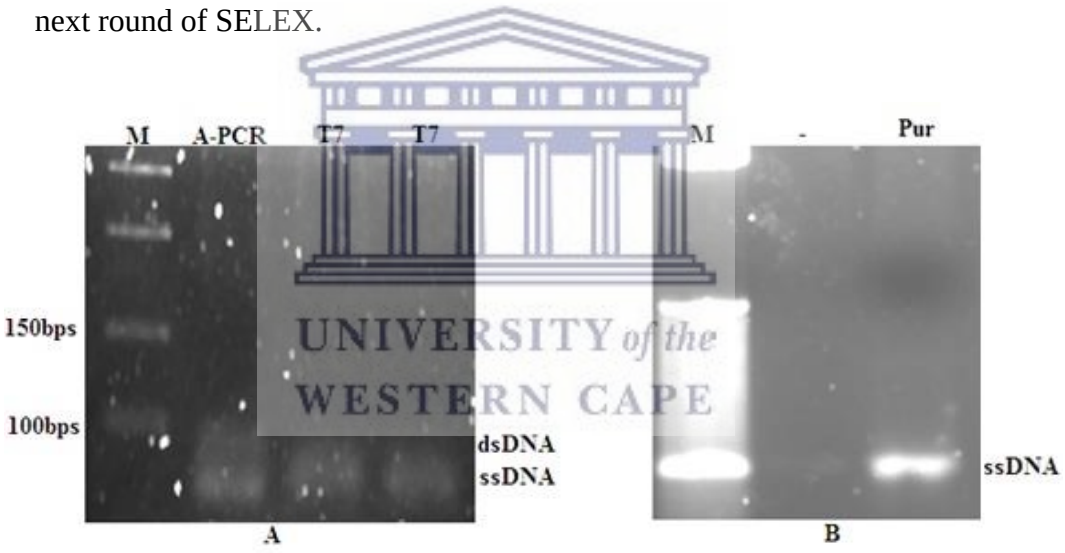

Figure 4. 4: Production of ssDNA by A-PCR following digestion (A) and purification of the ssDNA (B). M: 100 bp O'gene ruler, A-PCR: Asymmetry PCR sample used as the control, T7: the digested amplicons generated from A-PCR, -ve: the negative control and Pur: purified product.

4.2.2. Selection of aptamers against TAGLN2 protein

In this study 14 rounds of SELEX was performed to obtain DNA aptamers that are specific for histidine-tagged TAGLN2 protein. Figure 4.5 shows the results of the pilot PCRs for each of these SELEX rounds. PCR amplification was

http://etd.uwc.ac.za/

monitored at cycle (C) number 5, 10, 15 20 and 25. From figure 4.5, cycle numbers C10 from round 1 was selected for the large-scale PCR amplification while C15, C15, C15, C10, C15, C10, C15, C15, C15, C15, C20 and C15 were used for their large-scale PCR amplification from round 2 to 14 respectively.

There is a high probability that some of DNA aptamers in the library may have a higher affinity for the magnetic beads than the protein target (TAGLN2), resulting in the false positive selection of aptamers that bind to the beads and not TAGLN2.

To minimize this, a negative SELEX round (i.e. the incubation of the aptamer pool with the beads only) was introduced from SELEX round 2 (R2) to remove the aptamers that bind to the beads and not the TAGLN2 protein target. This means that all SELEX rounds from R2 were first performed using the magnetic beads as the target, followed by a positive SELEX (i.e. the incubation of the aptamer pool with the TAGLN2/bead complex). Aptamers that bound to the magnetic beads were removed and the supernatant containing unbound aptamers (which presumably do not bind to the beads) were used as the template for the positive SELEX.

To monitor the evolution and enrichment of the aptamers produced during SELEX process, pilot PCRs were performed on both negative (indicated by – sign and the PCR cycle number) and positive (indicated by + sign and the PCR cycle number) SELEX samples (Figure 4.5). No clear difference in the profile of the PCR amplicons for the positive and negative SELEX can be observed in SELEX round 2 (R2). However from SELEX round 3 (R3) to 9 (R9) a significant

http://etd.uwc.ac.za/

difference in the profiles of positive and negative SELEX can be observed. Figure 4.5 shows that pilot PCRs on negative SELEX samples yielded more intense bands and in some instances the PCR product also presented as a smear. This suggests that some aptamer sequences were successfully removed from the aptamer pool during negative SELEX.

It is also clear that the cycle numbers of around 15 produce the best result since a single PCR amplicon is produced in most SELEX rounds. Cycle numbers higher than 15 produce smearing and multiple PCR bands.

To further increase the selectivity and specificity of the aptamers for the target of interest, TAGLN2 counter SELEX was introduced from SELEX round 8 to 14. This was done by introducing an unrelated human protein, human serum albumin (HSA) into the SELEX procedure. From SELEX round 8 to 14 histidine-tagged TAGLN2 was replaced by recombinant histidine-tagged HSA as the target protein. Aptamers that bound to the HSA/bead complex were removed and the supernatant containing unbound aptamers were used as template for PCR amplification and the target for the next SELEX round. Counter SELEX can further assist the selection of aptamers that are specific for TAGLN2, since this will remove aptamers that can potentially bind to HSA, which is highly abundant in human serum. Since the aptamer that will be identified in this study will be used to detect TAGLN2 in serum samples, counter SELEX with HSA will also ensure that there is no undesirable binding of this aptamer to HSA, which is not a biomarker for TB, but is highly expressed in serum. This will limit false positive results in the diagnostic from serum samples. Based on the PCR profiles for SELEX rounds 8 to 14, there was no difference between positive and negative

UNIVERSITY of the
WESTERN CAPE

http://etd.uwc.ac.za/

SELEX (Figure 4.5). This showed that the selection was enriched and the quality of the PCR amplicon in R13, cycle number 20 was selected for the large-scale PCR amplification of aptamers before stopping at R14**.**

UNIVERSITY of the
WESTERN CAPE

http://etd.uwc.ac.za/

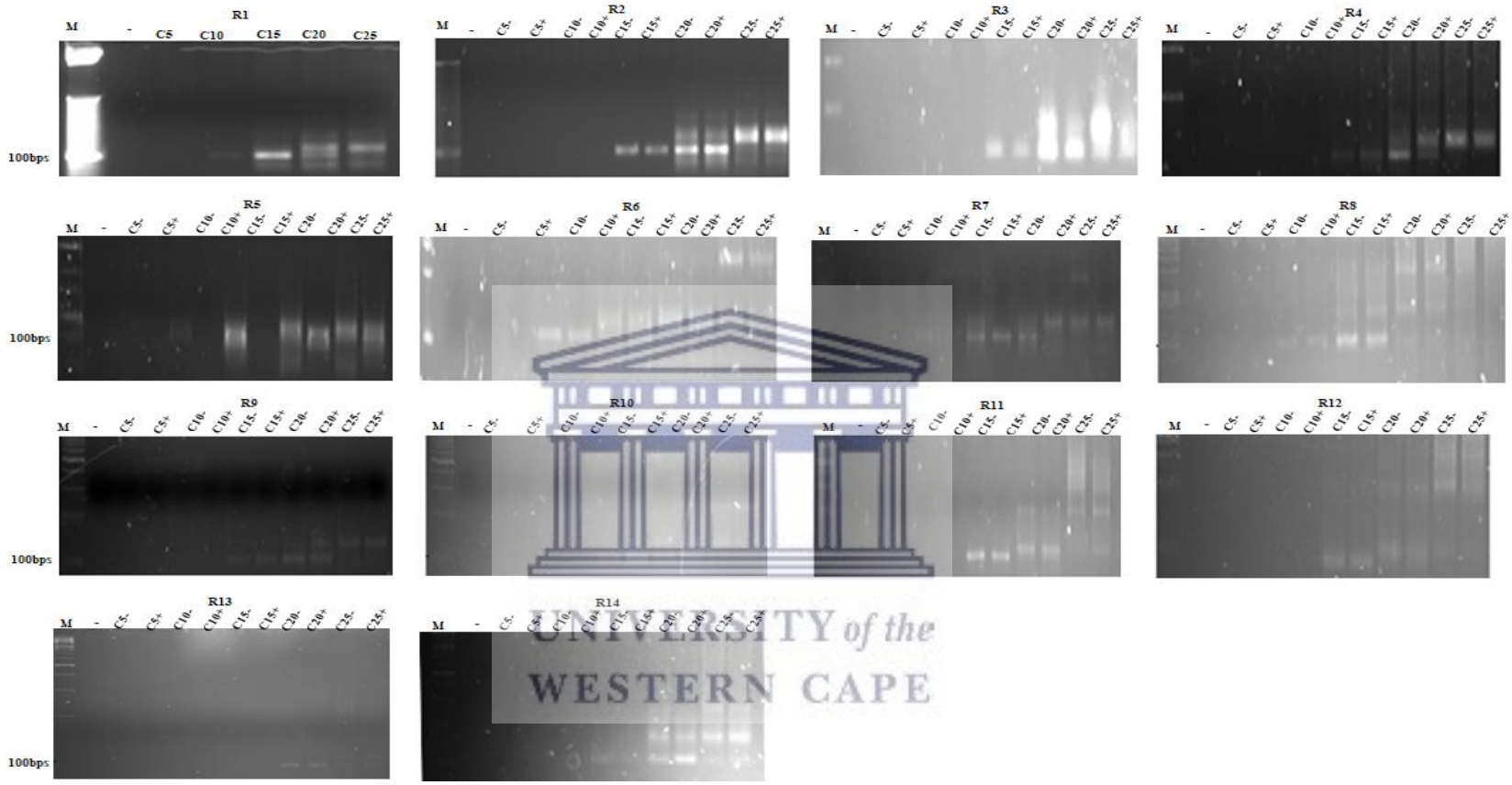

UNIVERSITY of the
WESTERN CAPE

Figure 4. 5: Analysis of TAGLN2 aptamer evolution and enrichment during SELEX using pilot PCR. R1 – R14 indicate the SELEX round, while C5 – C25 indicate the PCR cycle number. Negative SELEX (indicated by the – sign) were introduced from R2 to R14. Counter SELEX was introduced from R8 to R14. M: 100 bp O'gene ruler, -: negative control , C5 - C25: PCR cycle number.

http://etd.uwc.ac.za/

It is generally expected that as the number of SELEX rounds increase, the number of aptamer variants in the selected or bound pool of aptamers should decrease and become more specific. This is expected result in an increase in the concentration of the PCR product. To verify this, pilot PCR amplicons in cycle number 15 (C15) in SELEX rounds 6, 10 and 13 was analysed by AGE and the PCR products were quantified by densitometry (Figure 4.6). Figure 4.6B shows that the yield of PCR product in negative SELEX rounds was much lower than the yield in the positive SELEX rounds for R6, R10 and R13. It is also clear that the yield of product increase with increasing PCR cycles. This suggests that the aptamer pool is becoming selective towards the target protein.

UNIVERSITY of the
WESTERN CAPE

http://etd.uwc.ac.za/

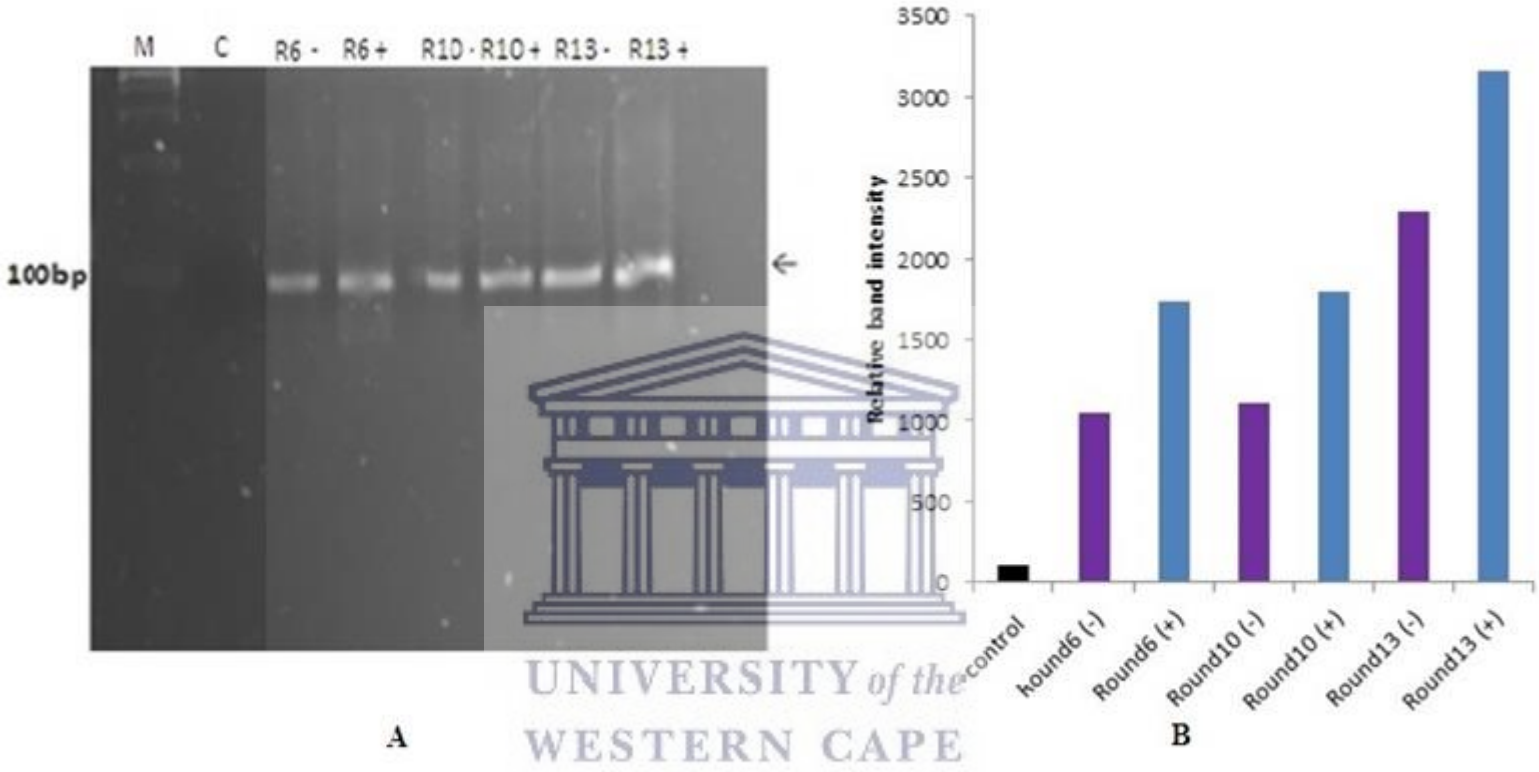

UNIVERSITY of the
WESTERN CAPE

Figure 4. 6: Monitoring of the evolution of TAGLN2 aptamers in R10 and R13. PCR yields were quantified by AGE (A) and densitometry analysis of the PCR bands (B). M: 100 bp O'gene ruler, C: negative control, the SELEX round (R) number with either – or + represent positive and negative SELEX. Densitometry analysis was done using ImageJ software.

http://etd.uwc.ac.za/

4.2.3 Analysis of aptamers using bioinformatics tools

The aptamers generated from the final round (Section 4.2.2) were prepared by PCR and the integrity confirmed by gel electrophoresis before being sent for sequence analysis. The resulting aptamer sequences were analysed by Bioinformatics (*in silico*) tools.

In silico tools Geneious, MEME Suite software and the Mfold Web Server were used to analyse the DNA sequences which represented the isolated aptamers. The raw data containing the DNA sequences were uploaded in the Geneious interface where they were filtered until conserved sequence motifs were produced. The motifs were then subjected and confirmed by the MEME Suite.

The selected aptamers were analysed by the Mfold Web browser to predict their secondary structures before synthesis. The aptamer structures provided insight into their binding patterns to the targets. These aptamers were then selected based on their binding capability to the target.

UNIVERSITY of the
WESTERN CAPE

4.2.3.1 Sample preparation and sequence analysis by Geneious

The PCR products from SELEX R13, PCR cycle 15 (C15) was submitted to Inqaba® Biotech for DNA sequence analysis to identify the sequence of potential TAGLN2 aptamers. Direct ultra-high-throughput deep DNA sequencing was performed on the sample.

Around 83,750 sequences were generated, which were further analysed using Geneious software (https://www.geneious.com/).

http://etd.uwc.ac.za/

The aim was to verify that these sequences resembled the DNA aptamer library (i.e. that the sequences contained the variable region which was flanked by the conserved primer regions on the 5' and 3' ends) and to determine if there were similarities between any of the aptamer sequences. Following analysis using Geneious software, the 83,750 sequences were reduced to about 30, 000 unique sequences. Several sequences appeared multiple times and only the sequences that mapped to the forward primer used during selection was selected. This is not unexpected since it is anticipated that the relative concentrations of the aptamers will differ depending on their affinity for the target and due to the introduction of mutations by PCR. Figure 4.7 shows a pairwise sequence alignment (generated using ClustalW) of a list of ten full-length (FL, i.e. including the conserved 5' and 3' primer sequences) aptamer sequences that were most frequently replicated amongst the 83,750 sequences. The sequences were named Apt_1 to Apt_10. The conserved primer regions on the 5' and 3' ends, as well as the variable region (VR) were appeared in all these sequences. The frequency of repetition of the same sequence differed between the sequences. Apt_1, for example appeared 15 times, while Apt_10 appeared only 4 times. The majority of the sequences were unique sequences, appearing only once. It is possible that the sequences that appear more frequently in the aptamer pool is more likely to bind to the protein target, TAGLN2.

UNIVERSITY of the
WESTERN CAPE

http://etd.uwc.ac.za/

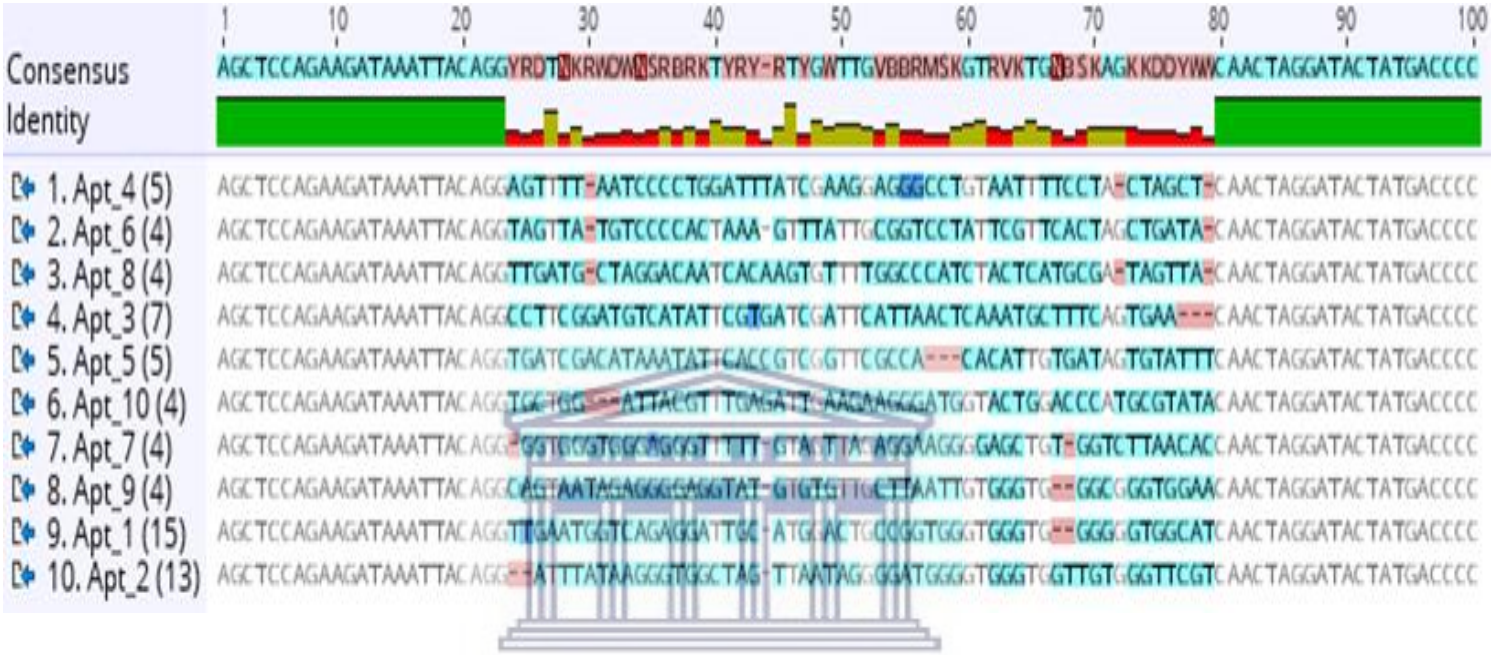

Figure 4. 7: ClustalW alignment of the ten most frequently repeated aptamer sequences. The aptamers were named Apt_1 to Apt_10. The frequency of repetition is indicated in brackets. The consensus sequence is indicated on top. The frequency of individual nucleotides in specific positions is also indicated and is colour coded. Nucleotides that are highly conserved are not highlighted, while nucleotides that show a degree of variation are highlighted in green. Nucleotides with unique nucleotide positions are highlighted in blue.

UNIVERSITY of the
WESTERN CAPE

http://etd.uwc.ac.za/

To determine the evolutionary development and diversification of the aptamer sequences, phylogenetic analysis of the 10 most frequently repeated aptamer sequences was performed (Figure 4.8). For this purpose the 5' and 3' primer ends were removed to leave a truncated (TR) aptamer sequence, which in essence is the variable region of the aptamer library.

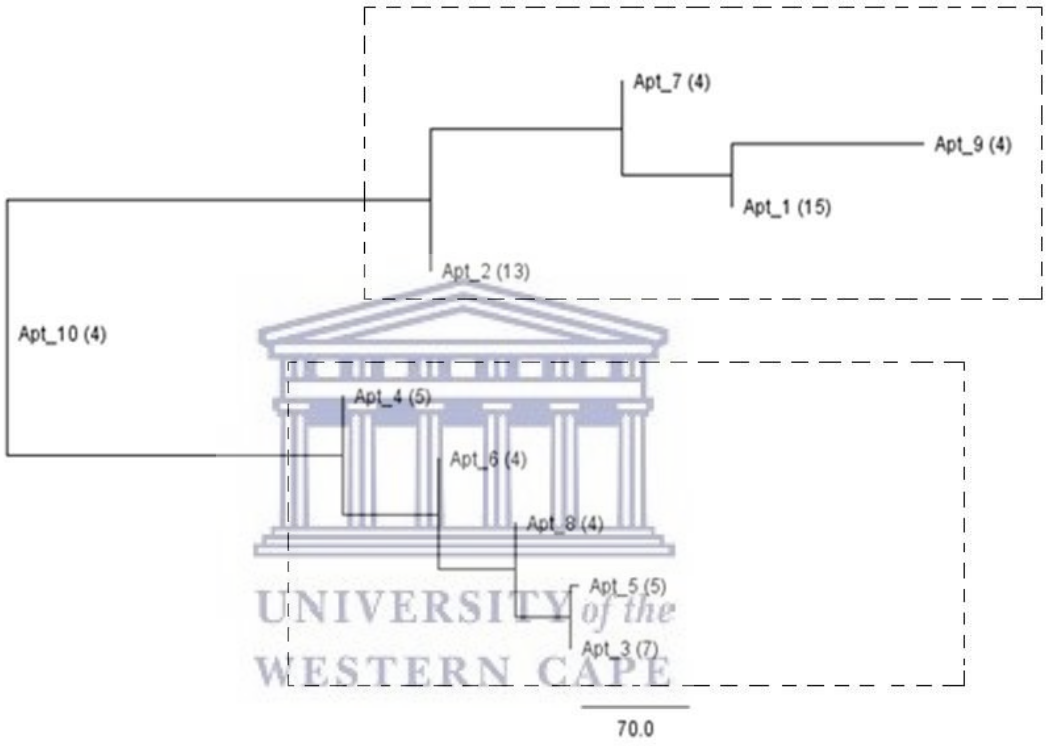

Figure 4. 8: Phylogenetic trees for the TR aptamers. The name of the aptamer (e.g. Apt_1, etc.) and number of repeats (in brackets) for each aptamer are indicated. The boxes indicate Clade 1 and 2 while 70.0 represent the frequency of evolution of the aptamers in the pool.

TR aptamers showed a distinct evolutionary tree as shown in Figure 4.8. Based on the phylogenetic tree, the aptamers appeared to have evolved from Apt_10. The evolving aptamers then diverged into two clades; Clade 1 is comprised of the Apt_1, Apt_2, Apt_7 and Apt_9, while clade 2 is comprised of Apt_3, Apt_4, Apt_5, Apt_6 and Apt_8. Aptamers in clade 1 contained Apt_1 and Apt_2, which are also the most recurring (frequent) aptamers with frequencies of 15 and 13.

http://etd.uwc.ac.za/

Since the selection pressure during SELEX will strengthen the evolution of aptamers with a higher affinity for the target protein, Apt_1 and Apt_2 might potentially be more suitable for application in the detection of TAGLN2. Apt_9, which was the last aptamer to evolve in clade 1, may also be a possibility. Clade 2 evolved before clade 1 and eventually produced Apt_4, which may therefore also be a possible consideration. The frequency of evolution (70.0) was attributed by the rate of mutations during PCR amplifications.

A pairwise sequence alignment analysis of clade 1 and 2 shows a distinct contrast attributed by the conserved regions in clade 1 (Figure 4.9). It is clear that the sequence alignment of the clade 1 was more homogenous compared to aptamers in clade 2. Therefore, based on this data, aptamer sequences from clade 1 (Apt_1, Apt_2, Apt_7 and Apt_9) were selected for further analysis.

UNIVERSITY of the
WESTERN CAPE

http://etd.uwc.ac.za/

Figure 4. 9: Pairwise sequence analysis of clade 1 and 2. Clade 1 has conserved regions that start from sequence ~35 to 50. The name of the aptamer (e.g. Apt_1, etc.) and number of repeats (in brackets) for each aptamer are indicated.

UNIVERSITY of the
WESTERN CAPE

http://etd.uwc.ac.za/

4.2.3.2 Identification of conserved motifs in clade 1.

The DNA sequence in the variable regions (VRs) of Apt_1, Apt_2, Apt_7 and Apt_9 were analysed using Multiple EM for Motif Elicitation (MEME) online software (http://meme-suite.org). MEME is an online tool that can be used to identify common sequence motifs in a group of related DNA sequences.

Conserved motifs in DNA aptamers have been shown to be involved in binding interactions between the aptamers and the target protein (Groher and Suess, 2016; Meng *et al.*, 2014; Murakami *et al.*, 2017; Percze *et al.*, 2017). Figure 4.10 shows the results for MEME analysis. Three recurring motifs (5'-GGGGTGG-3', 5'-TTTAT-3' and 5'-TAGTTA-3) were identified in aptamers from clade 1. The 5'-GGGGTGG-3' motif appeared more frequently than 5'-TTTAT-3' or 5'-TAGTTA-3'. The 5'-GGGGTGG-3' motif appeared 4 times in Apt_2 and 3 times in Apt_1, Apt_7 and Apt_9. It is known that DNA with a high GC content is more stable at higher temperatures, which may suggest that the aptamers from clade 1 can form high stable structures. The 5'-TTTAT-3' motif appeared only in Apt_2 and Apt_9, while the 5'-TAGTTA-3' motif only appeared in Apt_2 and Apt_7.

UNIVERSITY of the
WESTERN CAPE

http://etd.uwc.ac.za/

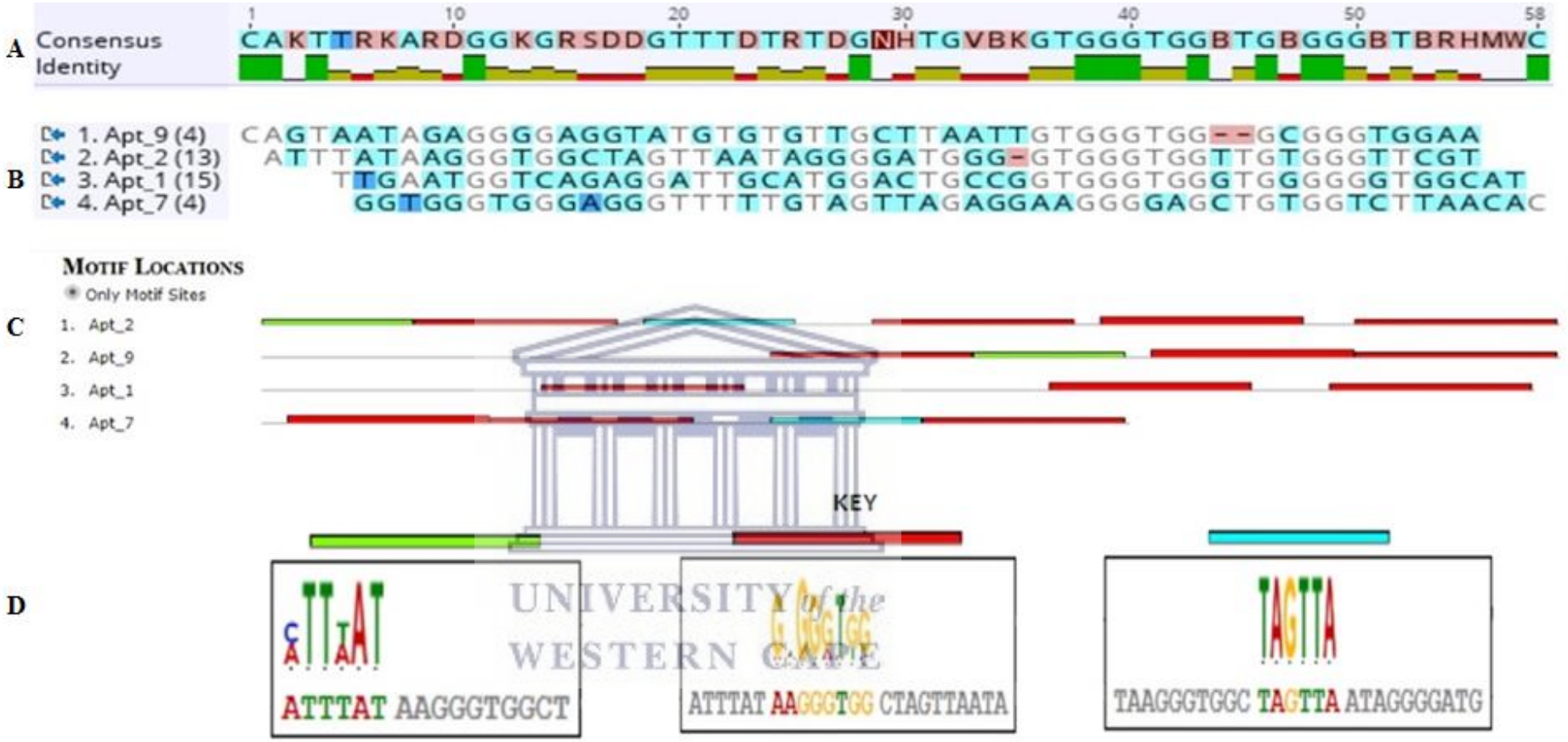

Figure 4. 10: MEME analysis of aptamer sequences from clade 1. A shows the consensus sequence, B shows the sequence alignment, C shows the positioning of the motifs in the VR of the aptamers, while D shows the sequence of the motifs and the variation of nucleotides within the motifs.

UNIVERSITY of the
WESTERN CAPE

http://etd.uwc.ac.za/

4.2.3.3 Aptamers secondary structures prediction by M-fold

M-fold (http://unafold.rna.albany.edu/?q=mfold) is a web-based online software tool that can be used to predict the suboptimal secondary structure of DNA by free energy minimization. Mfold was also used to confirm the location of conserved motifs within the secondary structures.

The formation of the aptamer secondary structure is dependent on the environmental conditions (i.e. pH, ionic strength and temperature) as this drive the formation of the helix structures supported by the hydrogen bonds of the stacked sequences (Bozza *et al*., 2006). The conditions for the structure predictions were set according to the constituents of the SELEX buffer (PBS) at 25 ^{0}C in 0.138mM NaCl and 1.5mM ions at pH 7.4. These conditions were selected, as it resembled the conditions used to do the aptamer selection in SELEX.

Since FL aptamer sequences were used during SELEX, structure predictions were done on both FL and TR aptamer sequences. The removal of the conserved primer sequences can have a significant effect on the folding of the aptamer, consequently affecting the binding negatively (Kaur and Yung, 2012). Conversely, the removal of the conserved primer sequences can also successfully reduce the length of an aptamer without any significant loss of its binding activity to the target (Akitomi *et al*., 2011). It is therefore advisable to perform an *in silico* prediction of the aptamer secondary structure with both FL and TR aptamer sequences. Figure 4.11 shows the *in silico* predicted structures of FL and TR for Apt_1, Apt_2, Apt_7 and Apt_9.

UNIVERSITY of the
WESTERN CAPE

http://etd.uwc.ac.za/

The aptamers were folded into unique structures that included loops and stems as shown in Figure 4.11. Structures generated for the FL sequences were more complex when compared to the TR sequences. The number of loops and stems in the FL sequences were much higher when compared to the TR sequences, which mostly consisted of one loop structure. The free energy (*dG*) predicted for the FL sequences was significantly lower (-7.14 to -9.65) when compared to the TR sequences (0.18 to -2.10). This suggests that FL structures are more likely to form under these environmental conditions. The structure predicted for Apt_2 had the lowest free energy (-9.65) suggesting that it will form more readily than the others. Amongst the TR sequences, Apt_1 had the lowest free energy (-2.10), while the TR sequence for Apt-9 was the only aptamer that produced a positive free energy (0.18), suggesting that this aptamer will only form if energy is applied in the form of heat.

UNIVERSITY of the
WESTERN CAPE

http://etd.uwc.ac.za/

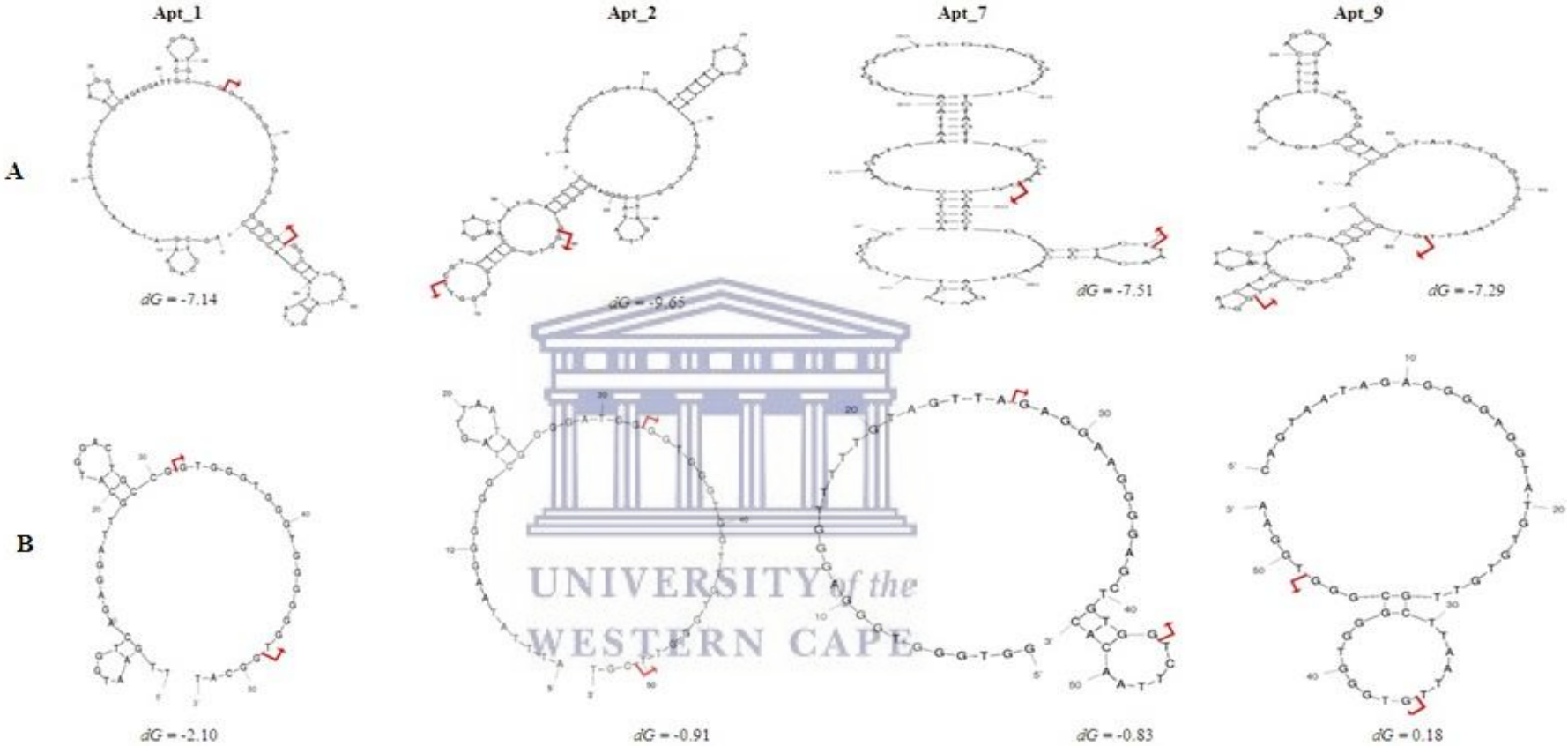

UNIVERSITY of the
WESTERN CAPE

Figure 4. 11: The predicted secondary structures for aptamers from clade 1. FL (A) and TR (B) sequences were analysed using M-fold. The red arrows in all the aptamers represent the conserved motifs regions. The free energy (*dG*) for each structure is also indicated.

http://etd.uwc.ac.za/

4.3 Conclusion

Four DNA aptamers (Apt_1, Apt_2, Apt_7 and Apt_9) that can potentially bind to TAGLN2, a potential serum TB biomarker protein were identified through 13 rounds of SELEX using a recombinant histidine tagged sample of this protein. The Apt_1 sequence appeared more frequently in the aptamer pool generated after 13 rounds of SELEX. Based on *in silico* structure prediction, the FL sequences for these aptamers are more likely to form using conditions that are comparable to the conditions used during SELEX. However, much of this is based on predictions, the actual binding of the aptamers to TAGLN2 needed to be verified experimentally using technologies such as EMSA, Isothermal Titration Calorimetry (ITC), Bio-Layer Interferometry (BLI) or Surface Plasmon Resonance (SPR).

UNIVERSITY of the
WESTERN CAPE

http://etd.uwc.ac.za/

CHAPTER 5
EVALUATING THE BINDING OF APT-1 TO RECOMBINANT TAGLN2 PROTEIN

5.1 Introduction

The Electrophoretic Mobility Shift Assay (EMSA) can be used to evaluate the interaction and formation of complexes between nucleic acids and proteins based on changes in the electrophoretic mobility of the complex (Hellman and Fried, 2007). The electrophoretic mobility of a molecule is determined by its net charge as well as its molecular weight. The higher the negative charge on the molecule, the faster the movement of the molecule through matrices such as agarose or acrylamide. Therefore, when a nucleic acid is bound to a protein the electrophoretic mobility will be reduced compared to the unbound nucleic acid, which move faster on the gel (Hellman and Fried, 2007). The nucleic acid/protein complex is also larger than either molecule on its own or therefore the nucleic acid/protein complex will also migrate slower.

UNIVERSITY of the
WESTERN CAPE

5.2 *In vitro* binding evaluation by EMSA

For logistical reasons not all 4 aptamers from clade 1 (Apt_1, Apt_2, Apt_7 and Apt_9) could be analysed by EMSA. Apt_1 was selected from the 4 aptamers to evaluate binding to TAGLN2. The selection of Apt_1 over the other 3 aptamers was based on the fact that DNA sequence analysis (discussed in Chapter 4) demonstrated that the Apt_1 aptamer sequence was more frequently amplified from an aptamer pool generated after 13 rounds of SELEX.

http://etd.uwc.ac.za/

The binding of Apt_1 to TAGLN2 was investigated using EMSA (Figure 5.1). Apt_1 (5 μM) was incubated with increasing concentrations (ranging from 5 to 500 nM) of target protein (TAGLN2). These protein/aptamer mixtures were analysed by polyacrylamide gel electrophoresis (PAGE). Figure 5.1 shows that the migration of bands produced for samples where the TAGLN2 and Apt_1 was mixed, was much slower than the migration of the band produced for free Apt_1 (FA). This suggests that Apt_1 was able to bind to TAGLN2. This shift can be observed for all 5 concentrations (5, 50, 15, 250 and 500nM) of Apt_1.

Two additional negative controls were performed. In Control 1, an unrelated known aptamer (this aptamer targets another cancer biomarker protein, Mucin-1, MUC-1) was incubated with TAGLN2. In Control 2, Apt_1 was incubated with HSA (which was used as a target in positive SELEX) but was not expected to bind Apt_1. The MUC-1 protein is known to be overexpressed in malignant cancer cells. The MUC-1 protein is coded for by the MUC-1 gene (Yang, *et al.*, 2017). Therefore, MUC-1 aptamer was used as a negative control since it has affinity for the MUC-1 protein and was not expected to bind to the TAGLN2 protein.

UNIVERSITY of the
WESTERN CAPE

Figure 5.1 shows that the migration of the band produced for samples from Control 1 was similar to the band produced for free Apt_1 (FA), suggesting no interaction between Mucin-1 aptamer and TAGLN2. However, the band produced for Control 2 shifted to the same position as was observed for the TAGLN2/Apt_1 mixture. This suggests that Apt_1 is able to bind HSA as well as TAGLN2 and is not able to discriminate between HSA and TAGLN2. It is therefore possible that not all aptamer sequences with an affinity for HSA were removed during positive SELEX.

http://etd.uwc.ac.za/

However, EMSA does not provide conclusive evidence of molecular interaction (Xie, *et al* 2016) and must be done in conjunction with other methods such as Isothermal Titration Calorimetry (ITC), Bio-Layer Interferometry (BLI) or Surface Plasmon Resonance (SPR), which is more definitive.

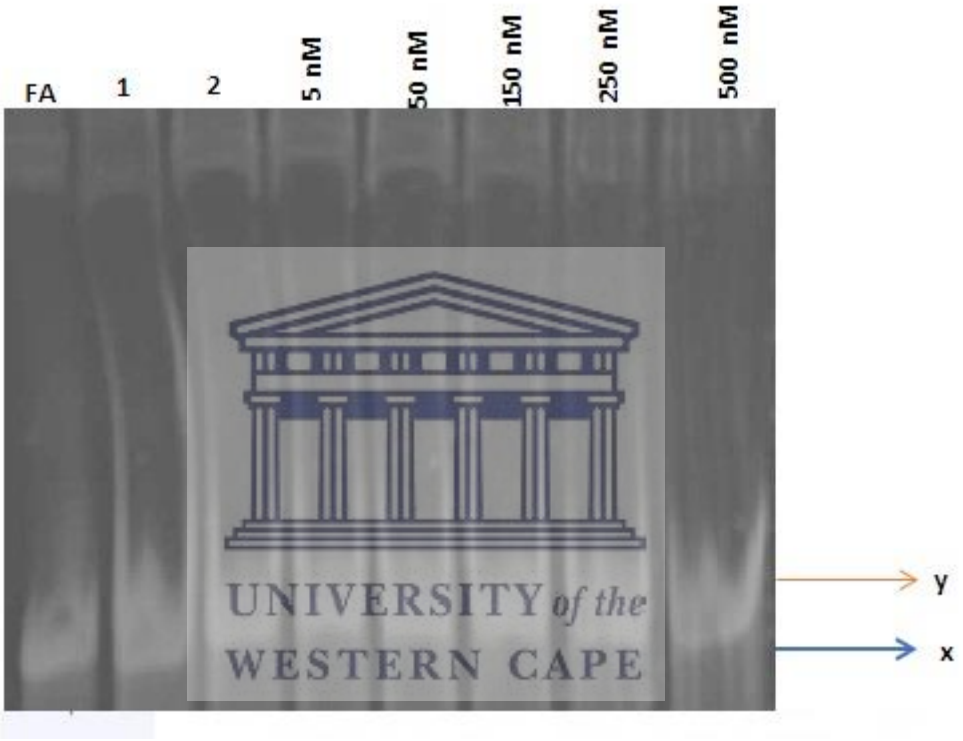

UNIVERSITY of the
WESTERN CAPE

Figure 5. 1: Analysis of Apt_1 binding to TAGLN2 using EMSA. FA: free aptamer; 1: Mucin-1 aptamer incubated with TAGLN2; 2: Apt-1 incubated with the HSA; 5 nM – 500 nM: increasing concentration of the TAGLN2 incubated with the Apt_1. The blue arrow (x) shows the migration of free aptamer, while the orange arrow (y) shows the migration of shifted aptamer/protein complex.

http://etd.uwc.ac.za/

5.3 Conclusion

EMSA provided preliminary evidence that Apt_1 binds to TAGLN2. However, the control experiment shows that Apt_1 binds also binds to HSA, which was used in the positive SELEX rounds.

EMSA does not provide information on the affinity or the rate of molecule/molecule interactions. It is also a very crude method to show that two molecules interact. Additional experimental work using technologies such as BLI and SPR is required to verify the interactions between Apt_1 and TAGLN2, and Apt_1 and HSA.

UNIVERSITY of the
WESTERN CAPE

http://etd.uwc.ac.za/

CHAPTER 6
CONCLUSIONS AND FUTURE WORK

The TAGLN2 recombinant protein was successfully expressed by recombinant DNA technology. The recombinant protein was successfully purified and lyophilized for further application in protein-aptamer interaction studies. The recombinant protein was used as a target for aptamers synthesis. Potential TB aptamers (Apt 1, 2, 7 and 9) were successfully synthesized by SELEX. The binding of these aptamers to TAGLN2 was further validated by Bioinformatics tools. Although EMSA showed potential binding of the aptamers to the target protein, the SPR ProteOn XPR36 analysis was inconclusive.

Binding of the aptamers to the TAGLN2 protein will be further characterized by other technologies such as the Biacore SPR or Isothermal Titration Colorimetry (ITC), UV-Vis absorption, BioLayer Interferometry (BLI), Quartz Micro Crystal Balance (QMCB) and the Nuclear Magnetic Resonance (NMR). These studies will facilitate the interaction mechanisms as well as demonstrate the potential selectivity, specificity and sensitivity of the aptamer to its target molecule. These techniques will also be used to determine the binding stoichiometry and *kd*s between the aptamers (FL and VR) and TAGLN2 protein as well as the protein-aptamer complex. Most importantly, the aptamers will be used in the development of a rapid and cost-effective nanotech-based detection system for diagnosis of TB positive patients at the POC.

UNIVERSITY of the
WESTERN CAPE

http://etd.uwc.ac.za/

References

Achkar, J. M., Cortes, L., Croteau, P., Yanofsky, C., Mentinova, M., Rajotte, I., Schirm, M., Zhou, Y., Junqueira-Kipnis, A. P., Kasprowicz, V. O., Larsen, M., Allard, R., Hunter, J., & Paramithiotis, E. (2015). Host Protein Biomarkers Identify Active Tuberculosis in HIV Uninfected and Co-infected Individuals. *EBioMedicine*, *2*(9), 1160–1168.

Afgan, E., Baker, D., van den Beek, M., Blankenberg, D., Bouvier, D., Čech, M., Chilton, J., Clements, D., Coraor, N., Eberhard, C., Grüning, B., Guerler, A., Hillman-Jackson, J., Von Kuster, G., Rasche, E., Soranzo, N., Turaga, N., Taylor, J., Nekrutenko, A., & Goecks, J. (2016). The Galaxy platform for accessible, reproducible and collaborative biomedical analyses. *Nucleic Acids Research*, *44*(Web Server issue).

AITC. (2019). AITC Immunization & Travel Clinic: *AITC Regular Prices* (online). Available: https://www.sfcdcp.org/aitc/aitc-regular-prices-low-cost-or-free-vaccines/. Date accessed 14 March, 2019.

Akitomi, J., Kato, S., Yoshida, Y., Horii, K., Furuichi, M., & Waga, I. (2011). ValFold: Program for the Aptamer Truncation Process. *Bioinformation 7*(1), 38-40.

Al-Nedawi, K., Meehan, B., Micallef, J., Lhotak, V., May, L., Guha, A., & Rak, J. (2008). Intercellular transfer of the oncogenic receptor EGFRvIII by microvesicles derived from tumour cells. *Nature Cell Biology*, *10*(5), 619–624.

Amano, R., Aoki, K., Miyakawa, S., Nakamura, Y., Kozu, T., Kawai, G., & Sakamoto, T. (2017). NMR monitoring of the SELEX process to confirm enrichment of structured RNA. *Scientific Reports*, *7*(1), 283.

Amatya, Y., Rupp, J., Russell, F. M., Saunders, J., Bales, B., & House, D. R. (2018). Diagnostic use of lung ultrasound compared to chest radiograph for suspected pneumonia in a resource-limited setting. *International journal of emergency medicine*, *11*(1), 8.

Angkawanish, T., Wajjwalku, W., Sirimalaisuwan, A., Mahasawangkul, S., Kaewsakhorn, T., Boonsri, K., & Rutten, V. (2010). Mycobacterium tuberculosis infection of domesticated Asian elephants, Thailand. *Emerging Infectious Diseases*, *16*(12), 1949–51.

Assinder, S. J., Stanton, J.-A. L., & Prasad, P. D. (2009). Transgelin: An actin-binding protein and tumour suppressor. *The International Journal of Biochemistry & Cell Biology*, *41*(3), 482–486.

UNIVERSITY of the WESTERN CAPE

http://etd.uwc.ac.za/

Ball, L., Vercesi, V., Costantino, F., Chandrapatham, K., & Pelosi, P. (2017). Lung imaging: how to get better look inside the lung. *Annals of Translational Medicine, 5*(14), 294.

Barberis, I., Bragazzi, N. L., Galluzzo, L., & Martini, M. (2017). The history of tuberculosis: from the first historical records to the isolation of Koch's bacillus. *Journal of preventive medicine and hygiene, 58*(1), E9-E12.

Behar, S. M., Divangahi, M., & Remold, H. G. (2010). Evasion of innate immunity by Mycobacterium tuberculosis: is death an exit strategy? *Nature Reviews Microbiology, 8*(9), 668–74.

Bell, L., & Noursadeghi, M. (2017). Pathogenesis of HIV-1 and Mycobacterium tuberculosis co-infection. *Nature Reviews Microbiology, 16*, 80-90.

Blouin, Y. (2015). A new scenario for the early evolution of Mycobacterium tuberculosis A new scenario for the early evolution of Mycobacterium tuberculosis. *PhD Thesis in Life and Health Sciences*.

Bock, L. C., Griffin, L. C., Latham, J. A., Vermaas, E. H., & Toole, J. J. (1992). Selection of single-stranded DNA molecules that bind and inhibit human thrombin. *Nature, 355*(6360), 564–566.

Boehme, C., & Nabeta, P. (2010). Rapid molecular detection of tuberculosis and rifampin resistance. *The New England Journal of Medicine*, 1005–1015.

Boum, Y., Orikiriza, P., Rojas-Ponce, G., Riera-Montes, M., Atwine, D., Nansumba, M., Bazira, J., Tuyakira, E., De Beaudrap, P., Bonnet, M., & Page, A.-L. (2013). Use of Colorimetric Culture Methods for Detection of Mycobacterium tuberculosis Complex Isolates from Sputum Samples in Resource-Limited Settings. *Journal of Clinical Microbiology, 51*(7), 2273–2279.

Bozza, M., Sheardy, R. D., Dilone, E., Scypinski, S., & Galazka, M. (2006). Characterization of the Secondary Structure and Stability of an RNA Aptamer That Binds Vascular Endothelial Growth Factor. *Biochemistry, 45*(24), 7639–7643.

Broger, T., Basu Roy, R., Filomena, A., Greef, C. H., Rimmele, .S, Havumaki, J., Danks, D., Schneiderhan-Marra, N., Gray, C. M., Singh, M., Rosenkrands, I., Andersen, P., Husar, G. M., Joos, T. O., Gennaro, M. L., Lochhead, M. J., Denkinger, C. M., & Perkins M. D. (2017). Diagnostic Performance of Tuberculosis-Specific IgG Antibody Profiles in Patients with Presumptive Tuberculosis from Two Continents. *Clinical Infectious Diseases. 64*(7), 947-955.

Budgell, E. P, Evans, D., Schnippel, K., Ive, P., Long, L., & Rosen, S. (2016). Outcomes of treatment of drug-susceptible tuberculosis at public sector

http://etd.uwc.ac.za/

primary healthcare clinics in Johannesburg, South Africa: A retrospective cohort study, *South African Medical Journal*, *106*(10), 1002-1009.

Caliskan, T., Ozkisa, T., Aribal, S., Kaya, H., Incedayi, M., Ulcay, A., & Ciftci, F. (2014). High resolution computed tomography findings in smear-negative pulmonary tuberculosis patients according to their culture status. *Journal of Thoracic Disease*, *6*(6), 706–712.

Carstens, C.-P., Bonnardel, J., Allen, R., & Waesche, A. (2001). BL21-CodonPlus™ cells correct expression problems caused by codon bias. *Strategies*, *14*, 50–52.

Chen, A., & Yang, S. (2015). Replacing antibodies with aptamers in lateral fl ow immunoassay. *Biosensors and Bioelectronic*, *71*, 230–242.

Chen, F., Zhang, X., Zhou, J., Liu, S., & Liu, J. (2012). Aptamer inhibits Mycobacterium tuberculosis (H37Rv) invasion of macrophage. *Molecular Biology Reports*, *39*(3), 2157–2162.

Chen, F., Zhou, J., Luo, F., Mohammed, A.-B., & Zhang, X.-L. (2007). Aptamer from whole-bacterium SELEX as new therapeutic reagent against virulent Mycobacterium tuberculosis. *Biochemical and Biophysical Research Communications*, *357*(3), 743–748.

Chen, L., Rashid, F., Shah, A., Awan, H., Wu, M., Liu, A., Wang, J., Zhu, T., Luo, Z., & Shan, G. (2015). The isolation of an RNA aptamer targeting to p53 protein with single amino acid mutation. *Proceedings of the National Academy of Sciences*, *112*(32), 10002–10007.

Chen, M., Yu, Y., Jiang, F., Zhou, J., Li, Y., Liang, C., Dang, L., Lu, A., & Zhang, G. (2016). Development of Cell-SELEX Technology and Its Application in Cancer Diagnosis and Therapy. *International Journal of Molecular Sciences*, *17*(12), 2079.

Cheng, C., & Shuman, S. (2000). DNA strand transfer catalyzed by vaccinia topoisomerase: ligation of DNAs containing a 3' mononucleotide overhang. *Nucleic Acids Research*, *28*(9), 1893–1898.

Cheng, Y., Liu, C., Zhang, N., Wang, S., & Zhang, Z. (2014). Proteomics analysis for finding serum markers of ovarian cancer. *BioMed research international*, *2014*, 179040.

Cho, W. C. S., Yip, T.-T., Chung, W.-S., Leung, A. W. N., Cheng, C. H. K., & Yue, K. K. M. (2006). Potential biomarkers found by protein profiling may provide insight for the macrovascular pathogenesis of diabetes mellitus. *Disease Markers*, *22*, 153–166.

http://etd.uwc.ac.za/

Caulfield, A. J., & Wengenack, N. L. (2016). Diagnosis of active tuberculosis disease: From microscopy to molecular techniques. *Journal of Clinical Tuberculosis and Other Mycobacterial Diseases, 4*: 33-43.

Comucci, E. B., Vasques, A. C., Geloneze, B., Calixto, A. R., Pareja, J. C., & Tambascia, M. A. (2014). Serum levels of retinol binding protein 4 in women with different levels of adiposity and glucose tolerance, *Arquivos Brasileiros de Endocrinologia Metabologia, 58*(7), 709-14.

Darmostuk, M., Rimpelova, S., Gbelcova, H., & Ruml, T. (2014). Current approaches in SELEX: An update to aptamer selection technology. *Biotechnology Advances, 33*(6), 1141–1161.

Davies, P., & Pai, M. (2008). The diagnosis and misdiagnosis of tuberculosis. *International Journal of Tuberculosis and Lung Disease, 12*(11), 1226–34.

Davis, L., Cattamanchi, A., Cuevas, L., Hopewell, P., & Steingart, K. (2013). Diagnostic accuracy of same-day microscopy versus standard microscopy for pulmonary tuberculosis: a systematic review and meta-analysis. *The Lancet. Infectious Diseases, 13*(2), 147–154.

Del Ciello, A., Franchi, P., Contegiacomo, A., Cicchetti, G., Bonomo, L., & Larici, A. R. (2017). Missed lung cancer: when, where, and why? *Diagnostic and Interventional Radiology, 23*(2), 118–126.

Ellington, D. A., & Szostak, W. J. (1990). In vitro selection of RNA molecules that bind specific ligands. *Nature, 346*(6287), 818-822.

Fagerberg, L., Hallström, B. M., Oksvold, P., Kampf, C., Djureinovic, D., Odeberg, J., Habuka, M., Tahmasebpoor, S., Danielsson, A., Edlund, K., Asplund, A., Sjöstedt, E., Lundberg, E., Szigyarto, C. A., Skogs, M., Takanen, J. O., Berling, H., Tegel, H., Mulder, J., Nilsson, P., Schwenk, J. M., Lindskog, C., Danielsson, F., Mardinoglu, A., Sivertsson, A., von Feilitzen, K., Forsberg, M., Zwahlen, M., Olsson, I., Navani, S., Huss, M., Nielsen, J., Ponten, F., & Uhlén, M. (2014). Analysis of the human tissue-specific expression by genome-wide integration of transcriptomics and antibody-based proteomics. *Molecular & Cellular Proteomics, 13*(2), 397–406.

Falzon, D., Timimi, H., Kurosinski, P., Migliori, G. B., Van Gemert, W., Denkinger, C., Isaacs, C., Story, A., Garfein, R. S., do Valle Bastos, L. G., Yassin, M. A., Rusovich, V., Skrahina, A., Van Hoi, L., Broger, T. , Abubakar, I., Hayward, A., Thomas, B. V., Temesgen, Z., Quraishi, S., von Delft, D., Jaramillo, E., Weyer, K., & Raviglione, M. C. (2016). Digital health for the End TB Strategy: developing priority products and making them work. *European Respiratory Journal, 48*(1):29-45. Date accessed 23 November, 2017.

http://etd.uwc.ac.za/

Fleige, S., & Pfaffl, M. W. (2006). RNA integrity and the effect on the real-time qRT-PCR performance. *Molecular Aspects of Medicine*, *27*, 126–139.

Foell, D., Wittkowski, H., Vogl, T., & Roth, J. (2007). S100 proteins expressed in phagocytes: a novel group of damage-associated molecular pattern molecules. *Journal of Leukocyte Biology*, *81*(1), 28–37.

Fogel, N. (2015). Tuberculosis: A disease without boundaries. *Tuberculosis 95*, 5:527-531

Fu, R., & Gong, J. (2017). Single Cell Analysis Linking Ribosomal (r)DNA and rRNA Copy Numbers to Cell Size and Growth Rate Provides Insights into Molecular Protistan Ecology. *The Journal of eukaryotic microbiology*, *64*(6), 885-896.

Fu, T., & Xie, J. (2011). Progress on the biomarkers for tuberculosis diagnosis. *Critical Reviews in Eukaryotic Gene Expression*, *21*(4), 379–91.

Gagoski, D., Polinkovsky, M. E., Mureev, S., Kunert, A., Johnston, W., Gambin, Y., & Alexandrov, K. (2016). Performance benchmarking of four cell-free protein expression systems. *Biotechnology and Bioengineering*, *113*(2), 292–300.

Gao, F., Koenitzer, J. R., Tobolewski, J. M., Jiang, D., Liang, J., Noble, P. W., & Oury, T. (2008). Extracellular superoxide dismutase inhibits inflammation by preventing oxidative fragmentation of hyaluronan. *Nat Rev Mol Cell Biol.*, *283*(10), 6058-66.

Gong, Q., Wang, J., Ahmad, K. M., Csordas, A., Zhou, J., Nie, J., Stewart, R., Thomson, S. A., Rossi, J. J., & Soh, H. T. (2013). Selection Strategy to Generate Aptamer Pairs that Bind to Distinct Sites on Protein Targets. *Anal Chem*, *84*(12), 5365–5371.

Gopal, R., Monin, L., Torres, D., Slight, S., Mehra, S., McKenna, K. C., Junecko, B. A. F., Reinhart, T. A., Kolls, J., Báez-Saldaña, R., Cruz-Lagunas, A., Rodríguez-Reyna, T. S., Kumar, N. P., Tessier, P., Roth, J., Selman, M., Becerril-Villanueva, E., Baquera-Heredia, J., Cumming, B., Kasprowicz, V. O., Steyn, A. J. C., Babu, S., Kaushal, D., Zúñiga, J., Vogl, T., Rangel-Moreno, J., & Khader, S. A. (2013). S100A8/A9 Proteins Mediate Neutrophilic Inflammation and Lung Pathology during Tuberculosis. *American Journal of Respiratory and Critical Care Medicine*, *188*(9), 1137–1146.

Groher, F., & Suess, B. (2016). In vitro selection of antibiotic-binding aptamers. *Methods*, *106*:42–50.

UNIVERSITY of the WESTERN CAPE

http://etd.uwc.ac.za/

Grote, D., Olmos, A., Kofoet, A., Tuset, J. J., Bertolini, E., & Cambra, M. (2002). Specific and Sensitive Detection of Phytophthora nicotianae By Simple and Nested-PCR. *European Journal of Plant Pathology*, *108*(3), 197–207.

Guggino, G., Orlando, V., Cutrera, S., La, M. P., Di Liberto, D., Vanini, V., Petruccioli, E., Dieli, F., Goletti, D., & Caccamo, N. (2015). Granzyme A as a potential biomarker of Mycobacterium tuberculosis infection and disease, *166*:87–91.

Hare, N. J., Chan, B., Chan, E., Kaufman, K. L., Britton, W. J., & Saunders, B. M. (2015). Microparticles released from Mycobacterium tuberculosis infected human macrophages contain increased levels of the type I interferon inducible proteins including ISG15. *Proteomics*, *15*(17), 3020–3029.

Haridas, T. K., & Thiruvengadam, S. (2014). Development of a PCR based nucleic acid lateral flow assay device for detection of mycobacterium tuberculosis complex. *International Journal of PharmTech Research*, *6*(5), 1695-1702.

He, C.-Z., Zhang, K.-H., Wang, T., Wan, Q.-S., Hu, P.-P., Hu, M.-D., Huang, D.-Q., & Lv, N.-H. (2013). Single-primer-limited amplification: A method to generate random single-stranded DNA sub-library for aptamer selection. *Analytical Biochemistry*, *440*(1), 63–70.

Hellman, L. M., & Fried, M. G. (2007). Electrophoretic mobility shift assay (EMSA) for detecting protein–nucleic acid interactions. *Nature Protocols*, *2*(8), 1849–1861.

Heo, E. Y., Chun, E. J., Lee, C. H., Kim, Y. W., Han, S. K., Shim, Y. S., Lee, H. J., & Yim, J. J. (2009). Radiographic improvement and its predictors in patients with pulmonary tuberculosis. *International Journal of Infectious Diseases*, *13*(6), e371-376.

Huddart, S., Nash, M., & Pai, M., (2016). Tuberculosis diagnosis: Challenges and solutions. *Journal of Health Specialties*, *4*(4), 230-237.

Hunter, R. L. (2016). Tuberculosis as a three-act play: A new paradigm for the pathogenesis of pulmonary tuberculosis. *Tuberculosis (Edinburgh, Scotland)*, *97*:8–17.

Invitrogen. (2006). Champion™ pET Directional TOPO® Expression Kits. *User Manual*. Available: https://assets.thermofisher.com/TFS-Assets/LSG/manuals/pettopo_man.pdf. Date accessed 13 April, 2017.

Jakovljevic, J., de Mayolo, P. A., Miles, T. D., Nguyen, T. M.-L., Léger-Silvestre, I., Gas, N., & Woolford, J. L. (2004). The carboxy-terminal extension of yeast ribosomal protein S14 is necessary for maturation of 43S preribosomes. *Molecular Cell*, *14*(3), 331–42.

UNIVERSITY of the WESTERN CAPE

http://etd.uwc.ac.za/

James, W. (2000). Aptamers. *Encyclopedia of Analytical Chemistry*. R. A. Meyers (Ed.), John Wiley & Sons Ltd, Chichester, 4848-4871.

Jarosch, F., Buchner, K., & Klussmann, S. (2006). In vitro selection using a dual RNA library that allows primerless selection. *Nucleic Acids Research*, *34*(12), e86.

Jasenosky, L. D., Scriba, T. J., Hanekom, W. A. & Goldfeld, A. E. (2015). T cells and adaptive immunity to Mycobacterium tuberculosis in humans. *Immunological Reviews, 264*(1), 74-87.

Jeong, Y. H., Hur, Y.-G., Lee, H., Kim, S., Cho, J.-E., Chang, J., Shin, S. J., Lee, H., Kang, Y. A., Cho, S.-N., Ha, S.-J., & Forbes, B. A. (2015). Discrimination between Active and Latent Tuberculosis Based on Ratio of Antigen-Specific to Mitogen-Induced IP-10 Production. *Journal of Clinical Microbiology, 53*(2): 504-510.

Kaur, H., & Yung, L. Y. L. (2012). Probing High Affinity Sequences of DNA Aptamer against $VEGF_{165}$. *PLoS One 7*, e31196.

Kearse, M., Moir, R., Wilson, A., Stones-Havas, S., Cheung, M., Sturrock, S., Buxton, S., Cooper, A., Markowitz, S., Duran, C., Thierer, T., Ashton, B., Meintjes, P., & Drummond, A. (2012). Geneious Basic: An integrated and extendable desktop software platform for the organization and analysis of sequence data, *Bioinformatics*, *28*(12), 1647–1649.

Kirwan, D. E., Ugarte-Gil, C., Gilman, R. H., Caviedes, L., Rizvi, H., Ticona, E., Chavez, G., Cabrera, J. L., Matos, E. D., Evans, C. A., Moore, D. A. J., & Friedland, J. S. (2016). Microscopic Observation Drug Susceptibility Assay for Rapid Diagnosis of Lymph Node Tuberculosis and Detection of Drug Resistance. *Journal of Clinical Microbiology*, *54*:185–189.

Kiso, K., Yoshifuji, H., Oku, T., Hikida, M., Kitagori, K., Hirayama, Y., Nakajima, T., Haga, H., Tsuruyama, T., & Miyagawa-Hayashino, A. (2017). Transgelin-2 is upregulated on activated B-cells and expressed in hyperplastic follicles in lupus erythematosus patients. *PLoS One*, *12*(9), e0184738.

Koczula, K. M., & Gallotta, A. (2016). Lateral flow assays. *Essays In Biochemistry*, *60*(1), 111–120.

Kurt, B. (2013). *Aptamers as a new alternative to antibodies* (online). Available: http://www.int.laborundmore.com/archive/826310/Aptamers-as-a-new-alternative-to-antibodies.html. Date accessed 29 August, 2018.

Kusser, W. (2000). Chemically modified nucleic acid aptamers for in vitro selections: evolving evolution. *Journal of Biotechnology*, *74*(1), 27–38.

http://etd.uwc.ac.za/

Lai, J.-C., & Hong, C.-Y. (2014). A novel protocol for generating high-affinity ssDNA aptamers by using alternating magnetic fields. *Journal of Materials Chemistry B*.

Lambert, L., Rajbhandary, S., Qualls, N., Budnick, L., Catanzaro, A., Cook, S., Daniels-Cuevas, L., Garber, E., & Reves, R. (2015). Costs of Implementing and Maintaining a Tuberculin Skin Test Program in Hospitals and Health Departments. *Infection Control & Hospital Epidemiology*, *24*(11), 814-820.

Lange, C., & Mori, T. (2010). Advances in the diagnosis of tuberculosis. *Respirology*, *15*(2), 220–240.

Lawn, S. D., & Churchyard, G. (2009). Epidemiology of HIV-associated tuberculosis Running Head: Epidemiology of TB /HIV Europe PMC Funders Group. *Curr Opin HIV AIDS*, *4*(4), 325–333.

Le Bouc, Y., Bellocq, A., Philippe, C., Perin, L., Garabedian, M., Fouqueray, B., Zacharias, C., Cadranel, J., & Baud, L. (1997). Insulin-like growth factors and their binding proteins in pleural fluid. *European Journal of Endocrinology*, *137*(5), 467–73.

Lee, J. Y. (2015). Diagnosis and Treatment of Extrapulmonary Tuberculosis. *Tuberculosis and Respiratory Diseases*, *78*(2), 47–55.

Lee, K.-A., Ahn, J.-Y., Lee, S.-H., Singh Sekhon, S., Kim, D.-G., Min, J., & Kim, Y.-H. (2015). Aptamer-based Sandwich Assay and its Clinical Outlooks for Detecting Lipocalin-2 in Hepatocellular Carcinoma (HCC). *Scientific Reports*, *5*(1), 10897.

Legiewicz, M., Lozupone, C., Knight, R., & Yarus, M. (2005). Size, constant sequences, and optimal selection. *RNA (New York, N.Y.)*, *11*(11), 1701-9.

Lewinsohn, D. M., Leonard, M. K., LoBue, P. A., Cohn, D. L., Daley, C. L., Desmond, E., Keane, J., Lewinsohn, D. A., Loeffler, A. M., Mazurek, G. H., O'Brien, R. J., Pai, M., Richeldi, L., Salfinger, M., Shinnick, T. M., Sterling, T. R., Warshauer, D. M., & Woods, G. L. (2017). Official American Thoracic Society/Infectious Diseases Society of America/Centers for Disease Control and Prevention Clinical Practice Guidelines: Diagnosis of Tuberculosis in Adults and Children. *Clinical Infectious Diseases : An Official Publication of the Infectious Diseases Society of America*, *64*(2), 111–115.

Li, C., Chen, H., Ding, F., Zhang, Y., Luo, A., Wang, M., & Liu, Z. (2009). A novel p53 target gene, S100A9, induces p53-dependent cellular apoptosis and mediates the p53 apoptosis pathway. *The Biochemical Journal*, *422*(2), 363–72.

UNIVERSITY of the WESTERN CAPE

http://etd.uwc.ac.za/

Lieberman, J. (2003). Cell death and immunity: The ABCs of granule-mediated cytotoxicity: new weapons in the arsenal. *Nature Reviews Immunology*, *3*(5), 361–370.

Lieberman, J. (2010). Granzyme A activates another way to die. *Immunological Reviews*, *235*(1), 93–104.

Lin, H., Zhang, W., Jia, S., Guan, Z., Yang, C. J., & Zhu, Z. (2014). Microfluidic approaches to rapid and efficient aptamer selection. *Biomicrofluidics*, *8*(4), 041501.

Little, K. M., Pai, M., & Dowdy, D. W. (2015). Costs and Consequences of Using Interferon-γ Release Assays for the Diagnosis of Active Tuberculosis in India. *PloS one*, *10*(4), e0124525.

Liu, J., & Lu, Y. (2006a). Fast Colorimetric Sensing of Adenosine and Cocaine Based on a General Sensor Design Involving Aptamers and Nanoparticles. *Angewandte Chemie International Edition*, *45*(1), 90–94.

Liu, J., & Lu, Y. (2006b). Preparation of aptamer-linked gold nanoparticle purple aggregates for colorimetric sensing of analytes. *Nature Protocols*, *1*(1), 246–252.

Lorenz, T. C. (2012). Polymerase chain reaction: basic protocol plus troubleshooting and optimization strategies. *Journal of Visualized Experiments : JoVE*, (63), e3998.

Low, S. Y., Hill, J. E., & Peccia, J. (2009). DNA aptamers bind specifically and selectively to (1→3)-β-d-glucans. *Biochemical and Biophysical Research Communications*, *378*(4), 701–705.

UNIVERSITY of the
WESTERN CAPE

Lu, C., Liu, Q., Sarma, A., Fitzpatrick, C., Falzon, D., & Mitnick, C. D. (2013). A systematic review of reported cost for smear and culture tests during multidrug-resistant tuberculosis treatment. *PloS one*, *8*(2), e56074.

Mahmoudi, S., Mamishi, S., & Pourakbari, B. (2016). *Potential Markers for the Discrimination of Active and Latent Tuberculosis Infection: Moving the Research Agenda Forward*. SMGroup publishers (1st Edition), 1-9.

Marko-Varga, G., Lindberg, H., Löfdahl, C.-G., Jönsson, P., Hansson, L., Dahlbäck, M., Lindquist, E., Johansson, L., Foster, M., & Fehniger, T. E. (2005). Discovery of biomarker candidates within disease by protein profiling: principles and concepts. *Journal of Proteome Research*, *4*(4), 1200–1212.

Meng, H.-W., Pagano, J. M., White, B. S., Toyoda, Y., Min, I. M., Craighead, H. G., Shalloway, D., Lis, J. T., & Jin, M. M. (2014). Discovering Aptamers by Cell-SELEX against Human Soluble Growth Factors Ectopically Expressed on Yeast Cell Surface. *PLoS One*, *9*(3), e93052.

http://etd.uwc.ac.za/

Meyer, S., Maufort, J. P., Nie, J., Stewart, R., McIntosh, B. E., Conti, L. R., Ahmad, K. M., Soh, H. T., & Thomson, J. A. (2013). Development of an Efficient Targeted Cell-SELEX Procedure for DNA Aptamer Reagents. *PLoS One*, *8*(8), e71798.

Michos, A. G., Daikos, G. L., Tzanetou, K., Theodoridou, M., Moschovi, M., Nicolaidou, P., Petrikkos, G., Syriopoulos, T., Kanavaki, S., & Syriopoulou, V. P. (2006). Detection of Mycobacterium tuberculosis DNA in respiratory and nonrespiratory specimens by the Amplicor® MTB PCR. *Diagnostic Microbiology and Infectious Disease*, *54*(2), 121–126.

Montales, M. T., Beebe, A., Chaudhury, A., & Patil, N. (2015). *Mycobacterium tuberculosis* infection in a HIV-positive patient. *Respiratory Medicine Case Reports, 16*:160–162.

Mozioglu, E., Gokmen, O., Tamerler, C., Kocagoz, Z. T., & Akgoz, M. (2016). Selection of Nucleic Acid Aptamers Specific for Mycobacterium tuberculosis. *Applied Biochemistry and Biotechnology*, *178*(4), 849–864.

Mukai, S., Shigemura, K., Yamamichi, F., Kitagawa, K., Takami, N., Nomi, M., Arakawa, S., & Fujisawa, M. (2017). Comparison of cost-effectiveness between the quantiFERON-TB Gold-In-Tube and T-Spot tests for screening health-care workers for latent tuberculosis infection. *International Journal of Mycobacteriol*, *6*(1), 83-86.

Murakami, K., Zhao, J., Yamasaki, K., & Miyagishi, M. (2017). Biochemical and structural features of extracellular vesicle-binding RNA aptamers. *Biomedical Reports*, *6*(6), 615–626.

UNIVERSITY of the
WESTERN CAPE

Muthelo, P. M., & Meyer, M. (2015). *Development of a nanoparticle based diagnostic using a novel breast cancer biomarker*. Unpublished Master's thesis. Capetown. University of the Western Cape.

Na, B.-R., Kwon, M.-S., Chae, M.-W., Kim, H.-R., Kim, C.-H., Jun, C.-D., & Park, Z.-Y. (2016). Transgelin-2 in B-Cells Controls T-Cell Activation by Stabilizing T Cell - B Cell Conjugates. *PloS One*, *11*(5), e0156429.

Ninan, M. M., Gowri, M., Christopher, D. J., Rupali, P., & Michael, J. S. (2016). The diagnostic utility of line probe assays for multidrug-resistant tuberculosis. *Pathogens and Global Health*, *110*(4-5), 194–199.

Niu, S., Lv, Z., Liu, J., Bai, W., Yang, S., & Chen, A. (2014). Colorimetric Aptasensor Using Unmodified Gold Nanoparticles for Homogeneous Multiplex Detection. *PLoS One*, *9*(10), e109263.

http://etd.uwc.ac.za/

Nozik-Grayck, E., Suliman, H. B., & Piantadosi, C. A. (2005). Extracellular superoxide dismutase. *The International Journal of Biochemistry & Cell Biology*, *37*(12), 2466–2471.

Ozer, A., Pagano, J. M., & Lis, J. T. (2014). New technologies provide quantum changes in the scale, speed, and success of SELEX methods and aptamer characterization. *Molecular Therapy - Nucleic Acids*, *3*:1–18.

Palange, P., Narang, R., & Kandi, V. (2016). Evaluation of Culture Media for Isolation of Mycobacterium Species from Human Clinical Specimens. *Cureus*, *8*(8), e757.

Palomino, J. C., Cardoso, S., & Ritacco, V. (2007). *Tuberculosis 2007: From basic science to patient care*. Flying publishers (1st Edition), 1–687.

Pandey, P., Pant, N. D., Rijal, K. R., Shrestha, B., Kattel, S., Banjara, M. R., Maharjan, B., & KC, R. (2017). Diagnostic Accuracy of GeneXpert MTB/RIF Assay in Comparison to Conventional Drug Susceptibility Testing Method for the Diagnosis of Multidrug-Resistant Tuberculosis. *PLoS One*, *12*(1), e0169798.

Pantoja, A., Kik, S. V., & Denkinger, C. M. (2015). Costs of novel tuberculosis diagnostics-will countries be able to afford it? *The Journal of Infectious Diseases*, *211*(2), S67–S77.

Parsons, S. D. C., Gous, T. A., Warren, R. M., & Van Helden, P. D. (2008). Pulmonary Mycobacterium tuberculosis (Beijing strain) infection in a stray dog. *Clinical Communication*, *79*(2), 95–98.

Percze, K., Szakács, Z., Scholz, É., András, J., Szeitner, Z., Kieboom, C. H., Ferwerda, G., Jonge, M. I., Gyurcsányi, R. E., & Mészáros, T. (2017). Aptamers for respiratory syncytial virus detection. *Scientific Reports*, *7*: 42794.

Peruń, A., Biedroń, R., Konopiński, M. K., Białecka, A., Marcinkiewicz, J., & Józefowski, S. (2017). Phagocytosis of live versus killed or fluorescently labeled bacteria by macrophages differ in both magnitude and receptor specificity. *Immunology & Cell Biology*, *95*(5), 424-435.

Phillips, M., Basa-Dalay, V., Bothamley, G., Cataneo, R. N., Lam, P. K., Natividad, M. P. R., Schmitt, P., & Wai, J. (2010). Breath biomarkers of active pulmonary tuberculosis. *Tuberculosis*, *90*(2), 145–151.

Pierce, K. E., Sanchez, J. A., Rice, J. E., & Wangh, L. J. (2005). Linear-After-The-Exponential (LATE)-PCR: primer design criteria for high yields of specific single-stranded DNA and improved real-time detection. *Proceedings of the National Academy of Sciences of the United States of America*, *102*(24), 8609–8614.

http://etd.uwc.ac.za/

Pieters, J. (2008). Mycobacterium tuberculosis and the macrophage: maintaining a balance. *Cell Host Microbe, 3*(6), 399-407.

Pingle, P., Apte, P., & Trivedi, R. (2014). Evaluation of Microscopy, Culture and PCR Methods in the Laboratory Diagnosis of Genito-urinary Tuberculosis. *American Journal of Infectious Diseases and Microbiology, 2*(1), 17–21.

Poste, G. (2011). Bring on the biomarkers. *Nature, 469*(7329), 156-157.

Qin, L., Zheng, R., Ma, Z., Feng, Y., Liu, Z., Yang, H., Wang, J., Jin, R., Lu, J., Ding, Y., & Hu, Z. (2009). The selection and application of ssDNA aptamers against MPT64 protein in Mycobacterium tuberculosis. *Clinical Chemistry and Laboratory Medicine, 47*(4), 405–411.

Qu, H., Csordas, A. T., Wang, J., Oh, S. S., Eisenstein, M. S., & Soh, H. T. (2016). Rapid and Label-Free Strategy to Isolate Aptamers for Metal Ions. *American Chemical Society Journal of Nanoscience and Nanotechnology, 10*(8), 7558–7565.

Ray, S., Reddy, P. J., Jain, R., Gollapalli, K., Moiyadi, A., & Srivastava, S. (2011). Proteomic technologies for the identification of disease biomarkers in serum: Advances and challenges ahead. *Proteomics, 11*(11), 2139–2161.

Reinemann, C., & Strehlitz, B. (2014). Aptamer-modified nanoparticles and their use in cancer diagnostics and treatment. *Swiss Medical Weekly, 144*, w13908.

Robertson, D. L., & Joyce, G. (1990). Selection in vitro of an RNA enzyme that specifically cleaves single-stranded DNA. *Nature, 344*(6265), 467–468.

Rodriguez-Campos, S., Smith, N. H., Boniotti, M. B., & Aranaz, A. (2014). Overview and phylogeny of Mycobacterium tuberculosis complex organisms: Implications for diagnostics and legislation of bovine tuberculosis. *Research in Veterinary Science, 97*(S), S5-S19.

Rodríguez-Piñeiro, A. M., Blanco-Prieto, S., Sánchez-Otero, N., Rodríguez-Berrocal, F. J., & Páez de la Cadena, M. (2010). On the identification of biomarkers for non-small cell lung cancer in serum and pleural effusion. *Journal of Proteomics, 73*(8), 1511–1522.

Rotherham, L. S., Maserumule, C., Dheda, K., Theron, J., & Khati, M. (2012). Selection and Application of ssDNA Aptamers to Detect Active TB from Sputum Samples. *PLoS One, 7*(10), e46862.

Sanchez, J. A., Pierce, K. E., Rice, J. E., & Wangh, L. J. (2004). Linear-after-the-exponential (LATE)-PCR: an advanced method of asymmetric PCR and its uses in quantitative real-time analysis. *Proceedings of the National Academy of Sciences of the United States of America, 101*(7), 1933–1938.

UNIVERSITY of the
WESTERN CAPE

http://etd.uwc.ac.za/

Senthilingam, M. (2015). *How animals can give you tuberculosis*. CNN Report (online). Available: https://edition.cnn.com/2015/12/23/health/tuberculosis-from-animals/index.html. Date accessed 17 May, 2017.

Shah, M., Chihota, V., Coetzee, G., Churchyard, G., & Dorman, S. E. (2013). Comparison of laboratory costs of rapid molecular tests and conventional diagnostics for detection of tuberculosis and drug-resistant tuberculosis in South Africa. *BioMed Central infectious diseases, 13*; 352.

Shigdar, S., Macdonald, J., O'Connor, M., Wang, T., Xiang, D., Al Shamaileh, H., Qiao, L., Wei, M., Zhou, S. F., Zhu, Y., Kong, L., Bhattacharya, S., Li, C., & Duan, W. (2013). Aptamers as theranostic agents: modifications, serum stability and functionalisation. *Sensors (Basel, Switzerland)*, *13*(10), 13624–13637.

Shum, K. T., Lui, E. L. H., Wong, S. C. K., Yeung, P., Sam, L., Wang, Y., Watt, R. M., & Tanner, J. A. (2011). Aptamer-Mediated Inhibition of Mycobacterium tuberculosis Polyphosphate Kinase 2. *Biochemistry*, *50*(15), 3261–3271.

Shuman, S. (1994). Novel Approach to Molecular Cloning and Polynucleotide Synthesis Using Vaccinia DNA Topoisomerase. *The Journal of Biological Chemistry*, *269*(51), 32678-32684.

Siddiqi, K., Lambert, M.-L., & Walley, J. (2003). Clinical diagnosis of smear-negative pulmonary tuberculosis in low-income countries: the current evidence. *The Lancet. Infectious Diseases, 3*(5), 288–96.

Singhal, R., & Myneedu, V. P. (2015). Microscopy as a diagnostic tool in pulmonary tuberculosis. *International Journal of Microbiology, 4*(1):1-6.

Song, K., Lee, S., & Ban, C. (2012). Aptamers and Their Biological Applications. *Sensors, 12*(12), 612–631.

Song, S., Wang, L., Li, J., Zhao, J., & Fan, C. (2008). Aptamer-based biosensors. *Trends in Analytical Chemistry*, *27*(2), 108-117.

Sperandeo, M., Tinti, M. G., & Rea, G. (2017). Chest ultrasound versus chest X-rays for detecting pneumonia in children: Why compare them each other if together can improve the diagnosis? *European Journal of Radiology*, *93*:291-292.

Stanier, P., Abu-Hayyeh, S., Murdoch, J. N., Eddleston, J., & Copp, A. J. (1998). Paralogous sm22alpha (Tagln) genes map to mouse chromosomes 1 and 9: further evidence for a paralogous relationship. *Genomics, 51*(1), 144-147.

http://etd.uwc.ac.za/

Steingart, K. R., Dendukuri, N., Henry, M., Schiller, I., Nahid, P., Hopewell, P. C., Ramsay, A., Pai, M., & Laal, S. (2009). Performance of purified antigens for serodiagnosis of pulmonary tuberculosis: A meta-analysis. *Clinical and Vaccine Immunology*, *16*(2), 260–276.

Steingart, K. R., Flores, L. L., Dendukuri, N., Schiller, I., Laal, S., Ramsay, A., Hopewell, P. C., & Pai, M. (2011). Commercial Serological Tests for the Diagnosis of Active Pulmonary and Extrapulmonary Tuberculosis: An Updated Systematic Review and Meta-Analysis. *PLoS Medicine*, *8*(8), e1001062.

Steingart, K. R., Ramsay, A., Dowdy, D. W., & Pai, M. (2012). Serological tests for the diagnosis of active tuberculosis: relevance for India. *The Indian journal of medical research*, *135*(5), 695-702.

Stevens, W. (2012). GeneXpert Implementation in South Africa Public Sector: One year later..Lessons Learnt. *4th WHO/GLI Meeting* (online). Available: http://www.stoptb.org/wg/gli/assets/html/day%203/Stevens%20-%20South%20Africa.pdf. Date accessed 14 March, 2019.

Stoltenburg, R., Schubert, T., & Strehlitz, B. (2015). In vitro selection and interaction studies of a DNA aptamer targeting Protein A. *PLoS One*, *10*(7), 1–23.

Strand, C., Enell, J., Hedenfalk, I., & Ferno, M. (2007). RNA quality in frozen breast cancer samples and the influence on gene expression analysis - a comparison of three evaluation methods using microcapillary electrophoresis traces. *BMC Molecular Biology*, *8*(1), 38.

Strimbu, K., & Tavel, J. A. (2010). What are biomarkers? *Current Opinion in HIV and AIDS*, *5*(6), 463–466.

Sun, H., Zhu, X., Lu, P. Y., Rosato, R. R., Tan, W., & Zu, Y. (2014). Oligonucleotide Aptamers: New Tools for Targeted Cancer Therapy. *Molecular Therapy Nucleic Acids*, *3*:e182.

Svobodova, M., Bunka, D. H., Nadal, P., Stockley, P. G., & O'Sullivan, C. K. (2013). Selection of 2'F-modified RNA aptamers against prostate-specific antigen and their evaluation for diagnostic and therapeutic applications. *Analytical and Bioanalytical Chemistry*, *405*(28):9149-57.

Tabb-Massey, A., Caffrey, J. M., Logsden, P., Taylor, S., Trent, J. O., & Ellis, S. R. (2003). Ribosomal proteins Rps0 and Rps21 of Saccharomyces cerevisiae have overlapping functions in the maturation of the 3' end of 18S rRNA. *Nucleic Acids Research*, *31*(23), 6798–6805.

Takahashi, M., Wu, X., Ho, M., Chomchan, P., Rossi, J. J., Burnett, J. C., & Zhou, J. (2016). High throughput sequencing analysis of RNA libraries

http://etd.uwc.ac.za/

reveals the influences of initial library and PCR methods on SELEX efficiency. *Scientific Reports*, *6*(1), 33697.

Tang, T., Liu, F., Lu, X., & Huang, Q. (2017). Evaluation of GeneXpert MTB/RIF for detecting *Mycobacterium tuberculosis* in a hospital in China. *The Journal of International Medical Research*, *45*(2), 816–822.

Taslim, N. A., Virani, D., Sumartini, N. K., Karmila, Bukhari, A., Aminuddin, As'ad, S., Satriono, R., Rasyid, H., & Djaharuddin I. (2017). Energy regulation in newly diagnosed TB with chronic energy deficiency: free fatty acids and RBP4. *Asia Pacific Journal of Clinical Nutrition*, *26*(1):S73-S78.

Thoring, L., Wüstenhagen, D. A., Borowiak, M., Stech, M., Sonnabend, A., & Kubick, S. (2016). Cell-Free Systems Based on CHO Cell Lysates: Optimization Strategies, Synthesis of "Difficult-to-Express" Proteins and Future Perspectives. *PLOS One*, *11*(9), e0163670.

Tsao, S.-M., Lai, J.-C., Horng, H.-E., Liu, T.-C., & Hong, C.-Y. (2017). Generation of Aptamers from A Primer-Free Randomized ssDNA Library Using Magnetic-Assisted Rapid Aptamer Selection. *Scientific Reports*, *7*:45478.

Tuerk, C., & Gold, L. (1990). Systematic evolution of ligands by exponential enrichment: RNA ligands to bacteriophage T4 DNA polymerase. *Science*, *249*(4968), 505–510.

Vater, A., Jarosch, F., Buchner, K., & Klussmann, S. (2003). Short bioactive Spiegelmers to migraine-associated calcitonin gene-related peptide rapidly identified by a novel approach: tailored-SELEX. *Nucleic Acids Research*, *31*(21), e130.

Wallis, R. S., Wang, C., Doherty, T. M., Onyebujoh, P., Vahedi, M., Laang, H., Olesen, O., Parida, S., & Zumla, A. (2010). Biomarkers for tuberculosis disease activity, cure, and relapse. *The Lancet Infectious Diseases*, *10*(2), 68–69.

Walters, S. B., Kieckbusch, J., Nagalingam, G., Swain, A., Latham, S. L., Grau, G. E. R., Britton, W. J., Combes, V., & Saunders, B. M. (2013). Microparticles from Mycobacteria-Infected Macrophages Promote Inflammation and Cellular Migration. *The Journal of Immunology*, *190*(2), 669–677.

Walzl, G., Haks, M. C., Joosten, S. A., Kleynhans, L., Ronacher, K., & Ottenhoff, T. H. M. (2015). Clinical Immunology and Multiplex Biomarkers of Human Tuberculosis. *Cold Spring Harbor Perspectives in Medicine*, *5*(4), a018515.

http://etd.uwc.ac.za/

Walzl, G., Ronacher, K., Hanekom, W., & Scriba, T. J. (2011). Immunological biomarkers of tuberculosis. *Nature Reviews Immunology*, *11*(5), 343–354.

Wang, J.-Y., Chou, C.-H., Lee, L.-N., Hsu, H.-L., Jan, I.-S., Hsueh, P.-R., Yang, P.-C., & Luh, K.-T. (2007). Diagnosis of tuberculosis by an enzyme-linked immunospot assay for interferon-gamma. *Emerging Infectious Diseases*, *13*(4), 553–558.

Wang, L., Ma, W., Chen, W., Liu, L., Ma, W., Zhu, Y., Xu, L., Kuang, H., & Xu, C. (2011). An aptamer-based chromatographic strip assay for sensitive toxin semi-quantitative detection. *Biosensors Bioelectronics*, *26*(6):3059-3062.

Wang, L. T., Cleveland, R. H., Binder, W., Zwerdling, R. G., Stamoulis, C., Ptak, T., Sherman, M., Haver, K., Sagar, P., Sagar, P., & Hibberd, P. (2018). Similarity of chest X-ray and thermal imaging of focal pneumonia: a randomised proof of concept study at a large urban teaching hospital. *British Medical Journal open*, *8*(1), e017964.

Wang, X.-F., Wu, Y.-H., Jiao, J., Guan, C.-P., Yang, X.-G., & Wang, M.-S. (2013). Diagnostic value of superoxide dismutase in tuberculous and malignant pleural effusions. *Asian Pacific Journal of Cancer Prevention*, *14*(2), 821–824.

Warner, D. F. (2015). Mycobacterium tuberculosis metabolism. *Cold Spring Harbor perspectives in medicine*, *5*(4), a021121.

Warren, E., Teskey, G., & Venketaraman, V. (2017). Effector Mechanisms of Neutrophils within the Innate Immune System in Response to *Mycobacterium tuberculosis* Infection. *Journal of Clinical Medicine*, *6*(2), 15.

UNIVERSITY of the
WESTERN CAPE

Wei, H., Li, B., Li, J., Wang, E., & Dong, S. (2007). Simple and sensitive aptamer-based colorimetric sensing of protein using unmodified gold nanoparticle probes. *Chemical Communications*, *0*(36), 3735.

Whitelaw, A., & Sturm, A. W. (2009). *Microbiological testing for Mycobacterium tuberculosis*. Tuberculosis a comprehensive clinical reference (1st Edition), 169-178.

Wilson, D. S., Keefe, A. D., & Szostak, J. W. (2001). The use of mRNA display to select high-affinity protein-binding peptides. *Proceedings of the National Academy of Sciences of the United States of America*, *98*(7), 3750–3755.

World Health Organization (WHO) (2011): Tuberculosis: Serodiagnostic Tests Policy Statement 2011. *Commercial serodiagnostic tests for diagnosis of active tuberculosis* (online). Available: https://www.who.int/tb/features_archive/factsheet_serodiagnostic_test.pdf?ua=1. Date accessed 14 March, 2019.

http://etd.uwc.ac.za/

World Health Organization (WHOa) (2018): Tuberculosis. https://www.who.int/news-room/fact-sheets/detail/tuberculosis. Date accessed 20 December, 2018.

World Health Organization (WHOb) (2018): Tuberculosis and gender. https://www.who.int/tb/publications/tb_women_factsheet.pdf?ua=1. Date accessed 20 Dec, 2018.

Xi, Z., Huang, R., Li, Z., He, N., Wang, T., Su, E., & Deng, Y. (2015). Selection of HBsAg-Specific DNA Aptamers Based on Carboxylated Magnetic Nanoparticles and Their Application in the Rapid and Simple Detection of Hepatitis B Virus Infection. *ACS Applied Materials & Interfaces*, *7*(21), 11215–11223.Xu, D. D., Deng, D. F., Li, X., Wei, L. L., Li, Y. Y., Yang, X. Y., Yu, W., Wang, C., Jiang, T. T., Li, Z. J., Chen, Z. L., Zhang, X., Liu, J. Y., Ping, Z. P., Qiu, Y. Q. and Li, J. C. (2015). Discovery and identification of serum potential biomarkers for pulmonary tuberculosis using iTRAQ-coupled two-dimensional LC-MS/MS. *Proteomics. 14*(2-3):322-331.

Xie, Y., Liu, Y-G., & Chen, L. (2016). Assessing protein-DNA interactions: Pros and cons of classic and emerging techniques. *Science China Life Sciences, 59* (4), 425–427.

Xu, D., Li, Y., Li, X., Wei, L. L., Pan, Z., Jiang, T. T., Chen, Z. L., Wang, C., Cao, W. M., Zhang, X., Ping, Z. P., Liu, C. M., Liu, J. Y., Li, Z. J., & Li, J. C. (2015). Serum protein S100A9, SOD3, and MMP9 as new diagnostic biomarkers for pulmonary tuberculosis by iTRAQ-coupled two-dimensional LC-MS/MS. *Proteomics. 15*(1):58-67.

UNIVERSITY of the
WESTERN CAPE

Yang, C., Murray, J. L., & Ibrahim, J. K. (2017). Chapter 15 - MUC1 and Cancer Immunotherapy. *Immunology:Immunotoxicology, Immunopathology, and Immunotherapy, 1*:225-240.

Yang, H., Kruh-Garcia, N. A., & Dobos, K. M. (2012). Purified Protein Derivatives of Tuberculin - Past, Present, and Future. *FEMS Immunology and Medical Microbiology*, *66*(3), 273–280.

Young, B. L., Mlamla, Z., Gqamana, P. P., Smit, S., Roberts, T., Peter, J., Theron, G., Govender, U., Dheda, K., & Blackburn J. (2014). The identification of tuberculosis biomarkers in human urine samples. *European Respiratory Journal, 43*:1719-1729.

Yüce, M., Ullah, N., & Budak, H. (2015). Trends in aptamer selection methods and applications. *Analyst*, *140*(16), 5379–5399.

Zhou, J. (2015). Early diagnosis of pulmonary tuberculosis using serum biomarkers. *Proteomics*, *15*(1), 6–7.

http://etd.uwc.ac.za/

Zhu, P., Martinvalet, D., Chowdhury, D., Zhang, D., Schlesinger, A., & Lieberman, J. (2009). The cytotoxic T lymphocyte protease granzyme A cleaves and inactivates poly (adenosine 5′-diphosphate-ribose) polymerase-1. *Blood*, *114*(6), 1205–1216.

http://etd.uwc.ac.za/